Appendix I: Publications

List of publications from thesis:

Research Articles

1. **Sharma N**, Gaikwad AB (2020), Ameliorative effect of AT2R and ACE2 activation on ischemic renal injury associated cardiac and hepatic dysfunction. *Environmental Toxicology and Pharmacology*, 80, 103501. [IF- 3.292]
2. **Sharma N**, Gaikwad AB (2020), Effects of renal ischemia injury on brain in diabetic and non-diabetic rats: Role of angiotensin II type 2 receptor and angiotensin converting enzyme 2. *European Journal of Pharmacology*, 882, 173241. [IF- 3.263]
3. **Sharma N**, Sankrityayan H, Kale A, Gaikwad AB (2020), Role of SET7/9 in the progression of ischemic renal injury in diabetic and non-diabetic rats. *Biochemical and Biophysical Research Communications*, 528, 14-20. [IF- 2.985]
4. **Sharma N**, Malek V, Mulay SR, Gaikwad AB (2019), Angiotensin II type 2 receptor and angiotensin-converting enzyme 2 mediate ischemic renal injury in diabetic and non-diabetic rats. *Life Sciences*, 235, 116796. [IF- 3.647]

Review Articles

5. **Sharma N**, Sircar A, Anders HJ, Gaikwad AB (2020), Crosstalk between kidney and liver in non-alcoholic fatty liver disease: mechanisms and therapeutic approaches, *Archives of Physiology and Biochemistry*, 1-15. [Impact Factor: 2.575]
6. **Sharma N**, Anders HJ, Gaikwad AB (2019), Fiend and friend in the renin angiotensin system: An insight on acute kidney injury. *Biomedicine and Pharmacotherapy*, 110:764-774. [Impact Factor: 4.545]

Book Chapter

7. **Sharma N**, Kulkarni YA, Shiva N, Gaikwad AB (2020), Role of Histone modifications in the development of Acute kidney injury, *Organ specific epigenetic regulations in human diseases*. Published by Elsevier. [in the process of publication].

Abstract published in International Conference from thesis

8. **Sharma N** and Gaikwad AB (2020), Hyperglycemia-associated acute kidney injury increases the susceptibility towards neurological dysfunction: role of angiotensin II type 2

receptor and angiotensin-converting enzyme 2. *Nephrology Dialysis Transplantation Supplement 3*, P0527.

List of National and International Conferences from thesis:

1. **Sharma N** and Gaikwad AB. Hyperglycemia-associated acute kidney injury increases the susceptibility towards neurological dysfunction: Role of Angiotensin II Type 2 Receptor and Angiotensin-converting Enzyme 2. **57th ERA-EDTA Congress-Fully virtual-2020**, June 2020, Milan, Italy. (***e-poster presentation***).
2. **Sharma N** and Gaikwad AB. Ischemic renal injury-associated cardiac dysfunction in diabetic and non-diabetic rats: Role of depressor arm of RAS. **International Conference of Cardiovascular Sciences-2020 (ICCS-2020),** February 2020, DPSRU-New Delhi, India. **(*Oral presentation- won Travel Grant Award*).**
3. **Sharma N** and Gaikwad AB. Angiotensin II type 2 receptor and angiotensin-converting enzyme 2 mediate ischemic renal injury in diabetic and non-diabetic rats. **2nd National Biomedical Research Competition (NBRCom-2019),** PGIMER Chandigarh, India. (***Oral presentation- won Appreciation Award under 4th-10th rank***).
4. **Sharma N**, Malek V, Gaikwad AB, Role of protective renin angiotensin system intervention in preventing renal ischemia/reperfusion injury in diabetic rats. **ISMM-2018.** December 2018, SGPGIMS-Lucknow, India. ***(Oral presentation- won Travel Grant Award)***.
5. **Sharma N**, Malek V, Gaikwad AB, Hyperglycemia worsens acute kidney injury by reducing AT_2 receptor/ ACE2 expression. **IPSCON-2017.** February 2018, NMIMS-Mumbai, India. ***(Poster presentation)***.

List of other publications:

- **Research Articles**

1. Malek V, **Sharma N**, Sankrityayan H, Gaikwad AB (2019), Concurrent neprilysin inhibition and renin-angiotensin system prevented diabetic nephropathy. *Life Sciences*, 221, 159-167. [IF- 3.647]
2. Malek V, **Sharma N,** Gaikwad AB (2019). Simultaneous inhibition of neprilysin and activation of ACE2 prevented diabetic cardiomyopathy. *Pharmacological Reports, 71*(5), 958-967. [IF- 2.754]

3. Malek V, **Sharma N**, Gaikwad AB (2019), Histone Acetylation Regulates Natriuretic Peptides and Neprilysin Gene Expressions in Diabetic Cardiomyopathy and Nephropathy. *Current Molecular Pharmacology*, 12 (1), 61-71. [IF- 3.283]

4. Goru SK, Kadakol A, Malek V, Pandey A, **Sharma N**, Gaikwad AB (2017), Diminazene aceturate prevents nephropathy by increasing glomerular ACE2 and AT2 receptor expression in a rat model of type1 diabetes. *British Journal of Pharmacology*, 174 (18), 3118-3130. [IF- 7.73]

5. Kadakol A, Malek V, Goru SK, Pandey A, **Sharma N**, Gaikwad AB (2017), Esculetin ameliorates insulin resistance and type 2 diabetic nephropathy through reversal of histone H3 acetylation and H2A lysine 119 monoubiquitination. *Journal of Functional Foods*, 35, 256-266. [IF-3.701]

6. Pandey A, Raj P, Goru SK, Kadakol A, Malek V, **Sharma N**, Gaikwad AB (2017), Esculetin ameliorates hepatic fibrosis in high fat diet induced non-alcoholic fatty liver disease by regulation of FoxO1 mediated pathway. *Pharmacological Reports*, 69 (4), 666-672. [IF- 2.754]

7. Goru SK , Kadakol A, Pandey A, Malek V, **Sharma N**, Gaikwad AB (2016), Histone H2AK119 and H2BK120 monoubiquitination modulate SET7/9 and SUV39H1 in type 1 diabetes induced renal fibrosis. *Biochemical Journal*, 131-68-76. [IF- 4.097]

8. Pandey A, Goru SK, Kadakol A, Malek V, **Sharma N**, Gaikwad AB (2016), H2AK119 monoubiquitination regulates Angiotensin II receptor mediated macrophage infiltration and renal fibrosis in type 2 diabetic rats. *Biochimie*, 131, 68-76. [IF- 3.413]

- **Review Articles**

9. Shiva N, **Sharma N**, Kulkarni YA, Mulay SR, Gaikwad AB (2020), Renal ischemia/reperfusion injury: an insight on *in vitro* and *in vivo* models. *Life Sciences*, 256:117860. [IF- 3.647]

10. Sankrityayan H, Kale A, **Sharma N**, Anders HJ, Gaikwad AB (2020), Evidence for Use or Disuse of Renin-Angiotensin System Modulators in Patients Having COVID-19 With an Underlying Cardiorenal Disorder. *Journal of Cardiovascular Pharmacology and Therapeutics*, 25 (4), 299-306. [IF 2.322]

11. Kadakol A, **Sharma N**, Kulkarni YA, Gaikwad AB (2016), Esculetin: A phytochemical endeavor fortifying effect against non-communicable diseases. *Biomedicine and Pharmacotherapy*, 84: 1442-1448 [Impact Factor: 4.545]

- **Book Chapter**

12. Malek V, Suryavanshi SV, **Sharma N**, Kulkarni YA, Mulay SR, Gaikwad AB (2020), Potential of Renin-Angiotensin-Aldosterone System Modulations in Diabetic Kidney Disease: Old Players to New Hope!. In: . Reviews of Physiology, Biochemistry and Pharmacology. Springer, Berlin, Heidelberg. https://doi.org/10.1007/112_2020_50.

13. **Sharma N**, Gaikwad AB**,** Kulkarni YA (2017). Folic Acid in Pain: An Epigenetic Link. *In: Nutritional Modulators of Pain in the Aging Population*. Academic Press: Elsevier, USA. Pp. 245-251.

Appendix II: Biographies

Brief Biography of the Supervisor:

Prof. Gaikwad Anil Bhanudas is currently working as an Associate Professor in the Department of Pharmacy, and Associate Dean- Practice School Division at Birla Institute of Technology and Science Pilani (BITS Pilani), Pilani campus, Rajasthan. He did his M.S. (Pharm.) and Ph.D. from the Department of Pharmacology and Toxicology, National Institute of Pharmaceutical Education and Research (NIPER), S.A.S. Nagar, Punjab, India. He was awarded prestigious DAAD (German Academic Exchange Services) Sandwich fellowship (2008-09) for conducting part of his Ph.D. work in the Nephrological Center, Medical Policlinic, Ludwig Maximilians-University, Munich, Germany. After completion of the doctoral degree, he worked as a visiting scientist in the Department of Medicine/Nephrology, Albert Einstein College of Medicine, Bronx, NY, USA and Nephrological Center, Ludwig-Maximilians-University, Munich, Germany, in the year of 2008-09 and in 2010, respectively. He has strong expertise in the field of metabolic diseases including diabetes mellitus, its associated cardiovascular and renal complications. His enthusiasm for research has been admitted by various government funding authorities and accepted his seven research proposals. So far, he has provided vast and novel evidence on histone PTMs in diabetic cardiomyopathy and nephropathy; the therapeutic intervention of Esculetin in development of cardiorenal syndrome under type 2 diabetes; regulation of NF-κβ by angiotensin receptor subtypes AT1 and AT2 in diabetic nephropathy; protective action of Esculetin on thoracic aorta; the critical role of histone ubiquitination and ubiquitin-proteasome system in the development of diabetic renal fibrosis; the therapeutic intervention of Dize, an ACE2 activator, in the progression of diabetic nephropathy; Epigenetic regulation of natriuretic peptide system and reno-protective effect of novel combinations of Telmisartan with Thiorphan and Dize in the progression of type 1 diabetic cardiomyopathy and nephropathy. Prof. Gaikwad has not only contributed in research but also in scientific writing by being one of the authors in

several book chapters, which are published under Elsevier production. His publications are the relevant contribution towards the scientific community, providing more than 45 peer-reviewed research publications. He guided four Ph.D. students for the successful completion of their research work. One post-doctoral fellow has also been mentored by him. Additionally, six M. Pharm and seven B. Pharm students have completed their dissertation under his supervision. At the moment, he is supervising three Ph.D. and two M. Pharm students.

Brief Biography of the Candidate:

Ms. Nisha Sharma has graduated in Pharmacy from Savitri Devi Memorial College of Pharmacy, (SDMCP), Kaithal, Haryana, India in the year 2012. She completed her M.S. (Pharm.) degree in Pharmacology and Toxicology from the National Institute of Pharmaceutical Education and Research (NIPER), S.A.S. Nagar, Punjab, India in the year 2015. She has joined Laboratory of Molecular Pharmacology, Department of Pharmacy, Birla Institute of Technology and Science Pilani (BITS Pilani), Pilani Campus to pursue her doctoral research work. She was awarded Indian Council of Medical Research- Senior Research Fellowship (ICMR-SRF), to pursue the doctoral degree studies, in the year 2019. Her areas of interest include acute kidney injury and its associated distant organ dysfunction, diabetes and its related cardiovascular and renal complications, and epigenetics. Moreover, she has published 12 original research and 5 review articles in various reputed, international, peer-reviewed journals. She has also authored two book chapters. She has received two travel grant awards to attend international conferences.

Life Sciences 235 (2019) 116796

Contents lists available at ScienceDirect

Life Sciences

journal homepage: www.elsevier.com/locate/lifescie

Angiotensin II type 2 receptor and angiotensin-converting enzyme 2 mediate ischemic renal injury in diabetic and non-diabetic rats

Nisha Sharma[a], Vajir Malek[a], Shrikant R. Mulay[b], Anil Bhanudas Gaikwad[a,*]

[a] Laboratory of Molecular Pharmacology, Department of Pharmacy, Birla Institute of Technology and Science Pilani, Pilani Campus, Rajasthan 333031, India
[b] Pharmacology Division, CSIR-Central Drug Research Institute, Lucknow 226031, India

ARTICLE INFO

Keywords:
Renin-angiotensin system
AT2R agonist
ACE2 activator
Diabetes
Ischemic renal injury

ABSTRACT

Aim: Depressor arm of the renin-angiotensin system (RAS) exerts reno-protective effects in chronic kidney diseases like diabetic nephropathy. However, same is still elusive under AKI and hyperglycaemia comorbidity. Hence, the present study delineates the role of angiotensin-II type 2 receptor (AT2R) and angiotensin-converting enzyme 2 (ACE2) in AKI under normal and hyperglycaemia condition.

Methods: Non-diabetic (ND) and Streptozotocin-induced diabetes mellitus (DM) rats were subjected to ischemic renal injury (IRI). Rats underwent IRI were treated with an AT2R agonist, C21 (0.3 mg/kg/day, *i.p.*) or ACE2 activator, Dize, (5 mg/kg/day, *p.o.*) either alone or as combination therapy. Renal histopathology and immunohistochemistry, proximal tubular fraction isolation, ELISA, immunoblotting and qRT-PCR were performed for subsequent analysis.

Key findings: Rats subjected to IRI displayed an increase in plasma ACE, AT1R, AT2R, Ang II, and reduction in ACE2, Ang-(1–7) expressions, with augmented renal inflammation and apoptosis. These changes were more prominent in diabetic rats with IRI. Co-administration of C21 and Dize augmented ACE2, Ang-(1–7), AT2R and MasR expressions, and attenuated tubular injury in both DM and ND rats.

Conclusion: We demonstrated that pharmacological activation of AT2R and ACE2 protects DM and ND rats from IRI by preventing oxidative stress, inflammation and apoptosis-mediated tubular damage.

1. Introduction

Clinically, acute kidney injury (AKI) is considered a catastrophic condition with incidences allied with high morbidity and mortality [1,2]. One of the major risk factors for AKI is diabetes mellitus (DM) [3,4]. As compared to non-diabetics, diabetic patients remain on the higher risk of AKI [5]. Adverse renal outcomes in DM and AKI individually are attributed mainly to the renin-angiotensin system (RAS) driven activation of mitogen-active protein kinase (MAPK)-mediated apoptosis, NF-κB mediated inflammation, and redox imbalance promoting oxidative stress [6–8]. Therefore, RAS inhibition via angiotensin II receptor blockers (ARB) or angiotensin-converting enzyme inhibitors (ACEi) was thought to prevent AKI. Surprisingly, it was observed that when ARB and ACEi were used to treat AKI patients, they increased the severity of AKI [8]. Hence, it highlights the need for new therapeutic approaches for the treatment of AKI.

The RAS is comprised of two counter regulatory arms, the pressor arm [angiotensin II (Ang-II)/angiotensin-converting enzyme (ACE)/Ang II type 1 receptor (AT1R)] and the depressor arm (Ang-(1–7)/ACE2/MasR), which induces vasoconstriction and vasodilation, respectively, thereby helping in maintaining blood pressure and other homeostasis [8]. Interestingly, the pressor arm of the RAS has been explored in depth concerning the pathophysiology and pharmacotherapy of the renal complications including AKI. However, no study has demonstrated the role of the depressor arm of RAS in the pathogenesis of AKI-DM co-morbidity till date; hence the present study focuses the same.

The depressor arm of RAS sets a compensatory mechanism by sensing the elevated cellular stress and pathological signalling, thus benefits the renal system [9,10]. Tourniquet-induced remote kidney injury mice demonstrated deregulation of ACE and ACE2 activity, which cause kidney damage. Interestingly, restoring the ACE/ACE2 balance by up-regulation of ACE2 prevented renal damage [11]. Lipopolysaccharide-induced endotoxemia significantly decreased mRNA levels of ACE2 and

Abbreviations: ACE, angiotensin-converting enzyme; ACE2, angiotensin-converting enzyme 2; AKI, acute kidney injury; Ang II, angiotensin II; Ang-(1–7), angiotensin-(1–7); AT2R, angiotensin II type 2 receptor; DM, diabetes mellitus; IRI, ischemic renal injury; ND, non-diabetic; RAS, renin-angiotensin system

* Corresponding author at: Department of Pharmacy, Birla Institute of Technology and Science, Pilani, Pilani Campus, Pilani 333 031, Rajasthan, India.
E-mail address: anil.gaikwad@pilani.bits-pilani.ac.in (A.B. Gaikwad).

https://doi.org/10.1016/j.lfs.2019.116796
Received 17 July 2019; Received in revised form 23 August 2019; Accepted 26 August 2019
Available online 27 August 2019

elevated Ang II, and inducible nitric oxide synthase levels in kidney, whereas restoration of ACE2 levels maintained endothelial porosity, glomerular filtration rate, and proximal tubular function, eventually protects the kidney against AKI [12]. Ruiz-Ortega et al. demonstrated overexpression of AT2R in renal tubular cells of Balb/c subjected to folic acid-induced AKI and proposed the potential role of AT2R in protecting the kidney damage [13]. Subsequently, overexpression of AT2R and activation of ACE2 activity significantly improved the renal function of mice in these models [11–13].

Therefore, in the present study, we hypothesised that the pharmacological activation of AT2R and ACE2 might protect rats from ischemic renal injury (IRI). Since hyperglycaemia remains a major risk factor for ischemic AKI, we also evaluated the protective effect of AT2R and ACE2 activation in diabetic rats with IRI.

2. Materials and methods

2.1. Materials

Streptozotocin and diminazene aceturate (Dize) were obtained from Sigma (St. Louis, MO, USA). Glucose, blood urea nitrogen (BUN) and creatinine kits were purchased from Accurex (Mumbai, India). ELISA kits for ACE, ACE2, Ang-(1–7) and Ang II were obtained from Fn Test (Wuhan, China). ACE, ACE2, AT1R, AT2R, and monocytes chemoattractant protein (MCP-1) primary antibodies were purchased from Santa Cruz Biotechnology (Dallas, TX, USA), and the remaining primary and secondary antibodies were purchased from Cell Signalling Technology (Danvers, MA, USA).

2.2. Development of streptozotocin-induced type 1 diabetes

The animal experiments were performed at Central Animal Facility (CAF), Birla Institute of Technology and Science Pilani (BITS-Pilani) as per the protocol approved by the Institutional Animal Ethics Committee (IAEC), BITS-Pilani (Protocol Approval No: IAEC/RES/21/08). Animal studies are reported ensuing the ARRIVE guidelines [14]. The male adult Wistar rats (200-220 g) were procured from the CAF of BITS-Pilani and were maintained under standard environmental conditions, with feed and water ad lib. Diabetes was induced by injecting a single dose of streptozotocin [55 mg/kg, *i.p.*, vehicle- sodium citrate buffer (0.01 M, pH 4.4)] in male Wistar rats, as described previously [15]. ND rats with same age group received only sodium citrate buffer ($n = 40$). After 48 h of streptozotocin injection, rats showing plasma glucose levels > 16 mmol/L were included in the study as DM rats ($n = 40$).

2.3. Ischemic renal injury in non-diabetic and diabetes mellitus rats

ND and DM rats were injected with saline (20 ml/kg, *s.c.*) to prevent fluid loss during laparotomy. Rats were anaesthetised with pentobarbital sodium (50 mg/kg, *i.p.*) and kept on a homoeothermic blanket to maintain body temperature (37 °C). After the loss of pedal pain and corneal reflexes, a half-inch incision was given on the left flank portion of abdomen and kidney was pulled out of the abdomen by holding the perirenal fat at the lower pole with blunt forceps. Followed by the clamping of renal vascular pedicle with a surgical clamp to induce ischemia [16]. After 45 min, the clamps were released, and 48 h of reperfusion was done. Then skeletal muscle and skin layers were sutured separately with absorbable and non-absorbable sutures, respectively. After suturing, topical (Betadine™) antiseptic and parenteral (Augmentin™, 324 mg/kg, *i.p.*) antibiotics were given to prevent post-surgical infection. Sham control animals were subjected to identical operation without renal vascular pedicle clamping. After 48 h of reperfusion; the rats were again anaesthetised with pentobarbital sodium (50 mg/kg, *i.p.*). Blood samples were collected from vena cava with a 5 mL syringe and plasma were separated (centrifugation) for biochemical parameters like plasma glucose (PGl), blood urea nitrogen (BUN), plasma creatinine (PCr), and ELISA. Th left kidney (I/R kidney) was then removed, washed and blotted dry, weighed and kept in −80 °C. Further, the left kidney was taken for tubular fraction isolation, western blot, ELISA, immunohistochemistry (IHC) and histological examinations.

2.4. Treatment regimens

Both ND and DM rats were subdivided into five groups each: (i) **ND/DM-** serve as respective controls, (ii) **ND − /DM-I/R-** ND or DM rats subjected to Ischemia-45 min/reperfusion-48 h (I/R), (iii) **ND − /DM-I/R + C21–** ND-I/R or DM-I/R rats receiving compound 21 (C21) (0.3 mg/kg/day, *i.p.*) [17], (iv) **ND − /DM-I/R + Dize-** ND-I/R or DM-I/R rats receiving diminazene aceturate (Dize) (5 mg/kg/day, *p.o.*) [9], (v) **ND − /DM-I/R + CD-** ND-I/R or DM-I/R rats receiving C21 (0.3 mg/kg/day, *i.p.*) and Dize (5 mg/kg/day, *p.o.*) combination therapy (Fig. 1A–B). We kept six rats in each experimental group considering an effect size of 0.92, α of 0.05, and power of 0.95 for statistical analysis.

2.5. Proximal tubules isolation from the whole kidney

Collected kidneys were placed in cold PBS (pH- 7.4), and tubular fractions were isolated using the percoll gradient centrifugation method with some modifications [18]. Briefly, the kidney was minced and digested with collagenase type IV in PBS, with constant oxygenation until a uniform suspension was formed. The suspension was filtered through a nylon 250-μm sieve and centrifuged at 100 *g* for 1 min. The pellets were suspended and washed two times in ice-cold PBS. The pellet suspension in PBS was mixed thoroughly with 40% Percoll and centrifuged at 26,000 *g* for 30 min. Four distinct bands (B1-B4) were separated. The B4 band, highly enriched proximal tubular fraction, was carefully collected, suspended, and washed in ice-cold PBS. Thus, the obtained tubular fraction was assessed under the light microscope and used for further analysis.

2.6. Histopathology

Renal histology was examined by Hematoxylin and Eosin (H and E) staining [19]. At least 4–5 sections (one microscopy slide) from each kidney and a total of $n = 6$ kidneys from each group were observed; and images of cortical tubules were captured at 400× magnification by using a Zeiss microscope (model: Vert.A1). 5–6 images from each stained kidney microscopy slide were evaluated for tubular necrosis. The histological findings were semi-quantitatively scored from 0 to 3 by a blinded observer: 0, none; 1, < 25% of tubules affected; 2, 25–50% of tubules affected; 3, > 50% of tubules affected. The average value of tubular necrosis score for each kidney was considered for statistical analysis ($n = 6$ kidneys/group).

2.7. Immunohistochemistry

IHC was performed as described previously [9]. Briefly, kidney sections (5 μm) were taken from paraffin blocks and deparaffinized with xylene, followed by antigen retrieval by heating in citrate buffer (10 mmol/L). We have used rabbit/mouse monoclonal antibodies against, ACE, ACE2, AT1R, and AT2R (Dilution: 1:200 *v/v*) as primary antibodies, and HRP-conjugated anti-rabbit/mouse IgG as a secondary antibody. Followed by detection with diaminobenzidine (DAB) as a chromogen. The slides were counterstained with hematoxylin, dehydrated with alcohol and xylene and mounted in DPX. At least 4–5 sections (one microscopy slide) from each kidney and a total of $n = 6$ kidneys from each group were observed; and images were captured at 400× magnification by using Zeiss microscope (model: Vert.A1). 5–6

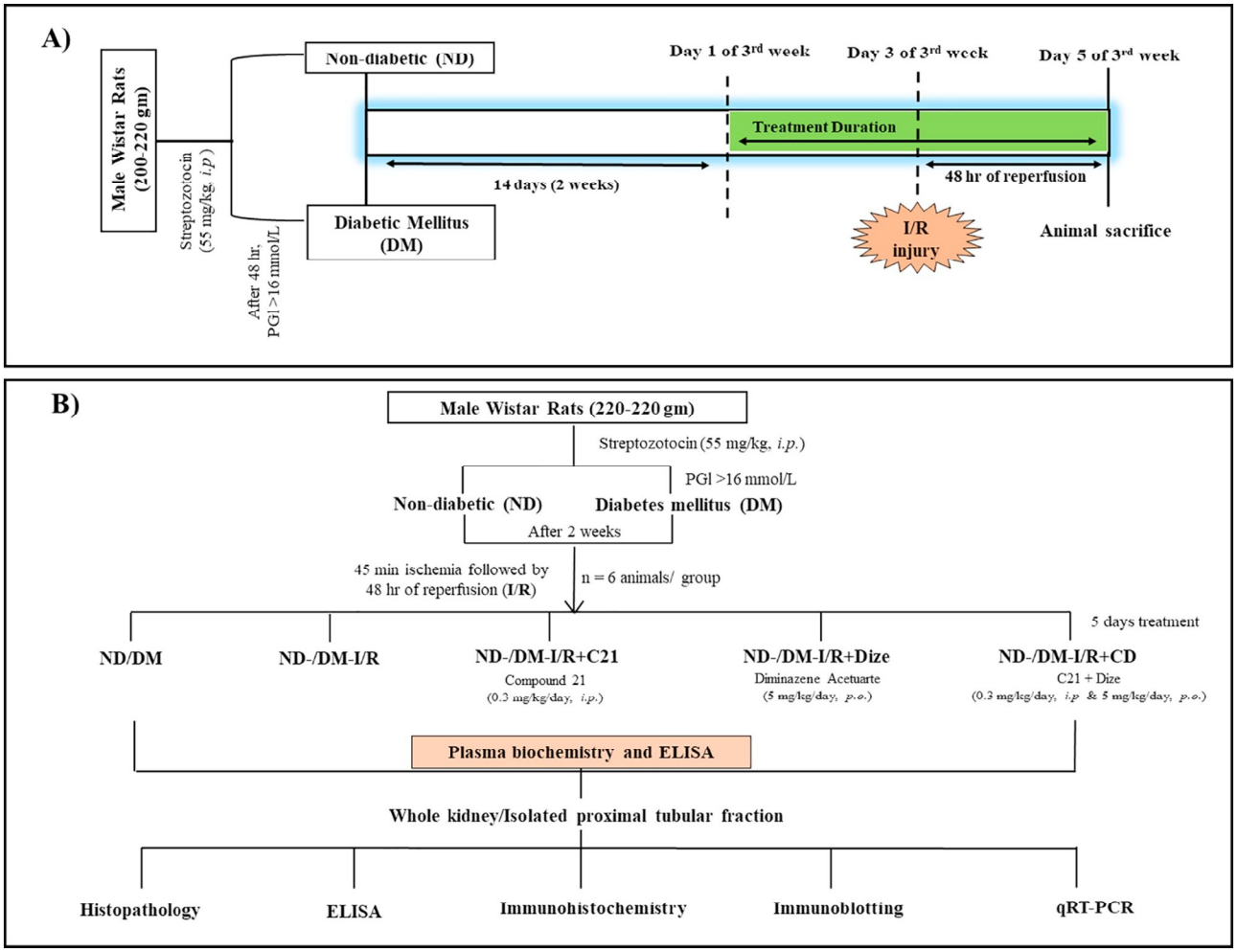

Fig. 1. Schematic representation of the interventional study.
A) Schedule for the induction of diabetes mellitus by streptozotocin-injection and acute kidney injury (AKI) by ischemia/reperfusion (I/Rin), and pharmacological intervention. B) Details of animal sub-grouping for an intervention study and further experimental design (n = 6 animals/group). **ND-** non-diabetic rats, **DM-** diabetes mellitus rats, **ND − /DM-I/R-** ND or DM rats subjected to Ischemia-45 min/reperfusion-48 h (I/R), **ND − /DM-I/R + C21–** ND-I/R or DM-I/R rats receiving compound 21 (0.3 mg/kg/day, *i.p.*) monotherapy, **ND − /DM-I/R + Dize-** ND-I/R or DM-I/R rats receiving Dize (5 mg/kg/day, *p.o.*) monotherapy, **ND − /DM-I/R + CD-** ND-I/R or DM-I/R rats receiving compound 21 (0.3 mg/kg/day, *i.p.*) and Dize (5 mg/kg/day, *p.o.*) combination therapy.

images from each stained kidney microscopy slide were analysed using ImageJ software (NIH, Bethesda, MD, USA) for calculating DAB-positive area.

2.8. Elisa

We homogenised isolated proximal tubular fraction in the recommended buffer solution, followed by total protein estimation by Lowry's method. Protein equalised proximal tubular samples, and diluted plasma were assayed for ACE, ACE2, Ang II and Ang-(1–7) protein levels by using ELISA kits (n = 6 rats/group) [9].

2.9. Immunoblotting

Protein isolation and immunoblotting were performed as previously described [9]. For immunoblotting, we have used rabbit/mouse/goat monoclonal antibodies against; p-NF-κB, c-Caspase-3, c-PARP1, Nrf2, MCP-1 and β-actin [Dilution 1:1000 (*v*/v)] as primary antibody and HRP conjugated anti-rabbit/mouse/goat IgG as secondary antibody [Dilution 1:20000 (v/v)]. Proteins were detected by using the ECL system and Hyperfilm, subsequently quantified by densitometric measurements using ImageJ software. The exposures were in linear dynamic range. Data analysis was performed by using GraphPad Prism software (San Diego, CA, USA), and results were expressed as fold change over control.

2.10. Quantitative real-time polymerase chain reaction

RNA was isolated from proximal tubular fraction using commercially available kits and qRT-PCR were performed using specific primers (Supplementary data, Table S1), designed and produced by Eurofins, India. [9,15]. Isolated RNA was reverse transcribed. qRT-PCR was done with LightCycler® 96 Real-Time PCR System using the FastStart Essential DNA Green Master and results were analysed by LightCycler® Software (Roche, Germany). Enrichment of targeted mRNA was normalized against 18s rRNA contents. Experiments were carried out in triplicate for each sample and results are expressed as fold changes over respective controls.

2.11. Statistical analysis

Experimental values are represented as mean ± SD, and 'n' refers to the number of samples studied. Statistical comparison between different groups was performed using one-way analysis of variance (ANOVA) followed by Tukey's Multiple Comparison post hoc test. Data were considered statistically significant if $p < 0.05$. GraphPad Prism

Table 1
Plasma biochemical parameters. Nondiabetic (ND) and diabetes mellitus (DM) (after 2 weeks of STZ-injection) rats were subjected to ischemic- 45 min and reperfusion of 48 h (I/R), followed by metabolic parameter measurement-plasma glucose (PGl), blood urea nitrogen (BUN), plasma creatinine (PCr).

Parameters	ND	ND-I/R	DM	DM-I/R
PGl (mmol/L)	4.9 ± 0.18	4.9 ± 0.42	16.9 ± 1.04[a]	17.3 ± 1.29[ab]
BUN (mmol/L)	7.1 ± 0.71	9.8 ± 0.53[a]	7.3 ± 0.49	13.8 ± 0.66[a,cb]
PCr (mg/dL)	1.56 ± 0.12	1.59 ± 0.16	1.57 ± 0.19	1.62 ± 0.11

Note: Each data is represented as mean ± SD (n = 6).
[a] $P < 0.05$ vs. ND.
[b] $P < 0.05$ vs. ND-I/R.
[c] $P < 0.05$ vs. DM.

software version 7.00 (San Diego, CA, USA) was used for all statistical processing.

3. Results

3.1. Hyperglycaemia increases the severity of ischemic renal injury

To check the effect of hyperglycaemia on IRI, we subjected ND and DM rats to ischemia followed by reperfusion (I/R) and evaluated the plasma biochemistry and extent of the oxidative stress markers in the isolated proximal tubular fraction. We observed that IRI in ND and DM rats significantly increased BUN levels when compared to respective controls. Interestingly, DM-I/R exhibited augmented BUN levels in comparison to ND-I/R rats. No change was observed in plasma creatinine levels among all the study groups (Table 1). Moreover, IRI in ND and DM rats significantly increased renal tubular oxidative stress, as demonstrated by augmented malondialdehyde (MDA) and GSH levels, nitrate/nitrite (NO_2/NO_3) ratio, and catalase activity compared to respective controls. Proximal tubules isolated from IR kidneys of DM rats showed significantly higher oxidative stress as compared to ND rats (Fig. 2A–D). Thus, our data indicated IRI hypersensitivity in diabetic rats.

Next, we analysed the expression of proinflammatory cytokines and apoptosis markers by western blot in I/R kidneys from ND and DM rats. IRI augmented tubular inflammation as evinced by increased p-NF-κB and MCP-1 expressions, as well as caused proximal tubular cell apoptosis as demonstrated by increased c-PARP1 and c-Cas-3 expressions when compared to respective controls (Fig. 2E–I). Interestingly, expressions of p-NF-κB, MCP-1, c-PARP1, and c-Cas-3 were significantly higher in I/R kidneys of DM as compared to ND rats (Fig. 2E–I).

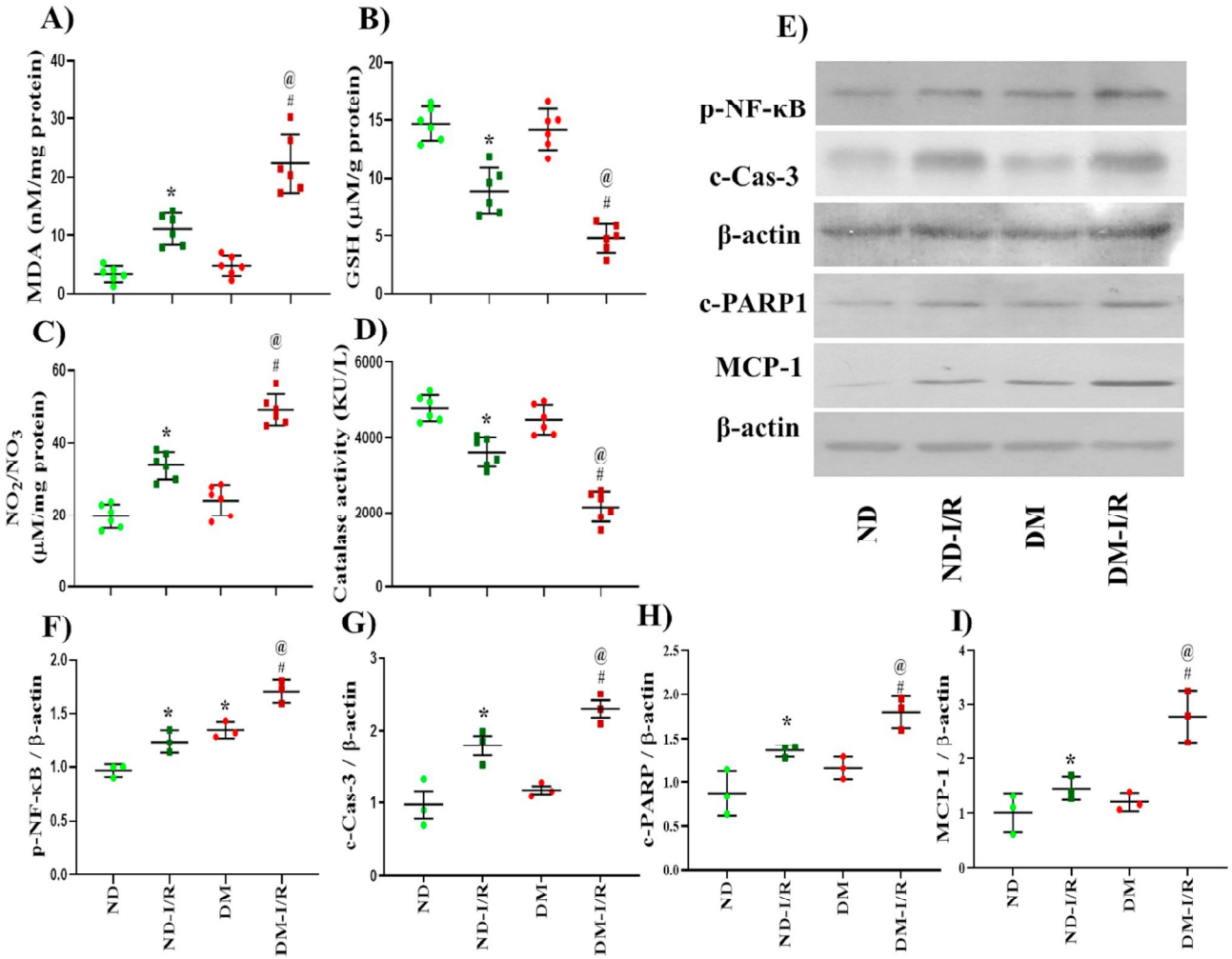

Fig. 2. Evaluation of oxidative stress, inflammation and apoptosis in IRI.
A-D: Estimation of oxidative stress markers e.g. malondialdehyde (MDA) (A), GSH (B), NO_2/NO_3 (Griess) (C), catalase activity (D) in kidneys of rats. ($n = 6$). E-I: Immunoblots for protein expressions of inflammatory and apoptotic markers in the isolated renal proximal tubular fraction with β-actin as a loading control (E). Immunoblots were quantified by densitometry analysis e.g. NF-κB(S-536) (F), c-Caspase-3 (G), c-PARP1 (H), and MCP-1 (I). Data are represented as mean ± SD from three independent experiments. For statistical comparison, one-way ANOVA with Tukey's multiple comparison test was used where (*) $p < 0.05$ vs ND; (#) $p < 0.05$ vs DM; (@) $p < 0.05$ vs ND-I/R.

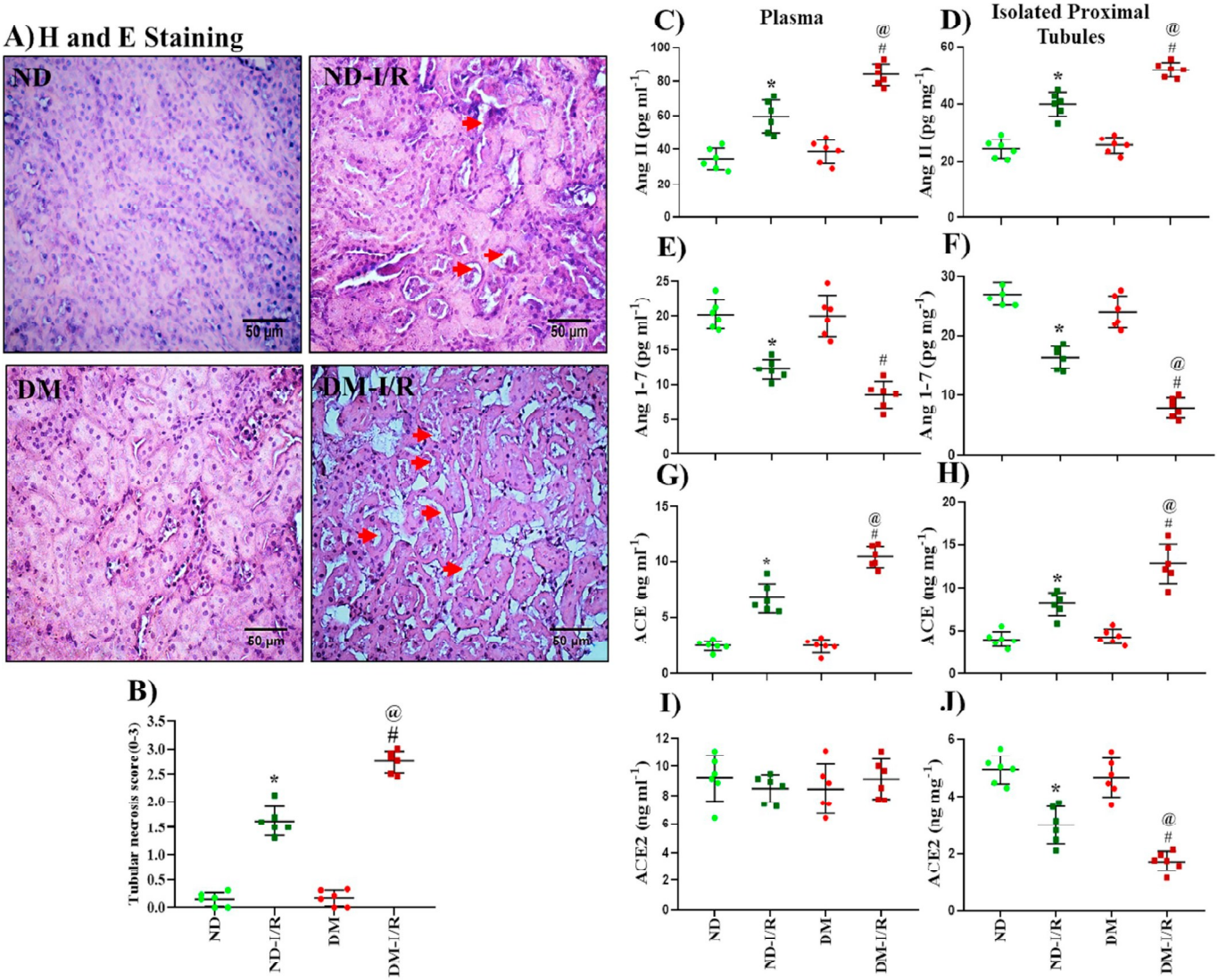

Fig. 3. IRI modulates tubular necrosis, and systemic and proximal tubular specific ACE, ACE2, Ang II and Ang-(1–7) levels.
A-B: Representative H & E staining images of the cortical region of kidney transverse sections (original magnification 400 × and scale bar- 50 µm). At least 4–5 images from each stained kidney section and a total of six different kidneys per group were observed by a blinded observer for tubular necrosis (arrow) (A). The tubular necrosis was analysed semi-quantitatively and scored from 0 to 3 (B). C-J: Protein expression of ACE, ACE2, Ang II and Ang-(1–7) in plasma (C, E, G, I) and isolated proximal tubules (D, F, H, J) was measured by ELISA ($n = 6$). Data are represented as mean ± SD. For statistical comparison, one-way ANOVA with Tukey's multiple comparison test was used where (*) $p < 0.05$ vs ND; (#) $p < 0.05$ vs DM; (@) $p < 0.05$ vs ND-I/R.

Furthermore, we also examined the histopathological alterations persuaded by unilateral renal ischemia in ND and DM rats by H and E staining. Tubular necrosis was observed in the outer cortex of DM-I/R rats and ND-I/R rats; however, DM-I/R rats showed extensive necrosis compared to ND-I/R rats (Fig. 3A–B). These results further confirm the higher susceptibility of diabetic kidney to I/R-induced AKI.

3.2. Ischemic renal injury alters systemic and tissue-specific renin-angiotensin system components in non-diabetic and diabetes mellitus rats

We measured the Ang II, Ang-(1–7) ACE, and ACE2 levels in plasma and proximal tubular fraction by ELISA kits (Fig. 3C–J). ND-I/R and DM-I/R rats demonstrated increased Ang II and decreased Ang-(1–7) levels in plasma and isolated tubules when compared to ND and DM rats, correspondingly (Fig. 3C–F). Furthermore, IRI to ND and DM rats increased ACE levels in plasma and isolated tubules, whereas decreased ACE2 levels only in isolated tubules with no change in plasma ACE2 levels (Fig. 3G–J). Interestingly, like our previous observations, IRI significantly altered the RAS components levels in the DM rats when compared to ND rats. Furthermore, IHC revealed increased ACE with no change in ACE2 expressions in I/R kidneys of ND as compared to control rats, whereas I/R kidneys of DM rats demonstrated increased ACE and reduced ACE2 tubular expression in comparison to DM and ND-I/R rats (Fig. 4A–B, E–F). In contrast, renal expression of AT1R and AT2R were significantly augmented in kidneys after IRI as compared to respective controls (Fig. 4C–D, G–H). Moreover, DM-I/R rats' kidneys exhibited increased tubular AT1R expression in comparison to ND-I/R rats' kidneys (Fig. 4C and G). Together our data suggest that the IRI altered the expression of the RAS depressor arm's components in both DM and ND conditions.

3.3. AT2R and ACE2 activation improved renal functions, inhibited renal oxidative stress and apoptosis in non-diabetic and diabetes mellitus rats upon ischemic renal injury

Based on our previous results we urged to check the role of RAS depressor arm's modulations on IRI, thus we treated ND-I/R and DM-I/R rats with AT2R agonist (C21, 0.3 mg/kg/day, *i.p.*) and ACE2 activator

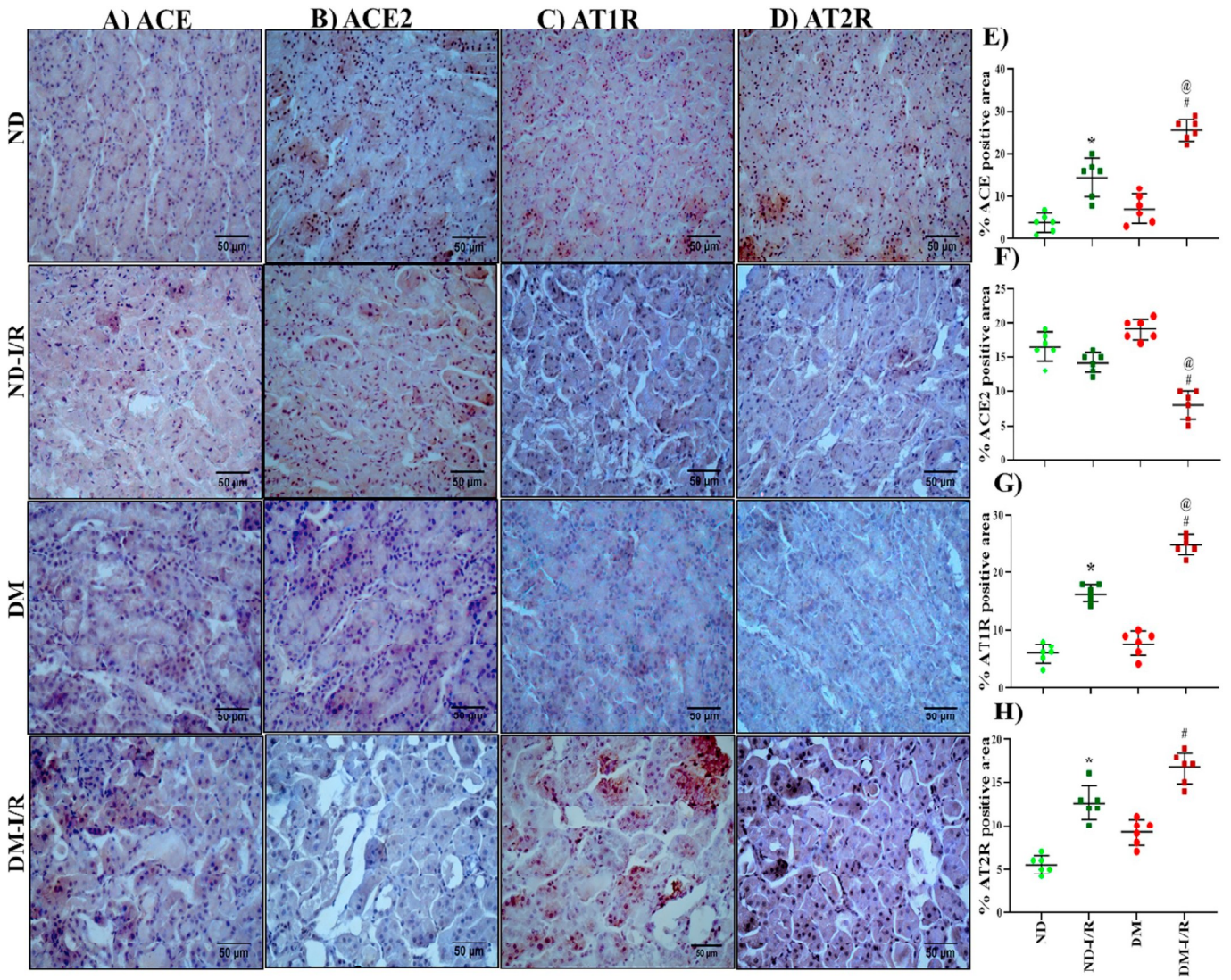

Fig. 4. Immunohistochemistry for ACE, ACE2, AT1R and AT2R.
A-D: Representative images of IHC staining for ACE, ACE2, AT1R and AT2R in the cortex of kidney (original magnification 400× and scale bar 50 µm). At least 4–5 sections from each stained kidney microscopy slide and total six different kidney slides per group were observed under microscope and images were captured. E-H: Semi-quantitative analysis of all the captured images using ImageJ (colour deconvolution plugin was utilized for analysis) for calculating DAB-positive area (indicates specific protein expressions). All Data are represented as mean ± SD. One-way ANOVA with Tukey's multiple comparison test, where (*) $p < 0.05$ vs ND; (#) $p < 0.05$ vs DM; (@) $p < 0.05$ vs ND-I/R.

Table 2
Plasma metabolic parameters: At the end of the treatment period, we have performed plasma biochemistry by assaying plasma glucose (PGL), blood urea nitrogen (BUN) levels in all the experimental groups.

Parameters	ND	ND-I/R	ND-I/R + C21	ND-I/R + Dize	ND-I/R + CD	DM	DM-I/R	DM-I/R + C21	DM-I/R + Dize	DM-I/R + CD
PGL (mmol/L)	6.1 ± 0.8	6.3 ± 1.0	5.9 ± 0.7	6.9 ± 0.9	6.6 ± 0.6	20.1 ± 1.7	19.3 ± 1.2	19.8 ± 2.0	18.5 ± 2.4	19.9 ± 0.9
BUN (mmol/L)	6.8 ± 0.3	9.2 ± 0.5[a]	9.8 ± 0.6	9.5 ± 0.5	7.6 ± 0.4[b]	7.5 ± 0.8	13.3 ± 0.4[a,c]	12.1 ± 0.5	11.8 ± 0.6	8.7 ± 0.4[d]

Note: Each data is represented as mean ± SD (n = 6).
[a] $P < 0.05$ vs. ND.
[b] $P < 0.05$ vs. ND-I/R.
[c] $P < 0.05$ vs. DM.
[d] $P < 0.05$ vs.DM-I/R.

(Dize, 5 mg/kg/day, *p.o.*), either alone as monotherapy or together as combination therapy. Plasma biochemistry revealed that, AT2R agonist and ACE2 activator combination therapy scientifically lower the BUN levels, whereas monotherapies had no effect on BUN levels in ND-I/R and DM-I/R rats (Table 2). C21 and Dize monotherapies to ND-I/R rats reduced MDA and increased Nrf2 expression, with no change in GSH levels. In contrast, both monotherapies could only increase Nrf2 expression in DM-I/R rats and had no effect on MDA and GSH levels. Interestingly, combination therapy significantly reduced MDA and increased GSH and Nrf2 levels in both ND-I/R and DM-I/R rats (Fig. 5A–D). Next, we checked the expression of apoptosis markers, c-Cas-3 and c-PARP1 by western blot. We found that combination therapy

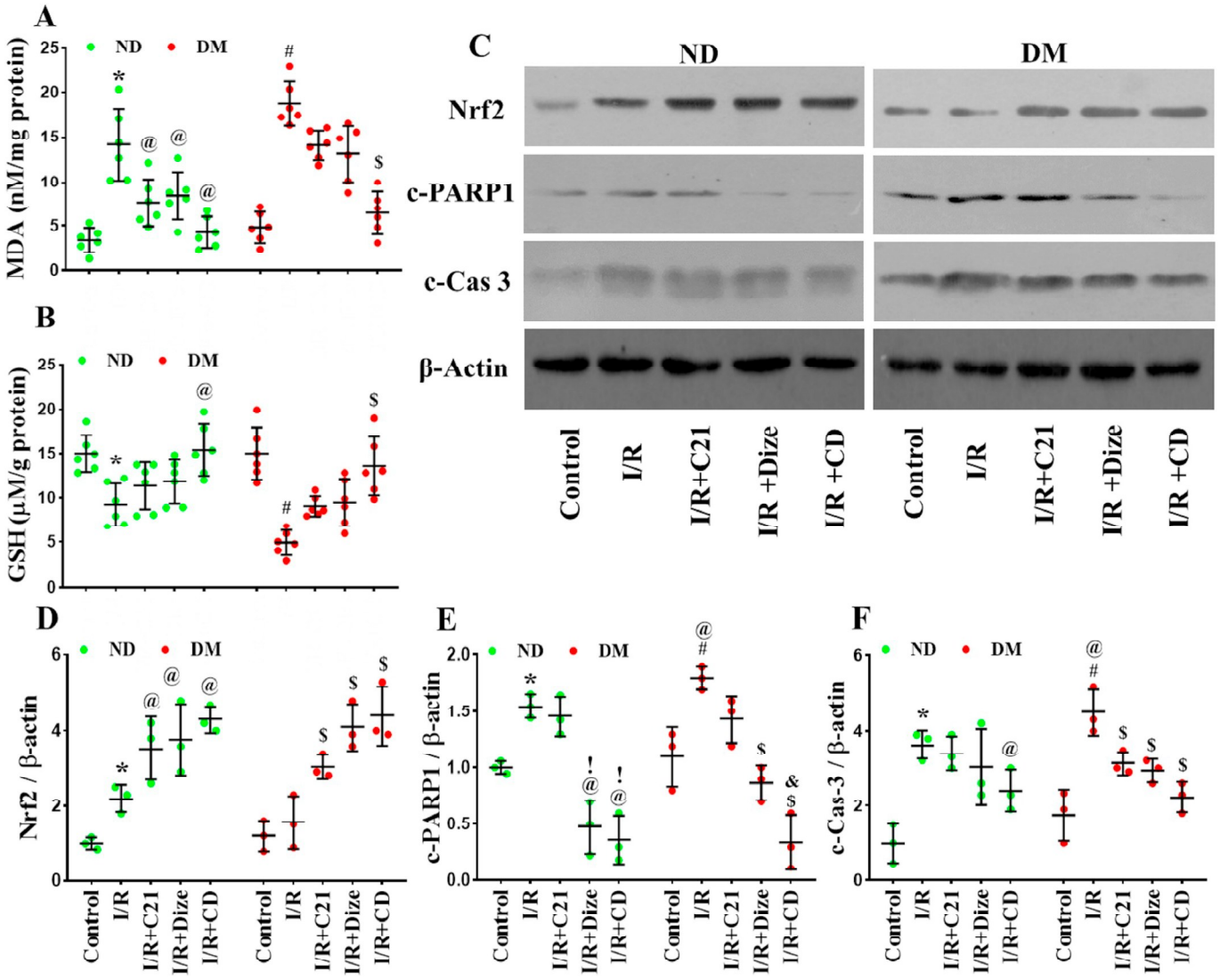

Fig. 5. AT2R agonist and ACE2 activator protects ND and DM rats against oxidative stress and apoptosis.
A-B: Estimation of oxidative stress markers e.g. malondialdehyde (MDA) (A), GSH (B) in proximal tubular fraction of kidneys of rats ($n = 6$). C-F: Representative western blot images for Nrf2, c-PARP1, c-Cas-3, and β-actin (loading control) protein expressions in isolated proximal tubular fraction (C). Immunoblots were quantified by densitometry analysis e.g. Nrf2 (D), c-PARP1 (E), and c-Cas-3 (F). Data are represented as mean ± SD from three independent experiments. One-way ANOVA with Tukey's multiple comparison test for statistical comparison. (*) $p < 0.05$ vs ND; (@) $p < 0.05$ vs ND-I/R; (#) $p < 0.05$ vs DM; ($) $p < 0.05$ vs DM-I/R; (&) $p < 0.05$ vs DM-I/R + C21.

significantly reduced c-Cas-3 and c-PARP1 levels in I/R kidneys of both ND and DM rats (Fig. 5C, E–F).

3.4. AT2R and ACE2 activation inhibits renal inflammation and prevented tubular damage in non-diabetic and diabetes mellitus rats upon ischemic renal injury

Inflammation is hallmark for the IRI [20], thus we analysed the alteration in the expressions of inflammatory molecules in the tubular fraction of I/R kidneys after AT2R and ACE2 activation. We observed that IRI increased protein expressions of p-NF-κB and MCP-1 in proximal tubules of ND and DM rats signifying renal inflammation. C21 and Dize monotherapies did not change the expression of p-NF-κB and MCP-1; except Dize monotherapy reduced MCP-1 expression in DM-I/R rats. In contrast, the combination therapy significantly inhibited p-NF-κB and MCP-1 expressions in the tubular fractions of both ND-I/R and DM-I/R rats (Fig. 6A–C). Furthermore, we found a significant increase in mRNA expressions of interleukin-6 (*Il6*), tumour necrosis factor-α (*Tnfa*) and *Mcp1* in the tubular fraction of ND and DM rats subjected to IRI (Fig. 6D–F). C21 or Dize monotherapy did not change mRNA expressions of *Tnfa* and *Mcp1* in ND-I/R and DM-I/R rats, whereas reduced *Il6* mRNA expression only in DM-I/R rats. In contrast, combination therapy significantly reduced *Il6* and *Mcp1* mRNA expressions in ND-I/R and DM-I/R rats, while decreased *Tnfa* mRNA expression in ND-I/R with no change in *Tnfa* mRNA expression in DM-I/R rats (Fig. 6D–F).

Next, we performed histopathological evaluation of kidney cortex by H and E staining. ND-I/R and DM-I/R rats exhibited significantly increased tubular necrosis, which was not prevented by C21 and Dize monotherapies. However, the combination therapy produced marked reduction in tubular necrosis in ischemic ND and DM kidneys' (Fig. 7). Therefore, our data suggest that simultaneous activation of AT2R and ACE2 inhibits renal inflammation and tubular damage in ND and DM rats upon IRI.

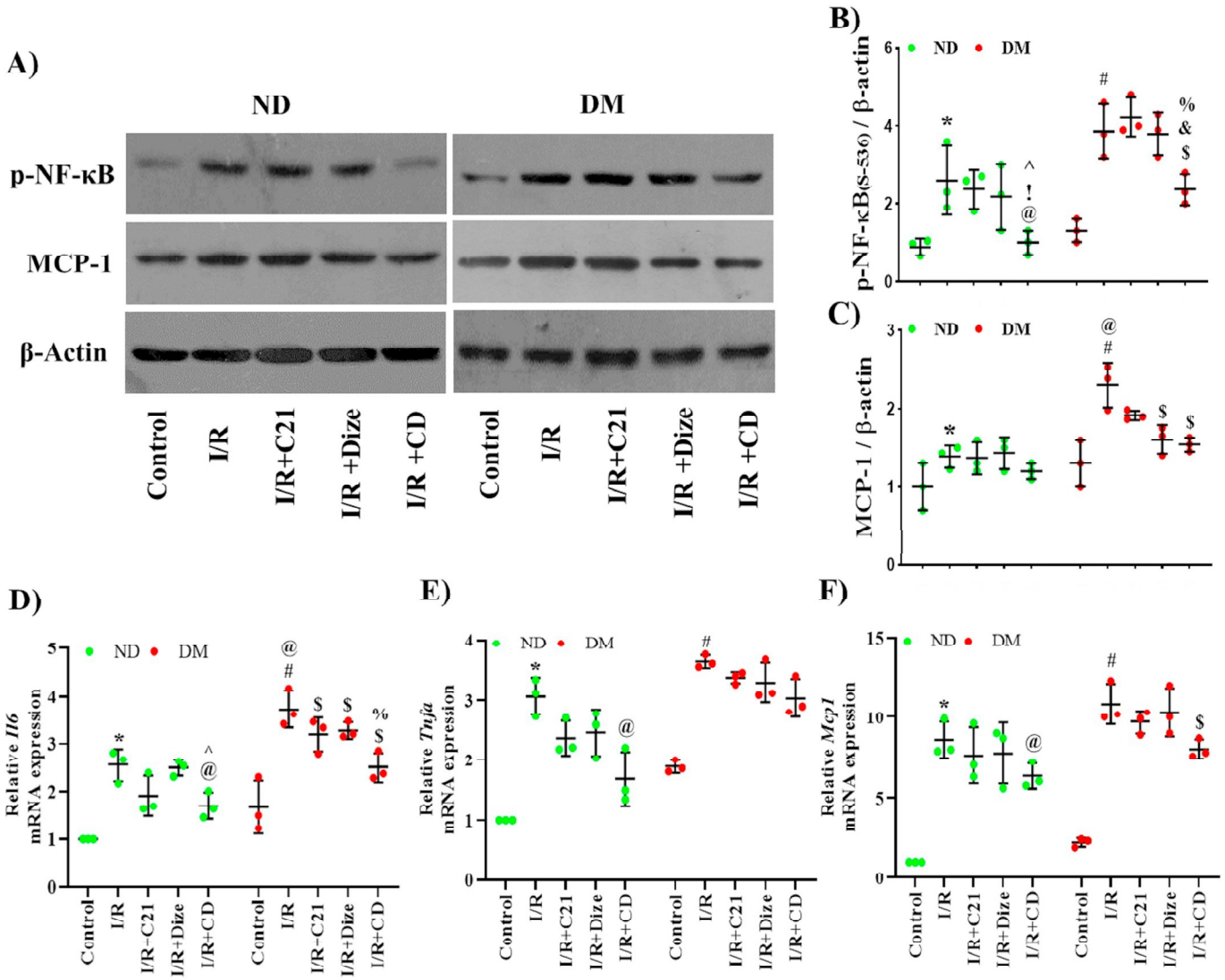

Fig. 6. Effect of C21, Dize and their combination therapy on protein and mRNA expressions of inflammatory markers.
A-C: Representative western blot images for protein expressions of p-NF-κB, MCP-1 and β-actin (loading control in isolated proximal tubular fraction (A). Immunoblots were quantified by densitometry analysis e.g. p-NF-κB (B), and MCP-1 (C). D-F: mRNA expression of *Il6, Tnfa* and *Mcp1* was assessed by qRT-PCR in isolated proximal tubules. 18s rRNA expression was used as internal control. Data are represented as mean ± SD from three independent experiments. One-way ANOVA with Tukey's multiple comparison test was used for statistical comparison. (*) $p < 0.05$ vs ND; (@) $p < 0.05$ vs ND-I/R; (!) $p < 0.05$ vs ND-I/R + C21; (^) $p < 0.05$ vs ND-I/R + Dize; (#) $p < 0.05$ vs DM; ($) $p < 0.05$ vs DM-I/R; (&) $p < 0.05$ vs DM-I/R + C21; (%) $p < 0.05$ vs DM-I/R + Dize.

3.5. AT2R and ACE2 activation restores the altered systemic and tissue-specific RAS components in non-diabetic and diabetes mellitus rats upon ischemic renal injury

According to our previous results, IRI altered the systemic and tissue-specific RAS components in ND and DM rats. Therefore, next we checked the effect of AT2R and ACE2 activator treatments on the same. All three-treatment regimen increased tubular ACE2 levels in ND-I/R and DM-I/R rats and reduced plasma ACE levels in DM-I/R rats, while only combination therapy reduced plasma ACE level in ND-I/R rats (Fig. 8A and F). None of the treatment regimens could alter the plasma ACE2 and tubular ACE levels in ND-I/R and DM-I/R rats (Fig. 8B and E). In plasma, Ang II and Ang-(1–7) levels remain unchanged after C21 monotherapy, while Ang-(1–7) levels significantly increased after Dize monotherapy in ND-I/R and DM-I/R rats. Interestingly, combination therapy significantly reduced Ang II levels and increased Ang-(1–7) levels in plasma of ND-I/R and DM-I/R rats (Fig. 8C–D). In isolated tubular fraction, all three-treatment regimen significantly reduced Ang II and augmented Ang-(1–7) levels in ND-I/R and DM-I/R rats; except C21 monotherapy did not change tubular Ang II and Ang-(1–7) levels in ND-I/R rats (Fig. 8G–H). One of the consistent features is that combination therapy was better in normalizing the RAS components levels when compared to respective monotherapies.

Next, we checked mRNA expressions of *At1r, At2r* and *Masr* in a tubular fraction using qRT-PCR. ND-I/R and DM-I/R rats exhibited increased mRNA expressions of *At1r, At2r* and *Masr* in a tubular fraction when compared to respective controls. C21 or Dize monotherapy did not change mRNA expressions of *At1r, At2r* and *Masr* in ND-I/R and DM-I/R rats. Interestingly, the combination therapy resulted in a further increase in *At2r* and *Masr* mRNA expressions, with no change in *At1r* mRNA expressions in ND-I/R and DM-I/R rats (Fig. 8I–K). Therefore, our data suggest that the protective effects seen after the combination therapy might relates to the restoration of systemic and tissue-specific RAS components in ND and DM rat upon IRI.

4. Discussion

We hypothesised that the depressor arm of RAS plays a major role in

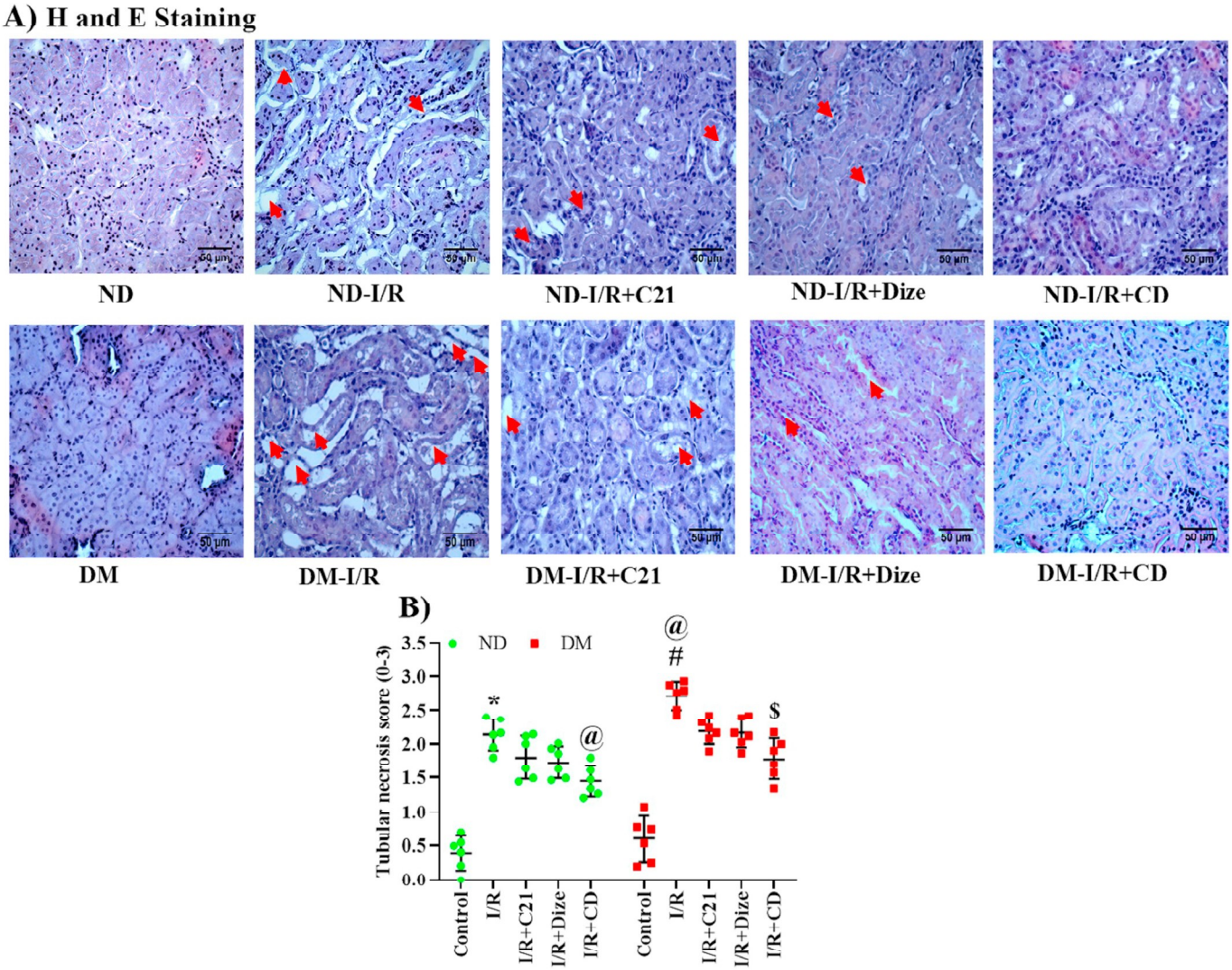

Fig. 7. AT2R agonist and ACE2 activator prevented tubular necrosis associated with IRI.
Representative images for H and E staining of kidney sections (original magnification 400× and scale bar- 50 µm). At least 4–5 images from each stained kidney section and a total of six different kidneys per group were observed by a blinded observer for tubular necrosis (Red arrow) (A). The tubular necrosis was analysed semi-quantitatively and scored from 0 to 3 (B). Data are represented as mean ± SD. One-way ANOVA with Tukey's multiple comparison test was applied for statistical comparison. (*) $p < 0.05$ vs ND; (@) $p < 0.05$ vs ND-I/R; (#) $p < 0.05$ vs DM; ($) $p < 0.05$ vs DM-I/R; (&) $p < 0.05$ vs DM-I/R + C21. (For interpretation of the references to colour in this figure legend, the reader is referred to the web version of this article.)

IRI under both diabetic and non-diabetic conditions. Our result demonstrated augmented AT1R, ACE, and Ang-II expressions, as well as AT2R and reduced ACE2 and Ang-(1–7) expression in proximal renal tubules of DM and ND rats subjected to IRI. Interestingly, administration of AT2R agonist (C21) and ACE2 activator (Dize) per se marginally ameliorated pathological changes associated with IRI including metabolic perturbation, increased renal tubular cells oxidative stress, apoptosis, and inflammation. However, their combination therapy significantly normalized the alterations in RAS components, thereby attenuated above-mentioned pathological consequences associated with IRI in diabetic and non-diabetic rats.

The epidemiologic reports advocated that AKI is more lethal in diabetic patients in comparison to non-diabetic individuals; however, responsible molecular mechanisms are still elusive [5]. In the present study, two weeks after STZ-injection, DM rats were subjected to I/R to induce AKI, we used this experimental animal model to mimic the pathophysiology of comorbid diabetes and AKI in humans (Fig. 1). We observed that IRI increased BUN levels and oxidative stress in DM rats compared to ND rats (Table 1, Fig. 2). Existing literature has speculated that critical pathogenic factors of AKI comprises compromised kidney perfusion and altered the intrarenal hemodynamic balance, which largely attributed to systemic and intrarenal RAS activation [21]. Individually, hyperglycaemia or IRI increased levels of Ang II; an octapeptide and the major effector of RAS pressor arm mediating pathological effects via activation of AT1R [8,22]. Consistent with this, we observed activation of the pressor arm of the RAS demonstrated by increased Ang II, ACE and AT1R expression in a renal proximal tubular fraction from kidneys of diabetic rats that underwent IRI (Figs. 3, 4).

On the other hand, the depressor arm components: AT2R, ACE2, Ang-(1–7) are identified for their positive feedback mechanism by recognising elevated cellular stress and activated pathological signalling [9,10]. Male Wistar rats subjected to left nephrectomy and 45 min ischaemia on right kidney demonstrated reduced renal ACE2 mRNA expression and Ang-(1–7) levels at 4 h reperfusion [10]. In subtotal nephrectomised rats, Dize (ACE2 activator) augmented cortical and medullary ACE2 activity and abridged cortical ACE activity [23]. Recently, we have reported that Dize monotherapy (5 mg/kg/day) marginally attenuated diabetic renal fibrosis, whereas Dize in combination with a neprilysin inhibitor thiorphan significantly attenuated the development of diabetic nephropathy [24]. Further, C21 has

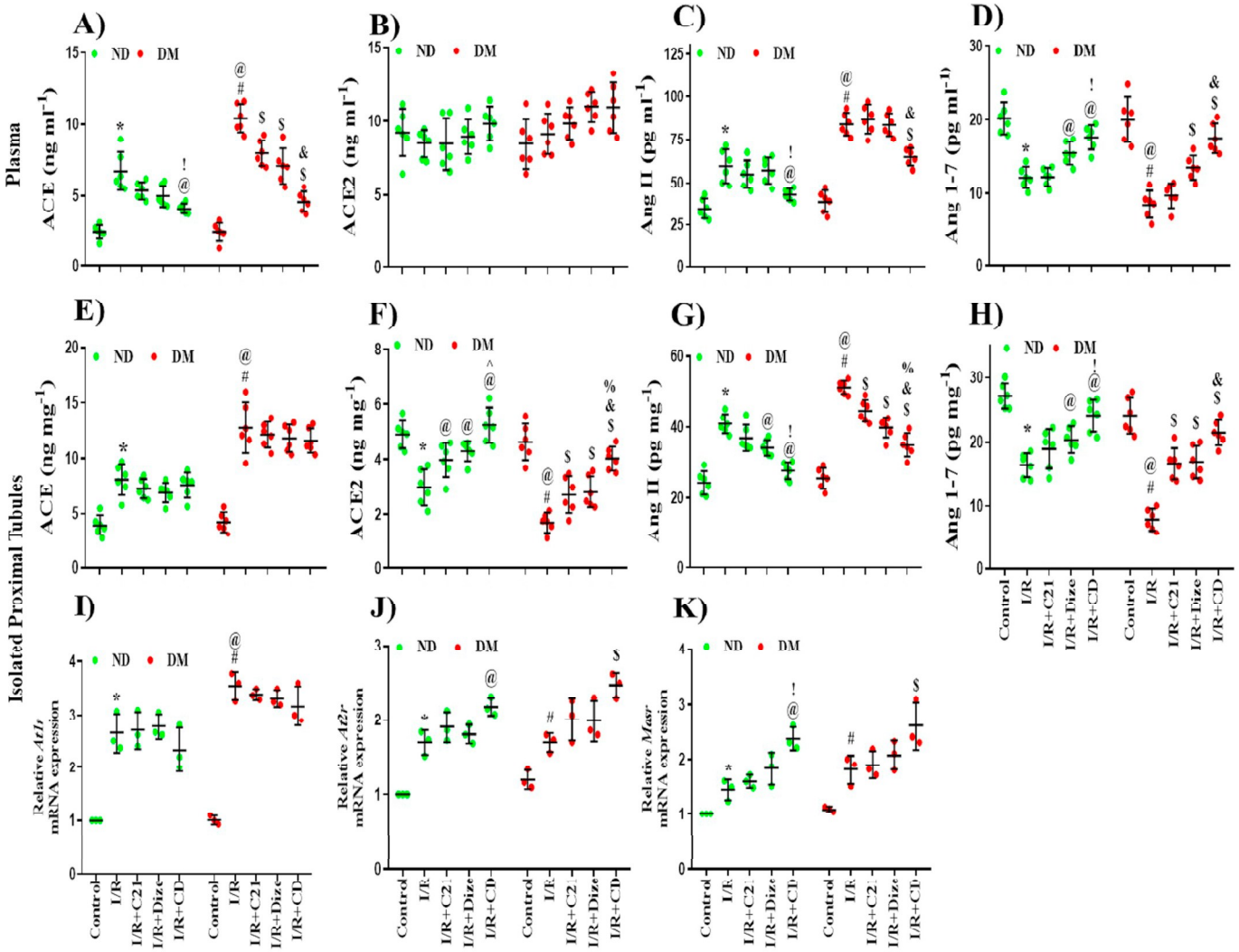

Fig. 8. Effect of C21, Dize and their combination therapy on protein and mRNA expressions of RAS components.
A-H: Protein expression of ACE, ACE2, Ang II and Ang-(1–7) in plasma (A-D) and isolated proximal tubules (D-J) was measured by ELISA (n = 6). I-K: mRNA expressions of *At1r*, *At2r* and *Masr* was assessed by qRT-PCR in isolated proximal tubules. 18s rRNA expression was used as internal control. Data are represented as mean ± SD from three independent experiments. One-way ANOVA with Tukey's multiple comparison test was applied for statistical comparison. (*) $p < 0.05$ vs ND; (@) $p < 0.05$ vs ND-I/R; (!) $p < 0.05$ vs ND-I/R + C21; (#) $p < 0.05$ vs DM; ($) $p < 0.05$ vs DM-I/R; (&) $p < 0.05$ vs DM-I/R + C21; (%) $p < 0.05$ vs DM-I/R + Dize.

demonstrated to halt the development of diabetic nephropathy in mice and rats [25,26]. Recently, we reported that C21 monotherapy at dose 0.3 mg/kg/day has partially improved renal functions, while C21 with Telmisartan combination has markedly mitigated diabetic nephropathy by attenuating apoptotic signalling [17].

In the present study, we observed reduced tubular ACE2 and Ang-(1–7) expressions and a compensatory increase in AT2R expression in DM-I/R rats when compared to DM and ND-I/R rats. Hence, we speculated that modulating RAS depressor arm by ACE2 activator or AT2R agonist might protect the kidney against IRI. On the basis of abovementioned reports, we treated ND-I/R and DM-I/R rats with AT2R agonist, C21 (0.3 mg/kg/day, *i.p.*) or ACE2 activator, Dize (5 mg/kg/day, *p.o.*) for five days. Our data suggest that the monotherapy using either AT2R agonist or ACE2 activator in ND-I/R and DM-I/R rats had only minor effect on tubular damage as evident from oxidative stress parameters and histopathological evaluations. Hence, we plan to administer AT2R agonist and ACE2 activator together as a combination therapy at same dose regimen in ND-I/R and DM-I/R rats. We found that concomitant AT2R agonism and ACE2 activation significantly attenuated oxidative stress associated with IRI in ND and DM rats (Fig. 5). Further, IRI has been reported to activate antioxidant transcription factor Nrf2 [27]. In this regard, we observed increased Nrf2 expression in renal tubular fraction of ND-I/R and DM-I/R rats. Interestingly, C21 and Dize combination therapy to ND-I/R and DM-I/R rats further amplified proximal tubular Nrf2 expression (Fig. 5). Interestingly, simultaneous AT2R agonist and ACE2 activator administration have attenuated proinflammatory cytokines *Il6, Tnfa* and *Mcp1* mRNA expressions and preventing NF-κB signalling-mediated inflammation, MCP-1-mediated leukocyte infiltration, and c-Cas-3 and cPARP-mediated apoptosis in the proximal tubular fraction of ND-I/R and DM-I/R rats (Figs. 5 and 6). Previous studies showed that C21 in combination with telmisartan or losartan alleviated glomerular damage, extracellular matrix accumulation, and increased glomerular nephrin expression in type 2 diabetic rats [17,28]. Similarly, we observed that C21, AT2R agonist along with Dize, ACE2 activator was better in mitigating morphological alterations (tubular necrosis) when compared to monotherapies (Fig. 7). Moreover, ELISA results revealed the superiority of C21 and Dize combination therapy over respective monotherapies in normalizing systemic (plasma) and local (proximal tubules) alteration in RAS components level [e.g. ACE, ACE2, Ang II and Ang-

(1–7)] associated with IRI in ND and DM rats (Fig. 8). The combination therapy further augmented mRNA expressions of renoprotective AT2R and MasR in IRI subjected ND and DM rats (Fig. 8). In brief, these results provide us with articulate evidence that AT2R and ACE2 are involved in the pathogenesis of ischemic AKI. In this study, elevated inflammatory, apoptotic and other pathogenic signalling can be correlated with dysregulated RAS depressor arm (reduced Ang-(1–7) and ACE2 levels) and severity of ischemic AKI. For the first time, we stated that the novel combination of AT2R agonist and ACE2 activator has significantly attenuated the IRI related kidney impairments in DM and ND rats.

5. Conclusion

To the best of our knowledge, this is the first report to revealed that suppression of the depressor arm of RAS precipitates ischemic AKI in ND and DM rats. However, the severity of ischemic AKI was found to be extensive in DM rats, which could be due to the presence of hyperglycaemia. The novel combination therapy of AT2R agonist and ACE2 activator targeting protective axis of RAS, significantly assuaged systemic and renal RAS alterations and prevented renal tubular damage associated with IRI in ND and DM rats. Thus, we suggested that targeting RAS depressor arm might serve as a novel therapeutic option against AKI in diabetic and non-diabetic conditions.

Supplementary data to this article can be found online at https://doi.org/10.1016/j.lfs.2019.116796.

Author contributions

A.B.G. and S.R.M conceived the idea and designed the experiments. N.S. and V.M. performed all the experiments and data analysis. All the authors were actively involved in manuscript writing.

Funding

This research was supported by the Science & Engineering Research Board -Department of Science & Technology (SERB-DST), Govt. of India [SERB/ECR/2017/000317].

Declaration of competing interest

The authors declare no potential conflicts of interest.

Acknowledgements

S.R.M. acknowledges the Department of Biotechnology (DBT), Govt. of India for supporting him [BT/RLF/*Re*-entry/01/2017]. N.S. sincerely acknowledges the Indian Council of Medical Research (ICMR) for senior research fellowship [45/54/2019/PHA/BMS]. The authors thank Anders Ljunggren, Vicore Pharma, Sweden, for his suggestions and for offering the drug sample, Compound 21.

References

[1] E.A. Hoste, et al., Global epidemiology and outcomes of acute kidney injury, Nat Rev Nephrol 14 (2018) 607–625, https://doi.org/10.1038/s41581-018-0052-0.
[2] S.A. Silver, et al., Causes of death after a hospitalization with AKI, J. Am. Soc. Nephrol. 29 (3) (2018) 1001–1010, https://doi.org/10.1681/ASN.2017080882.
[3] S.M.-W. Yu, J.V. Bonventre, Acute kidney injury and progression of diabetic kidney disease, Adv. Chronic Kidney Dis. 25 (2) (2018) 166–180, https://doi.org/10.1053/j.ackd.2017.12.005.
[4] Y. Takiyama, M. Haneda, Hypoxia in diabetic kidneys, Biomed. Res. Int. 2014 (2014) 1–10, https://doi.org/10.1155/2014/837421.
[5] C.V. Thakar, et al., Acute kidney injury episodes and chronic kidney disease risk in diabetes mellitus, Clin. J. Am. Soc. Nephrol. (2011), https://doi.org/10.2215/CJN.01120211.
[6] P. Newsholme, et al., Molecular mechanisms of ROS production and oxidative stress in diabetes, Biochem. J. 473 (24) (2016) 4527–4550, https://doi.org/10.1042/BCJ20160503C.
[7] L. Gnudi, R.J. Coward, D.A. Long, Diabetic nephropathy: perspective on novel molecular mechanisms, Trends Endocrinol. Metab. 27 (11) (2016) 820–830, https://doi.org/10.1016/j.tem.2016.07.002.
[8] N. Sharma, H.J. Anders, A.B. Gaikwad, Fiend and friend in the renin angiotensin system: an insight on acute kidney injury, Biomed. Pharmacother. 110 (2019) 764–774, https://doi.org/10.1016/j.biopha.2018.12.018.
[9] S.K. Goru, et al., Diminazene aceturate prevents nephropathy by increasing glomerular ACE2 and AT2 receptor expression in a rat model of type1 diabetes, Br. J. Pharmacol. 174 (18) (2017) 3118–3130, https://doi.org/10.1111/bph.13946.
[10] K.D. Da Silveira, et al., ACE2–angiotensin-(1–7)–mas axis in renal ischaemia/reperfusion injury in rats, Clin. Sci. 119 (9) (2010) 385–394, https://doi.org/10.1042/CS20090554.
[11] X.H. Yang, et al., Role of angiotensin-converting enzyme (ACE and ACE2) imbalance on tourniquet-induced remote kidney injury in a mouse hindlimb ischemia-reperfusion model, Peptides 36 (1) (2012) 60–70, https://doi.org/10.1016/j.peptides.2012.04.024.
[12] A. Gupta, et al., Activated protein C ameliorates LPS-induced acute kidney injury and downregulates renal INOS and angiotensin 2, Am J Physiol Renal Physiol 293 (1) (2007) F245–F254, https://doi.org/10.1152/ajprenal.00477.2006.
[13] M. Ruiz-Ortega, et al., Renal expression of angiotensin type 2 (AT2) receptors during kidney damage, Kidney Int. 64 (2003) S21–S26, https://doi.org/10.1046/j.1523-1755.64.s86.5.x.
[14] C. Kilkenny, et al., Improving bioscience research reporting: the ARRIVE guidelines for reporting animal research, PLoS Biol. 8 (6) (2010) e1000412, , https://doi.org/10.1371/journal.pbio.1000412.
[15] V. Malek, A.B. Gaikwad, Telmisartan and thiorphan combination treatment attenuates fibrosis and apoptosis in preventing diabetic cardiomyopathy, Cardiovasc. Res. 115 (2) (2018) 373–384, https://doi.org/10.1093/cvr/cvy226.
[16] N. Le Clef, et al., Unilateral renal ischemia-reperfusion as a robust model for acute to chronic kidney injury in mice, PLoS One 11 (3) (2016) e0152153, , https://doi.org/10.1371/journal.pone.0152153.
[17] A. Pandey, A.B. Gaikwad, Compound 21 and Telmisartan combination mitigates type 2 diabetic nephropathy through amelioration of caspase mediated apoptosis, Biochem. Biophys. Res. Commun. 487 (4) (2017) 827–833, https://doi.org/10.1016/j.bbrc.2017.04.134.
[18] A.C. Hakam, A.H. Siddiqui, T. Hussain, Renal angiotensin II AT2 receptors promote natriuresis in streptozotocin-induced diabetic rats, Am J Physiol Renal Physiol 290 (2) (2006) F503–F508, https://doi.org/10.1152/ajprenal.00092.2005.
[19] L. Danelli, et al., Early phase mast cell activation determines the chronic outcome of renal ischemia–reperfusion injury, J. Immunol. 198 (6) (2017) 2374–2382, https://doi.org/10.4049/jimmunol.1601282.
[20] H. Rabb, et al., Inflammation in AKI: current understanding, key questions, and knowledge gaps, J. Am. Soc. Nephrol. 27 (2) (2016) 371–379, https://doi.org/10.1681/ASN.2015030261.
[21] M. Matejovic, et al., Renal hemodynamics in AKI: in search of new treatment targets, J. Am. Soc. Nephrol. 27 (1) (2016) 49–58, https://doi.org/10.1681/ASN.2015030234.
[22] V. Malek, A.B. Gaikwad, Neprilysin inhibitors: a new hope to halt the diabetic cardiovascular and renal complications? Biomed. Pharmacother. 90 (2017) 752–759, https://doi.org/10.1016/j.biopha.2017.04.024.
[23] E. Velkoska, et al., Short-term treatment with Diminazene Aceturate ameliorates the reduction in kidney ACE2 activity in rats with subtotal nephrectomy, PLoS One 10 (3) (2015) e0118758, , https://doi.org/10.1371/journal.pone.0118758.
[24] V. Malek, et al., Concurrent neprilysin inhibition and renin-angiotensin system modulations prevented diabetic nephropathy, Life Sci. 221 (2019) 159–167, https://doi.org/10.1016/j.lfs.2019.02.027.
[25] C. Koulis, et al., AT2R agonist, compound 21, is Reno-protective against type 1 diabetic nephropathy, Hypertension 65 (5) (2015) 1073–1081, https://doi.org/10.1161/HYPERTENSIONAHA.115.05204.
[26] M. Malek, M. Nematbakhsh, The preventive effects of diminazene aceturate in renal ischemia/reperfusion injury in male and female rats, Adv. Prev. Med. 2014 (2014) 1–9, https://doi.org/10.1155/2014/740647.
[27] M.O. Leonard, et al., Reoxygenation-specific activation of the antioxidant transcription factor Nrf2 mediates cytoprotective gene expression in ischemia-reperfusion injury, FASEB J. 20 (14) (2006) 2624–2626, https://doi.org/10.1096/fj.06-5097fje.
[28] G. Castoldi, et al., Prevention of diabetic nephropathy by compound 21, selective agonist of the angiotensin type 2 receptors, in Zucker diabetic fatty rats, Am J Physiol Renal Physiol 307 (10) (2014) F1123–F1131, https://doi.org/10.1152/ajprenal.00247.2014.

Biochemical and Biophysical Research Communications 528 (2020) 14–20

Contents lists available at ScienceDirect

Biochemical and Biophysical Research Communications

journal homepage: www.elsevier.com/locate/ybbrc

Role of SET7/9 in the progression of ischemic renal injury in diabetic and non-diabetic rats

Nisha Sharma, Himanshu Sankrityayan, Ajinath Kale, Anil Bhanudas Gaikwad*

Laboratory of Molecular Pharmacology, Department of Pharmacy, Birla Institute of Technology and Science Pilani, Pilani Campus, Rajasthan, 333031, India

ARTICLE INFO

Article history:
Received 28 April 2020
Accepted 11 May 2020
Available online 22 May 2020

Keywords:
Ischemia renal injury
Diabetes
Histone methylation
Cyproheptadine
Kidney

ABSTRACT

SET domain with lysine methyltransferase 7/9 (Set7/9), a histone lysine methyltransferase (HMT), recently suggested to exert a critical role among kidney disorders, whereas its role in diabetes associated IRI co-morbidity remains complete elusive. The present study aimed to understand the role of SET7/9 and histone methylation in regulation of inflammatory signaling under IRI in diabetes mellitus and non-diabetic rats. Our results demonstrated that IRI caused renal dysfunction via increased blood urea nitrogen (BUN) levels in ND and DM rats. The NF-κB mediated inflammatory cascade like increased p-NF-κB, reduced IκBα levels followed by enhanced leukocyte infiltration as shown by increased MCP-1 expressions. IRI results in increased histone H3 methylation at lysine 4 and 36 (H3K4Me2, H3K36Me2), and decreased histone H3 methylation at lysine 9. Additionally, IRI increased the protein and mRNA expression of H3K4Me2 specific histone methyltransferase-SET7/9 in DM and ND rats. The above-mentioned results remain prominent in DM rats compared to ND rats followed by IRI. Further, treatment with a novel SET7/9 inhibitor; cyproheptadine, significantly improved renal functioning via reducing the BUN levels in ND and DM rats. Hence, this study demonstrated the role of SET7/9 in mediating active transcription via H3K4Me2, ultimately regulated the NFκB-mediated inflammatory cascade. Therefore, SET7/9 can be explored as novel target for drug development against IRI under DM and ND conditions.

1. Introduction

Acute kidney injury (AKI) is a serious clinical condition which imparts with high morbidity and mortality rates [1,2]. Ischemic renal injury (IRI) is the most common cause of AKI [3]. A growing body of experimental and clinical evidences has reported that the diabetic kidney has increased susceptibility towards ischemic insults [4–7]. Diabetes associated AKI co-morbidity results in adverse renal outcomes like free radical stress, disturbed hemodynamics triggered inflammatory and apoptotic signaling [8]. AKI is often associated with elevated proinflammatory cytokines and chemokines which leads to infiltration of leukocytes [9,10]. In AKI, inflammation is triggered by molecular signals delivered by apoptotic cells, activated pattern recognition receptors, diversified recruitment of immune cells [10]. However, the molecular mechanisms by which diabetes upsurges the jeopardy of IRI are unclear. As aforementioned, genetic proclivity alone is inadequate to explain the complex pathogenesis of IRI and the rationale to explore the epigenetic modifications came into the picture. Among posttranslational histone modifications (PTHMs), the role of histone lysine methylation (H3KMe), mediated in the regulation of pathogenic gene transcription in diabetic kidney diseases has been studied extensively [11].

SET domain containing lysine methyltransferase 7/9 (SET7/9), a histone methyltransferase (HMT) mediates active transcription through H3K4Me [12]. In diabetic nephropathy, increased H3K4me and SET7/9 leads to increased recruitment of MCP-1 and ECM-associated gene promoters in diabetic renal fibrosis [11,13–15]. In IRI, increased TGF-β levels result in upregulation of H3K4Me and its specific HMT-SET7/9, which was successfully suppressed by Apelin treatment and further protect kidney from ischemic insult [16]. SET7/9 also attain a crucial role in inflammation and diabetes, as evidenced by augmented NF-κB associated inflammatory gene expressions and SET7/9 recruitment in macrophages of diabetic mice. TNF-α-induced recruitment of NF-κB p65 on inflammatory gene promoters was effectively reduced by targeted silencing of SET7/9 with siRNA [17].

Cyproheptadine, a clinically approved antiallergy drug, has been

* Corresponding author. Department of Pharmacy, Birla Institute of Technology and Science, Pilani, Pilani Campus, Pilani, 333 031, Rajasthan, India.
E-mail address: anil.gaikwad@pilani.bits-pilani.ac.in (A.B. Gaikwad).

https://doi.org/10.1016/j.bbrc.2020.05.075
0006-291X/

recently identified as a novel SET7/9 inhibitor [18]. Hang et al. has suggested that cyproheptadine exerts anti-nociceptive effect in cancer-induced bone pain via inhibiting SET7/9 and RANTES cytokine expressions [19]. SET7/9 is crucial for the estrogen-dependent transactivation of Estrogen Receptor (ER) target genes. Thus, Takimoto et al. has demonstrated that cyproheptadine effectively reduced estrogen receptor-α expression and transcriptional activity, and suppressing estrogen-dependent cell growth, ultimately helpful against breast cancer. However, the role of SET7/9 in regulation of inflammation under diabetes-AKI comorbidity is highly unclear. Hence, the current study aims to check the effect of HMT-SET7/9 and its inhibitor-cyproheptadine on NF-κB mediated inflammation, and histone H3 methylation against AKI in diabetic mellitus (DM) and non-diabetic (ND) rats.

2. Materials and methods

2.1. Materials

Cyproheptadine was obtained from Tocris Bioscience (Bristol, UK). Glucose, Blood urea nitrogen (BUN), creatinine kit was purchased from Accurex (Mumbai, India). Monocytes chemoattractant protein (MCP-1) primary antibody was purchased from Santa Cruz Biotechnology (Dallas, TX, USA), and rest of the primary and secondary antibodies were purchased from Cell Signaling Technology (Danvers, MA, USA). All the other chemicals were procured from Sigma Aldrich (St. Louis, MO, USA), unless otherwise mentioned.

2.2. Development of type 1 diabetic rat model

The male adult Wistar rats (200–220 g) were procured from the Central Animal Facility (CAF) of Birla Institute of Technology and Science Pilani (BITS-Pilani) in accordance with the protocol approved by the Institutional Animal Ethics Committee (IAEC), BITS-Pilani ((Protocol Approval No: IAEC/RES/21/08). Animals were maintained under standard environmental conditions with feed and water *ad lib*. Animal studies are reported ensuing the ARRIVE guidelines [20]. For Type 1 diabetes induction, male Wistar rats were injected with single dose of STZ [55 mg/kg, *i.p.*, vehicle-sodium citrate buffer (0.01 M, pH 4.4] [21]. Age-matched ND rats received only sodium citrate buffer. After 48 h of STZ injection, rats with plasma glucose levels >16 mmol/L were included in the study as DM rats.

2.3. Ischemic renal injury protocol

IRI was performed as per the protocol described previously [4]. Briefly, rats were anesthetized with pentobarbital sodium (50 mg/kg, *i.p.*), a half-inch incision was performed on the left flank portion of abdomen. Then, left renal pedicle was identified and occluded with a surgical clamp to induce ischemia [22]. After 45 min, the clamp was released, skeletal muscle and skin layers of abdominal incision were sutured discretely with absorbable and non-absorbable sutures, respectively. Sham control animals underwent identical operation without left renal pedicle clamping. After 48 h of reperfusion; the rats were re-anaesthetised with pentobarbital sodium (50 mg/kg, *i.p.*) and blood samples were collected from vena cava with a 5 mL syringe intended for plasma biochemistry. Kidneys were then removed, cleaned and blotted dry, and kept in −80 °C. The left kidney was utilised for further experiments.

2.4. Drug treatment

The ND and DM rats were divided into four groups each: (a) **ND/DM-**serve as respective controls, (b) **ND-/DM-IRI-** ND or DM rats subjected to unilateral ischemia (IRI) after completion of two weeks of diabetes induction, (c) **ND-/DM-IRI + Cp-LD-** ND- IRI or DM- IRI rats receiving cyproheptadine low dose (10 mg/kg/day, *i.p.*), (d) **ND-/DM-IRI + Cp-HD-** ND- IRI or DM- IRI rats receiving cyproheptadine high dose (20 mg/kg/day, *i.p.*) [18,23]. The treatment was given 30 min prior to IRI and after 24 h of reperfusion.

2.5. Proximal tubules isolation from the whole kidney

Isolation of proximal tubular fraction from whole kidney was done using percoll gradient centrifugation method as described earlier [4].

2.6. Immunoblotting

Protein isolation and immunoblotting were performed as previously described protocols [4,21].

2.7. Quantitative real-time polymerase chain reaction

RNA was isolated from proximal tubules by using commercially available kit and qRT-PCR was performed using specific primers which were designed and produced by Eurofins, India (Table 1) [11], as per described protocol.

2.8. Statistical analysis

Experimental values are represented as mean ± SD, and 'n' refers to the number of studied samples. Statistical comparison between groups was performed using one-way analysis of variance (ANOVA) pursued by Tukey's Multiple Comparison *post hoc* test or two-way ANOVA pursued by Tukey's Multiple Comparison *post hoc* test, using GraphPad Prism software version 8.0.2 (San Diego, CA, USA. Data showing $p < 0.05$, was measured statistically significant.

3. Results

3.1. Alteration in the renal functional parameters of diabetic and non-diabetic ischemic rats

STZ administration in rats result in the development of type 1 diabetes. We found that plasma glucose level of DM and DM-I/R rats remain significantly higher compared to ND and ND-I/R rats (Fig. 1 A). BUN levels were found to be elevated in ND-IRI and DM-IRI rats as compared to their respective controls. However, DM-IRI rats showed significant elevation in BUN levels than ND-IRI rats (Fig. 1 B). PCr levels were found to be elevated in DM-IRI rats, but not significantly increased compared to ND-IRI rats (Fig. 1 C).

Table 1
List of primers used for qRT-PCR.

Gene Name	Primer sequences of qRT-PCR
Nfkb p65	Forward:5′-CATCACACGGAGGGCTTC-3 Reverse:5′-GAACGATAACCTTTGCAGGC-3′
Tnfa	Forward:5′-GATCGGTCCCAACAAGGAGG-3′ Reverse:5′-CTTGGTGGTTTGCTACGACG-3′
Mcp1	Forward 5′- GTCTCAGCCAGATGCAGTTA-3′ Reverse 5′- CCTTATTGGGGTCAGCACAG-3′
Set7/9	Forward 5′-AGGTTGACAGCAGGGATT-3′ Reverse 5′-CAGTTCGGAGAAGGGAGT-3′

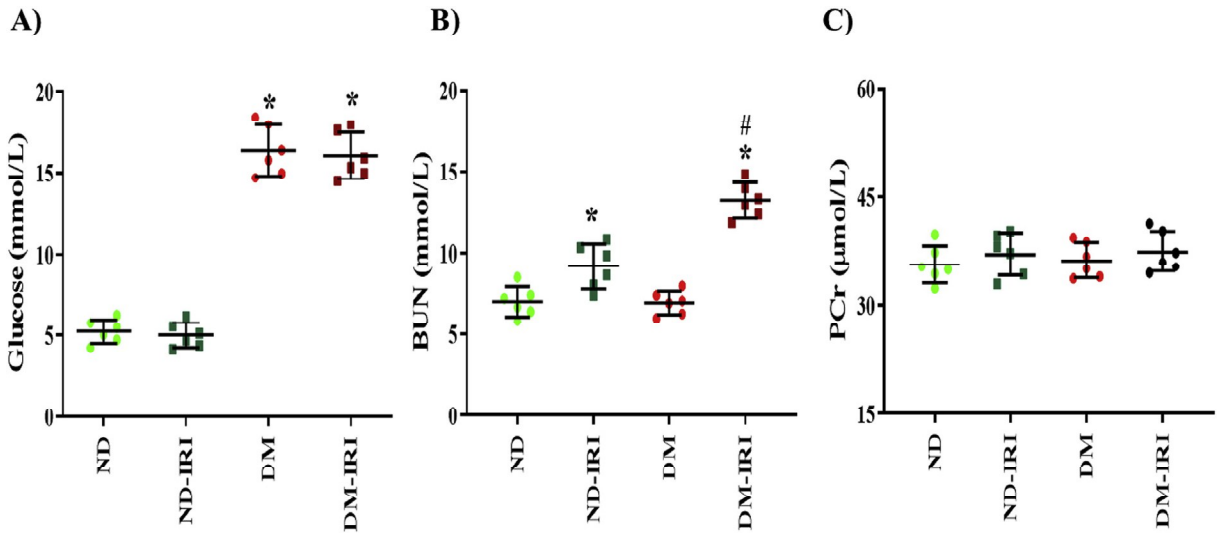

Fig. 1. Plasma Biochemistry.
A-C: Representative scattered plots of plasma glucose (PGl) (A), blood urea nitrogen (BUN) (B), creatinine (PCr) (C). Data are represented as mean ± SD (n – 6). For statistical comparison, one-way ANOVA with Tukey's multiple comparison test was used where (*) $p < 0.05$ vs ND; (#) $p < 0.05$ vs DM; (@) $p < 0.05$ vs ND-IRI.

3.2. Hyperglycemia increases inflammatory cascade following ischemic renal injury

Under the pathogenesis of AKI, the plethora of inflammatory response has been elucidated as the primary mechanism of IRI [10]. In the present study, isolated proximal tubules from DM and ND ischemic kidneys showed active NF-κB signaling demonstrated by elevated protein expression of p-NF-κB (S536) and decreased IκBα expression (negative regulator of NF-κB), when compared to their respective controls (Fig. 2A–C). In comparison to ND-IRI rats, DM-IRI rats showed significant higher and diminished expressions of p-NF-κB (S536) and IκBα, respectively. In addition, we also observed markedly increased mRNA levels of *Nfkb p65* in DM-IRI rats in comparison to ND-IRI rats (Fig. 2E). Further, we have checked the protein (MCP-1) expression of down-stream inflammatory signaling molecules in ND and DM group of rats. We have found marked elevation in MCP-1 protein expression in DM-IRI and ND-IRI rats as compared to DM and ND rats (Fig. 2A, D). Although, DM-IRI rats showed marked upregulation of MCP-1 protein expression than ND-IRI rats (Fig. 2A, D). We checked the mRNA expressions of *Mcp1* and *Tnfa*, we found that DM-IRI and ND-IRI rats showed elevated mRNA expressions of *Mcp1* and *Tnfa* as compared to DM and ND rats, respectively (Fig. 2F and G). Whereas DM-IRI rats showed significant elevation in *Mcp1* and *Tnfa* mRNA expressions compared to ND-IRI rats. Therefore, in comparison to ND rats, DM rats are more susceptible towards inflammatory response under IRI.

3.3. Hyperglycemia altered histone H3 dimethylation in isolated proximal tubules of ischemic kidney

Epigenetic machinery exerts a substantial role in the pathogenesis of AKI [24]. In the present study, we have checked the expression of histone H3K4Me2, H3K9Me2 and H3K36Me2 in the isolated proximal tubules. We found that permissive histone methylation marks i.e. histone H3K4Me2 and H3K36Me2 were significantly elevated in isolated proximal tubules of DM-IRI and ND-IRI rats compared to respective controls (Fig. 3 A, B, D). However, diabetic rats underwent IRI showed marked elevation of histone H3K4Me2 and H3K36Me2 expressions compared to non-diabetic rats underwent IRI (Fig. 3 A, B, D). Further, H3K9Me2 expression (repressive histone methylation mark) were observed to be decreased in ischemic DM and ND rats. Even though, DM-IRI rats showed profound alterations in histone di-methylation at H3K9 as compared to ischemic ND-IRI rats (Fig. 3 A, C).

3.4. Hyperglycemia upregulates the protein and mRNA expression of H3K4 specific histone methyltransferase-SET7/9 in ischemic renal injury

Histone methyltransferases (HMTs) play crucial role in chromatin remodeling and gene expression [24]. In our study, we found that protein and mRNA expression of H3K4Me2-specific methyltransferase, SET7/9 was highly upregulated after ischemic insult in DM and ND rats (Fig. 3A, E-F). Interestingly, DM-IRI rats showed significant elevated protein and mRNA expressions of SET7/9 as compared to ND-IRI rats (Fig. 3A, E-F).

3.5. Cyproheptadine shows improvement in renal biochemistry in diabetic and non-diabetic rats upon ischemic renal injury

In this study, cyproheptadine treatment was administered using low (10 mg/kg/day, *i.p.*) and high (20 mg/kg/day, *i.p.*) doses in DM-IRI and ND-IRI rats. None of the therapy has any effect on plasma glucose of DM-IRI compared to DM rats (Fig. 4A). Furthermore, in ND group, we found that elevated BUN levels were significantly attenuated by high dose of cyproheptadine (ND-IRI + Cp-HD) compared to low dose of cyproheptadine (ND-IRI + Cp-LD) and ND-IRI rats (Fig. 4B). In DM group, high dose of cyproheptadine has markedly reduced the BUN levels compared to DM-IRI rats (Fig. 4B). Among Cp-HD groups, DM-IRI rats showed lesser recovery as compared to ND rats (10.85 ± 2.36 vs. 7.158 ± 1.53).

4. Discussion

Despite different molecular and epigenetic mechanisms participated in the development of IRI are well demonstrated, the current remediation is scarce to prevent IRI. Therefore, it is a desideratum to focus on novel mechanisms which take part in the development of IRI. Therefore, we focused on histone methylation, H3K4-Specific

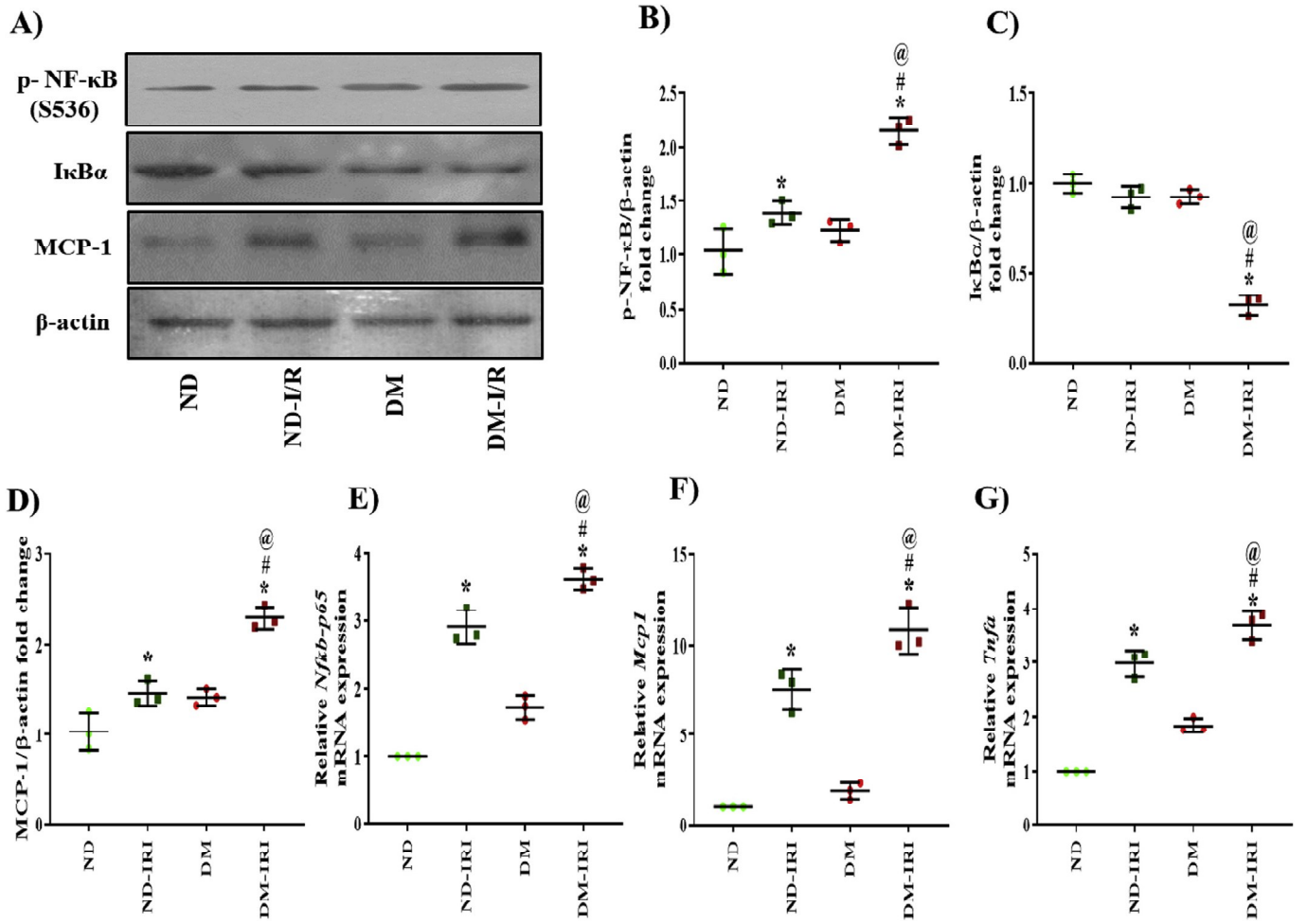

Fig. 2. Effect of hyperglycemia on protein and mRNA expressions of inflammatory markers following ischemic renal injury.
A-D: Immunoblots for protein expressions of inflammatory markers in the isolated renal proximal tubular fraction with β-actin as a loading control (A). Immunoblots were quantified by densitometry analysis e.g. p-NF-κB(S-536) (B), IKBα (C), MCP-1 (D). E-G: mRNA expression of *NF-κB, Mcp1 and Tnfa* was assessed by qRT-PCR in isolated proximal tubules. 18s rRNA expression was used as internal control. Data are represented as mean ± SD from three independent experiments. For statistical comparison, one-way ANOVA with Tukey's multiple comparison test was used where (*) $p < 0.05$ vs ND; (#) $p < 0.05$ vs DM; (@) $p < 0.05$ vs ND-IRI.

HMT i.e. SET7/9, involved the development of IRI under DM and ND rats. We found increased BUN levels which confirmed the renal functional impairment in IRI (Fig. 1). In our study, we also observed the increased inflammatory NF-κB signaling and enhanced leukocyte infiltration (Fig. 2) in ischemic ND and DM rats. Moreover, we also observed the augmented mRNA expressions of critical inflammatory mediators such as *Nf-κb, Mcp1* as well as *Tnfa* in ischemic ND and DM rats (Fig. 2). These results are more pronounced in DM-IRI rats compared to ND-IRI rats. During IRI, cytokines and other pathological mediators remain strong intermediaries of NF-κB. Particularly, ischemic insult persuades the generation of TNF-α in NF-κB-dependent manner, which in turns binds to TNF-α receptor to stimulate NF-κB activation. This induced a positive feedback mechanism of NF-κB regulation [25,26]. Thus, this signaling cascade has a major contribution in the pathogenesis of IRI [10,25]. Inflammation is also characterized by the recruitment of leukocytes, which is shown by the increased expressions of MCP-1 [27]. Apart from it, the presence of hyperglycemia also triggers the inflammatory loop and progress the kidney damage [28]. Therefore, in our study, we can correlate that the increased protein and mRNA expressions of NF-κB under the presence of hyperglycemia, could be involved in the renal ischemic damage by increasing cytokines and leukocyte infiltration (Fig. 2).

Furthermore, to check the inflammation and histone methylation crosstalk, we examined H3K4Me2, H3K9Me2 and H3K36Me2 in proximal tubules of DM-IRI and ND-IRI rats. Increasing evidence shows that histone H3 methylation is involved in the pathogenesis of kidney diseases likes diabetic kidney disease and ischemic renal damage. H3K4Me2 and H3K36Me2 are correlated with gene activation, while H3K9Me2 can be associated with gene silencing and transcriptional repression [29].

In diabetic kidney diseases, H3K4Me2 showed increased enrichment at p65, TNF-α and col1a1 gene [11,30]. H3K36Me2 showed higher levels at MCO-1 loci analyzed in the glomeruli from db/dbH2O mice compared with db/+H2O mice [31]. Isolated Glomeruli from diabetic nephropathy rats depicted the higher levels of H3K9Me2 at col1a1 gene in Refs. [11]. In addition, VSMCs derived from diabetic db/db mice, showed decreased occupancy of H3K9Me2 at inflammatory gene promoters [32]. These facts advocate that the enhancement of H3K4Me and suppressed repressive H3K9Me mark can upregulate the expression of pathological genes under diabetic kidney disorders. In our study, H3K4Me2 and H3K36Me2 expression were found to be increased in isolated proximal tubules, where H3K9Me2 expression was reduced in proximal tubules of diabetic and non-diabetic animals (Fig. 3). However, the abovementioned results were highly

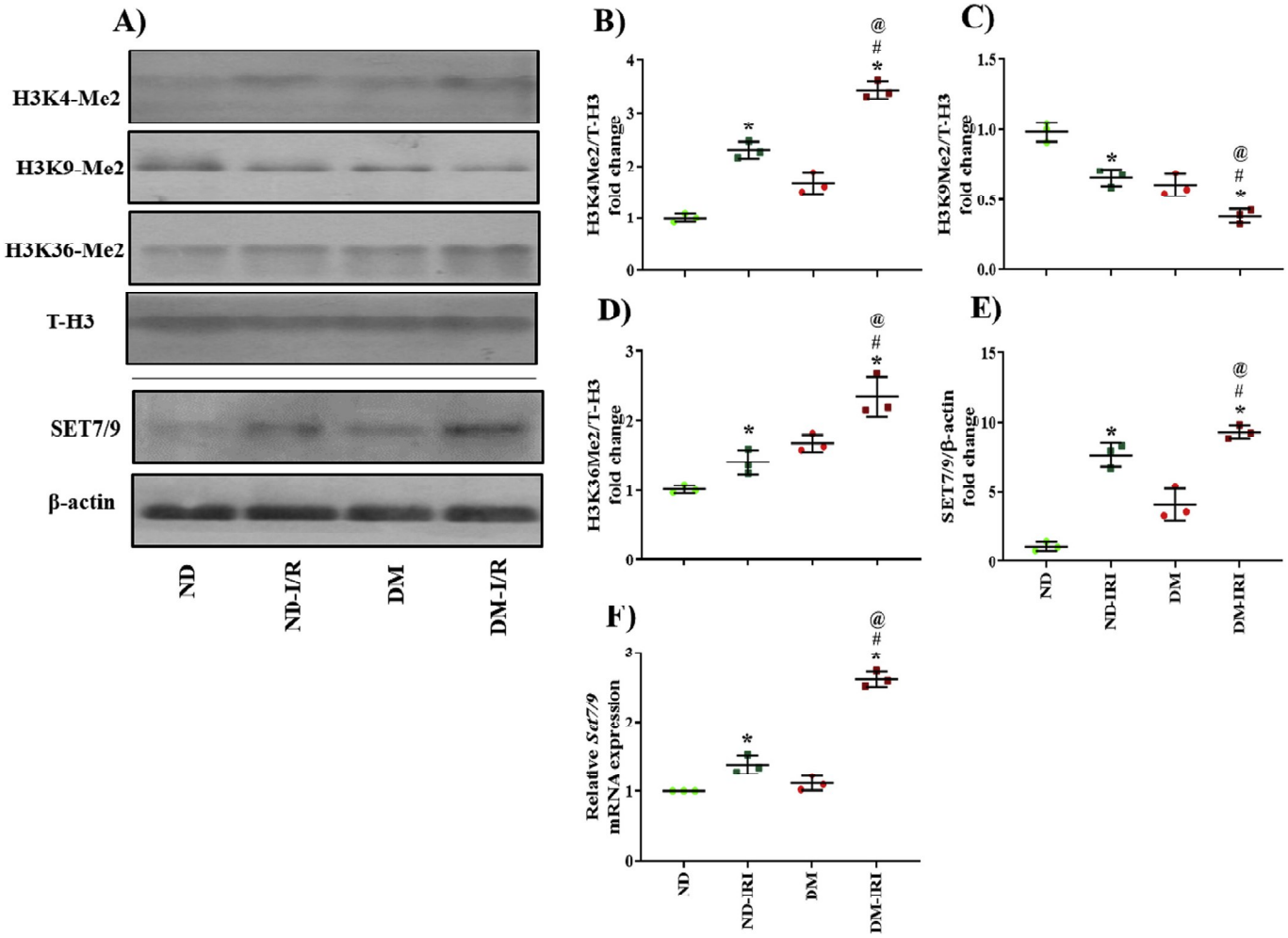

Fig. 3. Expression of H3K4Me2, H3K36Me2, H3K9Me2 and SET7/9 in isolated proximal tubules of ischemic kidney obtained from diabetic and non-diabetic rats.
A-E: Western blot analysis of H3K4Me2, H3K9Me2, H3K36Me2 and SET7/9. (B, C, D, E) Quantitative analysis of H3K4Me2, H3K9Me2, H3K36Me2 and SET7/9. F: mRNA expression of *Set7/9*. was assessed by qRT-PCR in isolated proximal tubules. 18s rRNA expression was used as internal control. Data are represented as mean ± SD from three independent experiments. For statistical comparison, one-way ANOVA with Tukey's multiple comparison test was used where (*) $p < 0.05$ vs ND; (#) $p < 0.05$ vs DM; (@) $p < 0.05$ vs ND-IRI.

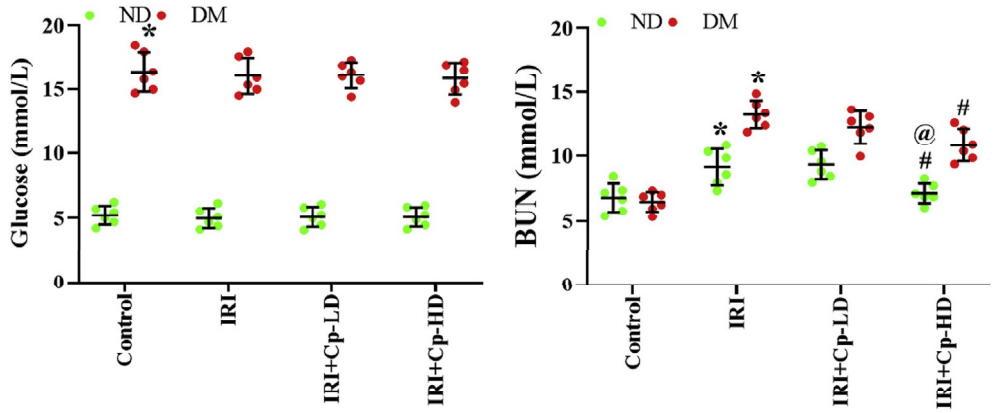

Fig. 4. Cyproheptadine improves renal function associated with IRI.
A-B: Representative scattered plots of plasma glucose (PGl) (A), blood urea nitrogen (BUN) (B). Data are represented as mean ± SD (n = 6). For statistical comparison, two-way ANOVA with Tukey's multiple comparison test was used where (*) $p < 0.05$ vs control; (#) $p < 0.05$ vs IRI; (@) $p < 0.05$ vs IRI-Cp-LD.

prominent in DM-IRI rats (Fig. 3). Next, we checked the protein expression of HMT-SET7/9 in proximal tubules of ND-IRI and DM-IRI rats. SET7/9 is mostly involved in H3K4Me [33]. In a cell culture study, silencing of SET7/9 gene with small interfering RNAs in monocytes markedly inhibited TNF-α induced inflammatory genes and H3K4Me2 on the TNF-α promoters [17]. Sasaki et al.

showed that knockdown of SET7/9 expression with small interfering RNA significantly attenuated renal fibrosis in unilateral ureteral obstruction (UUO) mice [34]. In addition, renal mesangial cells showed enhanced H3K4me1/3 expression and SET7/9 occupancies at the p21 promoter under diabetic condition [35]. These studies highlighted that SET7/9 are potential therapeutic targets in preventing IRI under DM as well as ND rats. In our study, we found that renal ischemic insult caused increased protein and mRNA expressions of SET7/9 in DM and ND rats. However, these results are more significant in DM-IRI rats compared to ND rats.

In recent studies, researchers have demonstrated the connection of increased expression of SET7/9 expressions and increased inflammatory cascade in diabetes and AKI conditions. It provides an insight towards the use of SET7/9 inhibitor under these conditions. Sinefungin, a SET7/9 inhibitor, ameliorated the renal fibrosis by inhibiting TGF-b1 and H3K4me1 in both cell lines (NRK-52E and NRK-49F cells) and UUO mice [34]. Recently, cyproheptadine, a novel SET7/9 inhibitor has been reported to exert protective role against breast cancer [18]. SET7/9 has claimed to methylated non-histone proteins including estrogen receptor (ER) α. ER-α methylation activates the pathogenic transcriptional activities and precipitate carcinogenesis of breast cancer. Cyproheptadine, clinically approved antiallergy drug, used as a SET7/9 inhibitor, which hinders substrate-binding pocket of Set7/9 along with its enzymatic activity via competing with the methyl group acceptor [18]. Hang et al. demonstrated the cyproheptadine reduced cancer induced bone pain via decreasing spinal SET7/9 and RANTES expression. Administration of SET7/9 (0.2 μg) in mice significantly abolished the anti-nociceptive effects of cyproheptadine, proved the selectively of cyproheptadine for SET7/9 [19]. In our study, we used cyproheptadine against IRI in DM and ND rats. We found that high dose of cyproheptadine has effectively improved the renal functions via reducing BUN levels in DM-IRI and ND-IRI rats (Fig. 4).

In conclusion, despite there is an association between inflammation, histone methylation and SET7/9 under diabetic kidney diseases, the underlying pathways are still not clear. This is the first report presenting the role of SET7/9 in epigenetic regulating NF-κB inflammatory signaling, directed via H3K4Me2 under IRI in DM and ND condition. For the first time, cyproheptadine has effectively prevent IRI in DM and ND condition, and provides a vast idea to conduct pathological studies exploring HMT-SET7/9 which is a novel and enticing target under the same.

Author contributions

A.B.G. conceived the idea and designed the experiments. N.S., H.S. and A.K. performed all the experiments, analyzed the data and completed the manuscript writing.

Funding

This research was supported by the Science & Engineering Research Board -Departmentof Science & Technology (SERB-DST), Govt. of India [SERB/ECR/2017/000317] and [SERB/EEQ/2019/000308].

Declaration of competing interest

The authors declare no potential conflicts of interest.

Acknowledgment

Sharma N. sincerely acknowledges the Indian Council of Medical Research (ICMR) for giving the senior research fellowship [45/54/2019/PHA/BMS].

References

[1] E.A. Hoste, J.A. Kellum, N.M. Selby, A. Zarbock, P.M. Palevsky, S.M. Bagshaw, S.L. Goldstein, J. Cerdá, L.S. Chawla, Global epidemiology and outcomes of acute kidney injury, Nat. Rev. Nephrol. 14 (2018) 607–625.
[2] S.A. Silver, Z. Harel, E. McArthur, D.M. Nash, R. Acedillo, A. Kitchlu, A.X. Garg, G.M. Chertow, C.M. Bell, R. Wald, Causes of death after a hospitalization with AKI, J. Am. Soc. Nephrol. 29 (2018) 1001–1010.
[3] S. Kumar, Cellular and molecular pathways of renal repair after acute kidney injury, Kidney Int. 93 (2018) 27–40.
[4] N. Sharma, V. Malek, S.R. Mulay, A.B. Gaikwad, Angiotensin II type 2 receptor and angiotensin-converting enzyme 2 mediate ischemic renal injury in diabetic and non-diabetic rats, Life Sci. 235 (2019) 116796.
[5] H. Shi, D. Patschan, T. Epstein, M.S. Goligorsky, J. Winaver, Delayed recovery of renal regional blood flow in diabetic mice subjected to acute ischemic kidney injury, Am. J. Physiol. Ren. Physiol. 293 (2007) F1512–F1517.
[6] S. Shi, S. Lei, C. Tang, K. Wang, Z. Xia, Melatonin attenuates acute kidney ischemia/reperfusion injury in diabetic rats by activation of the SIRT1/Nrf2/HO-1 signaling pathway, Biosci. Rep. 39 (2019).
[7] B.E. Hursh, R. Ronsley, N. Islam, C. Mammen, C. Panagiotopoulos, Acute kidney injury in children with type 1 diabetes hospitalized for diabetic ketoacidosis, JAMA pediatrics 171 (2017) e170020-e170020.
[8] J. Melin, O. Hellberg, E. Larsson, L. Zezina, B.C. Fellström, Protective effect of insulin on ischemic renal injury in diabetes mellitus, Kidney Int. 61 (2002) 1383–1392.
[9] J.V. Bonventre, A. Zuk, Ischemic acute renal failure: an inflammatory disease? Kidney Int. 66 (2004) 480–485.
[10] H. Rabb, M.D. Griffin, D.B. McKay, S. Swaminathan, P. Pickkers, M.H. Rosner, J.A. Kellum, C. Ronco, Inflammation in AKI: current understanding, key questions, and knowledge gaps, J. Am. Soc. Nephrol. 27 (2016) 371–379.
[11] S.K. Goru, A. Kadakol, A. Pandey, V. Malek, N. Sharma, A.B. Gaikwad, Histone H2AK119 and H2BK120 mono-ubiquitination modulate SET7/9 and SUV39H1 in type 1 diabetes-induced renal fibrosis, Biochem. J. 473 (2016) 3937–3949.
[12] C. Yu, S. Zhuang, Histone methyltransferases as therapeutic targets for kidney diseases, Front. Pharmacol. 10 (2019).
[13] J. Chen, Y. Guo, W. Zeng, L. Huang, Q. Pang, L. Nie, J. Mu, F. Yuan, B. Feng, ER stress triggers MCP-1 expression through SET7/9-induced histone methylation in the kidneys of db/db mice, Am. J. Physiol. Ren. Physiol. 306 (2014) F916–F925.
[14] G. Sun, M.A. Reddy, H. Yuan, L. Lanting, M. Kato, R. Natarajan, Epigenetic histone methylation modulates fibrotic gene expression, J. Am. Soc. Nephrol. 21 (2010) 2069–2080.
[15] V.G. Shuttleworth, L. Gaughan, L. Nawafa, C.A. Mooney, S.L. Cobb, N.S. Sheerin, I.R. Logan, The methyltransferase SET9 regulates TGFB1 activation of renal fibroblasts via interaction with SMAD3, J. Cell Sci. 131 (2018), jcs207761.
[16] H. Chen, D. Wan, L. Wang, A. Peng, H. Xiao, R.B. Petersen, C. Liu, L. Zheng, K. Huang, Apelin protects against acute renal injury by inhibiting TGF-β1, Biochim. Biophys. Acta (BBA) - Mol. Basis Dis. 1852 (2015) 1278–1287.
[17] Y. Li, M.A. Reddy, F. Miao, N. Shanmugam, J.-K. Yee, D. Hawkins, B. Ren, R. Natarajan, Role of the histone H3 lysine 4 methyltransferase, SET7/9, in the regulation of NF-κB-dependent inflammatory genes relevance to diabetes and inflammation, J. Biol. Chem. 283 (2008) 26771–26781.
[18] Y. Takemoto, A. Ito, H. Niwa, M. Okamura, T. Fujiwara, T. Hirano, N. Handa, T. Umehara, T. Sonoda, K. Ogawa, M. Tariq, N. Nishino, S. Dan, H. Kagechika, T. Yamori, S. Yokoyama, M. Yoshida, Identification of cyproheptadine as an inhibitor of SET domain containing lysine methyltransferase 7/9 (Set7/9) that regulates estrogen-dependent transcription, J. Med. Chem. 59 (2016) 3650–3660.
[19] L.H. Hang, Z.K. Xu, S.Y. Wei, W.W. Shu, H. Luo, J. Chen, Spinal SET 7/9 may contribute to the maintenance of cancer-induced bone pain in mice, Clin. Exp. Pharmacol. Physiol. 44 (2017) 1001–1007.
[20] C. Kilkenny, W.J. Browne, I.C. Cuthill, M. Emerson, D.G. Altman, Improving bioscience research reporting: the ARRIVE guidelines for reporting animal research, PLoS Biol. 8 (2010), e1000412.
[21] V. Malek, A.B. Gaikwad, Telmisartan and thiorphan combination treatment attenuates fibrosis and apoptosis in preventing diabetic cardiomyopathy, Cardiovasc. Res. 115 (2018) 373–384.
[22] N. Le Clef, A. Verhulst, P.C. D'Haese, B.A. Vervaet, Unilateral renal ischemia-reperfusion as a robust model for acute to chronic kidney injury in mice, PloS One 11 (2016), e0152153.
[23] K.C. Murray, A. Nakae, M.J. Stephens, M. Rank, J. D'Amico, P.J. Harvey, X. Li, R.L.W. Harris, E.W. Ballou, R. Anelli, C.J. Heckman, T. Mashimo, R. Vavrek, L. Sanelli, M.A. Gorassini, D.J. Bennett, K. Fouad, Recovery of motoneuron and locomotor function after spinal cord injury depends on constitutive activity in 5-HT2C receptors, Nat. Med. 16 (2010) 694–700.
[24] M. Fontecha-Barriuso, D. Martin-Sanchez, O. Ruiz-Andres, J. Poveda, M.D. Sanchez-Niño, L. Valiño-Rivas, M. Ruiz-Ortega, A. Ortiz, A.B. Sanz, Targeting epigenetic DNA and histone modifications to treat kidney disease, Nephrol. Dial. Transplant. 33 (2018) 1875–1886.
[25] H. Zhang, S.-C. Sun, NF-κB in inflammation and renal diseases, Cell Biosci. 5 (2015) 63.
[26] K.K. Donnahoo, B.D. Shames, A.H. Harken, D.R. Meldrum, Review article: the role of tumor necrosis factor in renal ischemia-reperfusion injury, J. Urol. 162 (1999) 196–203.

[27] F.L. Sung, T.Y. Zhu, K.K. Au-Yeung, Y.L. Siow, O. Karmin, Enhanced MCP-1 expression during ischemia/reperfusion injury is mediated by oxidative stress and NF-kappaB, Kidney Int. 62 (2002) 1160–1170.
[28] N. Song, F. Thaiss, L. Guo, NFκB and kidney injury, Front. Immunol. 10 (2019) 815.
[29] A.J. Bannister, T. Kouzarides, Regulation of chromatin by histone modifications, Cell Res. 21 (2011) 381–395.
[30] D. Brasacchio, J. Okabe, C. Tikellis, A. Balcerczyk, P. George, E.K. Baker, A.C. Calkin, M. Brownlee, M.E. Cooper, A. El-Osta, Hyperglycemia induces a dynamic cooperativity of histone methylase and demethylase enzymes associated with gene-activating epigenetic marks that coexist on the lysine tail, Diabetes 58 (2009) 1229–1236.
[31] M.A. Reddy, P. Sumanth, L. Lanting, H. Yuan, M. Wang, D. Mar, C.E. Alpers, K. Bomsztyk, R. Natarajan, Losartan reverses permissive epigenetic changes in renal glomeruli of diabetic db/db mice, Kidney Int. 85 (2014) 362–373.
[32] L.M. Villeneuve, M.A. Reddy, L.L. Lanting, M. Wang, L. Meng, R. Natarajan, Epigenetic histone H3 lysine 9 methylation in metabolic memory and inflammatory phenotype of vascular smooth muscle cells in diabetes, Proc. Natl. Acad. Sci. U. S. A. 105 (2008) 9047–9052.
[33] A.J. Ruthenburg, C.D. Allis, J. Wysocka, Methylation of lysine 4 on histone H3: intricacy of writing and reading a single epigenetic mark, Mol. Cell. 25 (2007) 15–30.
[34] K. Sasaki, S. Doi, A. Nakashima, T. Irifuku, K. Yamada, K. Kokoroishi, T. Ueno, T. Doi, E. Hida, K. Arihiro, N. Kohno, T. Masaki, Inhibition of SET domain–containing lysine methyltransferase 7/9 ameliorates renal fibrosis, J. Am. Soc. Nephrol. 27 (2016) 203–215.
[35] X. Li, C. Li, X. Li, P. Cui, Q. Li, Q. Guo, H. Han, S. Liu, G. Sun, Involvement of histone lysine methylation in p21 gene expression in rat kidney in vivo and rat mesangial cells in vitro under diabetic conditions, J. Diabetes Res. 2016 (2016) 3853242.

European Journal of Pharmacology 882 (2020) 173241

Contents lists available at ScienceDirect

European Journal of Pharmacology

journal homepage: www.elsevier.com/locate/ejphar

Full length article

Effects of renal ischemia injury on brain in diabetic and non-diabetic rats: Role of angiotensin II type 2 receptor and angiotensin-converting enzyme 2

Nisha Sharma, Anil Bhanudas Gaikwad*

Laboratory of Molecular Pharmacology, Department of Pharmacy, Birla Institute of Technology and Science Pilani, Pilani Campus, Rajasthan, 333031, India

ARTICLE INFO

Keywords:
Ischemia renal injury
Renin-angiotensin system
Depressor arm
Kidney
Brain

ABSTRACT

Clinically, patients with diabetes mellitus (DM) are more susceptible to ischemic renal injury (IRI) than non-diabetic (ND) patients. Besides, IRI predisposes distant organ dysfunctions including, neurological dysfunction, in which the major contributor remains renin-angiotensin system (RAS). Interestingly, the role of depressor arm of RAS on IRI-associated neurological sequalae remains unclear. Hence, this study aimed to delineate the role of angiotensin II type 2 receptor (AT2R) and angiotensin-converting enzyme 2 (ACE2) under the same. ND and Streptozotocin-induced DM rats with bilateral IRI were treated with AT2R agonist-Compound 21 (C21) (0.3 mg/kg/day, *i.p.*) or ACE2 activator-Diminazene Aceturate (Dize), (5 mg/kg/day, *p.o.*) either alone or as combination therapy. Effect of IRI on neurological functions were assessed by behavioural, biochemical, and histopathological analysis. Immunohistochemistry, ELISA and qRT-PCR experiments were conducted for evaluation of the molecular mechanisms. We found that in ND and DM rats, IRI causes increased hippocampal MDA and nitrite levels, augmented inflammatory cytokines (granulocyte-colony stimulating factor, glial fibrillary acidic protein), altered protein levels of Ang II, Ang-(1–7) and mRNA expressions of *At1r*, *At2r* and *Masr*. Treatment with C21 and Dize effectively normalised above-mentioned pathological alterations. Moreover, the protective effect of C21 and Dize combination therapy was better than respective monotherapies, and more likely, exerted via augmentation of protein and mRNA levels of depressor arm components. Thus, AT2R agonist and ACE2 activator therapy prevents the development of IRI-associated neurological dysfunction by attenuating oxidative stress and inflammation, upregulating depressor arm of RAS in brain under ND and DM conditions.

1. Introduction

Ischemic renal injury (IRI) remains the most common cause of acute kidney injury (AKI) (Kumar, 2018). On the other hand, the clinical settings are often multifaceted with patients having co-morbidities like diabetes that make patients more susceptible for IRI (Monseu et al., 2015). Besides, the diabetic patients suffering from AKI are at higher risk of central nervous system dysfunctions than with chronic kidney diseases like end stage renal disease (Baumgaertel et al., 2014; Wu et al., 2014). Even though, AKI-associated neurological impairments are well known, the pathogenesis of the same is poorly understood. Existing reports suggest that IRI elevated hippocampal pyknotic neurons and cerebral microglial cells, activates neurons due to stress responses, and retarded motor activity (Liu et al., 2008; Palkovits et al., 2009). These could be due to systemic inflammation which consequently increases the blood-brain barrier permeability (Liu et al., 2008; Chou et al., 2014).

In our recent review article, we have discussed the role of renin-angiotensin system (RAS) activation, as an unavoidable pathogenic signalling and contributes AKI (Sharma et al., 2019a). Clinically, treatment with conventional RAS inhibitors i.e. angiotensin-converting enzyme inhibitor (ACEi) and angiotensin II type 2 receptor blockers (ARBs), produces vasodilation of the renal efferent arterioles, thereby reduces glomerular filtration rate and deteriorates hypovolemic condition of kidney which eventually worsens the extent of AKI (Mansfield et al., 2016). Thus, recently, we tested the role of depressor arm of RAS modulations in IRI under diabetes mellitus (DM) and non-diabetic (ND) conditions (Sharma et al., 2019b). The diabetic unilateral-ischemic rats exhibited upregulation of the pressor RAS and down-regulation of depressor RAS components, leading to abrupt increase in inflammation, cell apoptosis and oxidative stress, consequently severe tubular damage. Upon treatment with angiotensin II type 2 receptor (AT2R) agonist, Compound 21 (C21) and angiotensin-converting enzyme 2 (ACE2) activator, Diminazene aceturate (Dize), the depressor arm of RAS get upregulated which depleted pathogenic markers of IRI and improved tubular morphology in kidney tissue (Sharma et al., 2019b).

* Corresponding author. Department of Pharmacy, Birla Institute of Technology and Science, Pilani, Pilani Campus, Pilani, 333 031, Rajasthan, India.
E-mail address: anil.gaikwad@pilani.bits-pilani.ac.in (A.B. Gaikwad).

https://doi.org/10.1016/j.ejphar.2020.173241
Received 22 April 2020; Received in revised form 28 May 2020; Accepted 29 May 2020
Available online 18 June 2020

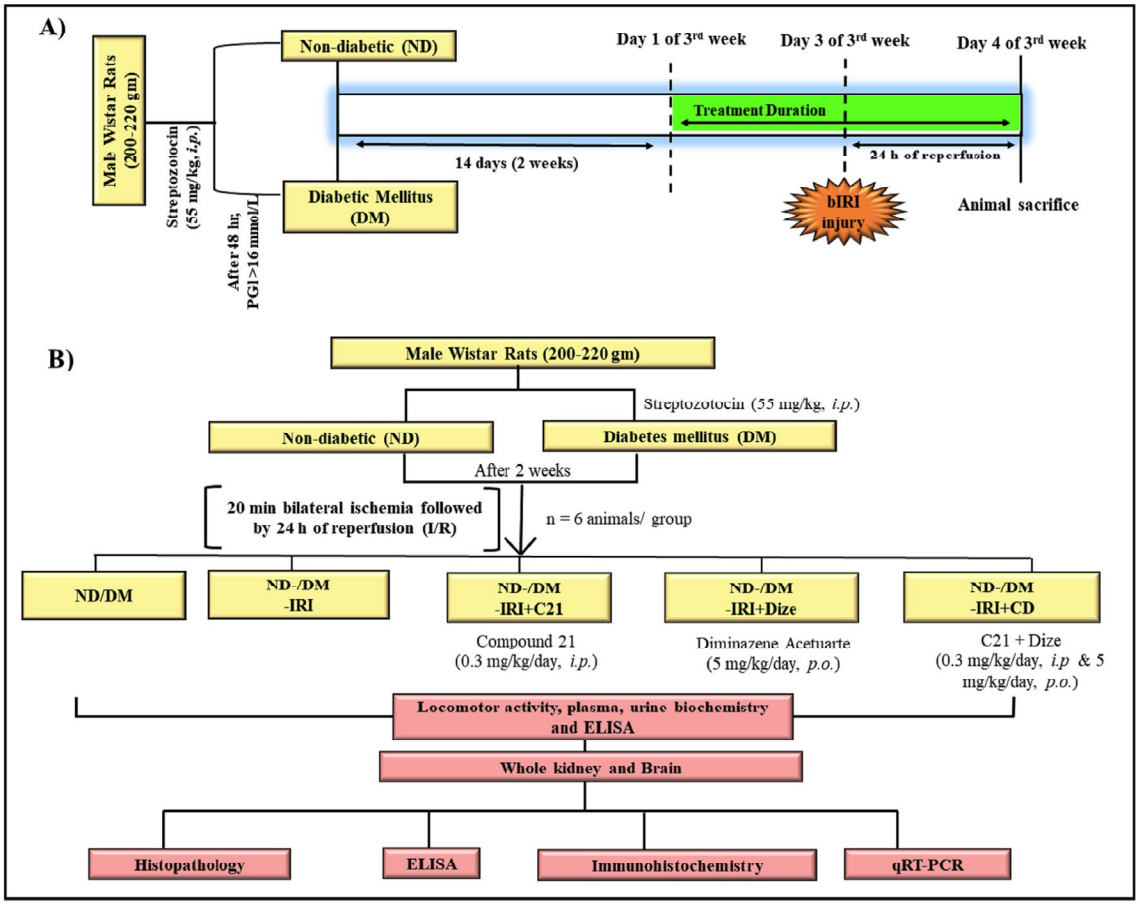

Fig. 1. Schematic representation of the study design. A) Timeframe for the induction of diabetes mellitus via streptozotocin-injection and acute kidney injury (AKI) by bilateral ischemia/reperfusion (bIRI), and pharmacological intervention. B) Experimental details of animal sub-grouping for an intervention study followed by experimental design (n = 6 animals/group). **ND**-non-diabetic rats, **DM**-diabetes mellitus rats, **ND-/DM-IRI**- ND or DM rats subjected to Ischemia-30min/reperfusion-24 h (IRI), **ND-/DM-IRI + C21**- ND-IRI or DM-IRI rats receiving compound 21 (0.3 mg/kg/day, *i.p.*) monotherapy, **ND-/DM-IRI + Dize**- ND-IRI or DM-IRI rats receiving Dize (5 mg/kg/day, *p.o.*) monotherapy, **ND-/DM-IRI + CD**- ND-IRI or DM-IRI rats receiving compound 21 (0.3 mg/kg/day, *i.p.*) and Dize (5 mg/kg/day, *p.o.)* combination therapy.

Prevailing body of preclinical and clinical evidences revealed that most of the organs control their own local RAS that is compartmentalized from the systemic circulation (Campbell, 2014). Recently, Cao et al. has described that IRI resulted in the local activation of RAS not only in kidney, but also in the brain tissue (Cao et al., 2017). The renal and brain RAS are interlinked via reno-cerebral sympathetic reflex that is activated by renal afferent sympathetic nerves, ultimately increases cerebral pressor arm components like angiotensinogen (AGT) and angiotensin II (Ang II) levels, intensifies inflammation and oxidative stress. Thus, there might be an upsurge of the brain RAS through neuronal pathways (Cao et al., 2015, 2017). However, the role of depressor arm of RAS in IRI-associated neurological dysfunction is still unknown. Therefore, in the present study we used diabetic and non-diabetic rats bilateral renal IRI model to test the hypothesis that IRI could alter the AT2R and ACE2 levels of the brain local RAS that could mediate cerebral inflammation and oxidative stress.

2. Materials and methods

2.1. Materials

Streptozotocin and Diminazene aceturate (Dize) were obtained from Sigma (St. Louis, MO, USA). Glucose, creatinine and blood urea nitrogen (BUN) kits were obtained from Accurex (Mumbai, India). ELISA kits for Kidney injury molecule-1 (Kim-1), ACE, ACE2, Ang-(1–7) and Ang II were purchased from Fn Test (Wuhan, China); granulocyte-colony stimulating factor (GCSF) and glial fibrillary acidic protein (GFAP) ELISA kits were purchased from Elabsciences (China). TNF-α primary antibody was procured from Santa Cruz Biotechnology (Dallas, TX, USA), and secondary antibody was procured from Cell Signaling Technology (Danvers, MA, USA).

2.2. Development of streptozotocin-induced type 1 diabetes

The animal experiments were carried out at Central Animal Facility (CAF) of Birla Institute of Technology and Science Pilani (BITS-Pilani) as per the protocol approved by the Institutional Animal Ethics Committee (IAEC), BITS-Pilani (Protocol Approval No: IAEC/RES/23/19/Rev-2/25/18). Reported animal studies are ensued the ARRIVE guidelines (Kilkenny et al., 2010). The male adult Wistar rats (200–220g) were acquired from the CAF of BITS-Pilani and maintained under standard environmental conditions, with feed and water *ad lib*.

Diabetes mellites (DM) was induced by single dose of Streptozotocin [55 mg/kg, *i.p.*, vehicle-sodium citrate buffer (0.01 M, pH 4.4)] in male Wistar rats (Sharma et al., 2019b). ND rats of same age group received only vehicle. After 48 h of Streptozotocin-injection, rats having plasma glucose levels > 16 mmol/L were involved in the study as DM rats.

2.3. Ischemia-reperfusion renal injury

ND and DM rats underwent bilateral ischemia reperfusion injury (IRI) (Lima-Posada et al., 2019; Sharma et al., 2019b). Briefly, rats were

given saline (20 ml/kg, *s.c.*) to prevent fluid loss during laparotomy. Then, rats were anaesthetised with pentobarbital sodium (50 mg/kg, *i.p.*) and were kept on surgical platform in dorsal position and body temperature (37°C) was maintained with homoeothermic blanket. The flank incisions were made to expose both kidneys, followed by occlusion of renal pedicles using non-traumatic clamps. After 20 min, the clamps were removed and after observing renal blood flow, the skeletal muscle and skin layers were sutured separately with absorbable and non-absorbable sutures, respectively. To prevent post-surgical infection, rats were given topical application of (Betadine™) antiseptic and parenteral (Augmentin™, 324 mg/kg, *i.p.*) antibiotics. Sham control animals were subjected to identical operation and length of time of surgery but without renal vascular pedicles clamping. After 24 h, blood was collected from vena cava with a 5 ml syringe for plasma biochemistry. The kidney and brain tissues were then removed, washed and blotted dry, weighed and kept in −80 °C for further experimentations. For histology, brain was harvested and separately fixed with formalin to proceed it for hematoxylin and eosin and immunohistochemical staining.

2.4. Drug treatments

The ND and DM rats were divided into five groups each: (a) **ND/DM-**serve as respective controls, (b) **ND-/DM-IRI**- ND or DM rats subjected to bilateral ischemia (IRI) after completion of two weeks of diabetes induction, (c) **ND-/DM-IRI + C21-** ND- IRI or DM- IRI rats receiving compound 21 (C21) (0.3 mg/kg/day, *i.p.*) (Pandey and Gaikwad, 2017), (d) **ND-/DM-IRI + Dize-** ND- IRI or DM- IRI rats receiving Dize (5 mg/kg/day, *p.o.*) (Goru et al., 2017), (e) **ND-/DM-IRI + CD-** ND- IRI or DM- IRI rats receiving C21 (0.3 mg/kg/day, *i.p.*) and Dize (5 mg/kg/day, *p.o.*) combination therapy. Both monotherapies and combination therapy were administered two days prior to IRI and continued to next day (24 h of reperfusion time) (Fig. 1).

2.5. Assessment of renal functions by plasma and urine biochemistry

After reperfusion time, blood samples were collected and plasma was separated by centrifugation (5 min at 5000 g, 4 °C). These plasma samples were used for estimation of BUN and creatinine (PCr) levels using spectrometric kits. Urine sampled were collected using metabolic cages and utilised for assessment of urinary kim-1 using ELISA kits.

2.6. Behavioural assessment: spontaneous locomotor activity

After 24 h of renal ischemia, behavioural assessment was performed between 09:00 and 17:00 h using a digital actophotometer (INCO, India). Briefly, each rat was placed inside a square closed chamber (30 × 30 cm^2) and spontaneous locomotor activity for a period of 10 min was recorded using infra-red light-sensitive photocells (Sharma and Taliyan, 2016).

2.7. Hematoxylin and eosin staining

Brain histology was examined by Hematoxylin and Eosin (H and E) staining (Liu et al., 2008). At least 4–5 sections (one microscopy slide) from each brain and a total of n = 6 brain from each group were observed; and images of CA1 region of hippocampus were captured at 400 × magnification by using a Zeiss microscope (model: Vert.A1). 5–6 images from each stained brain microscopy slide were evaluated for neuronal cells with a condensed, darkly stained cell body and nucleus which were considered as pyknotic. Pyknotic cells were counting by a blind observer and presented the damaged neuronal cells as the numbers of pyknotic cells per section. The average value of pyknotic cells count for each slide was considered for statistical analysis.

2.8. Immunohistochemistry

Immunohistochemistry (IHC) was performed as described previously (Sharma et al., 2019b). Briefly, brain sections (5 μm) were taken from paraffin blocks and deparaffinized with xylene, followed by antigen retrieval by heating in citrate buffer (10 mmol/L). Mouse primary antibody incubation was performed against TNF-α (Dilution: 1:200 v/v), followed by secondary antibody incubation with HRP-conjugated anti-mouse IgG. For detection, diaminobenzidine (DAB) were used as a chromogen. The slides were counterstained with hematoxylin, dehydrated with alcohol and xylene and mounted in DPX. At least 4–5 sections (one microscopy slide) from each brain and a total of n = 6 brain from each group were observed; and images were taken at 400 × magnification by using Zeiss microscope (model: Vert.A1). 5–6 images from each stained brain microscopy slide were analysed using ImageJ software (NIH, Bethesda, MD, USA) for calculating DAB-positive area.

2.9. Isolation of proximal tubular fraction

Proximal tubules were isolated form the kidney tissue as described previously (Sharma et al., 2019b). Briefly, the kidney was crushed and digested with collagenase type IV in PBS, followed by constant oxygenation until a uniform suspension was formed. The suspension was filtered using nylon 250-μm sieve followed by centrifugation at 100*g* for 1 min. After washing with ice-cold PBS, pellet suspension was mixed thoroughly with 40% Percoll followed by centrifugation at 26,000 *g* for 30 min. Centrifugation tubes showed four distinct bands (B1–B4). The B4 band, highly enriched proximal tubular fraction, was cautiously collected, suspended, and washed in ice-cold PBS. Finally, the isolated tubular fraction was examined under the light microscope and used for further analysis.

2.10. Measurements of oxidative stress level in proximal tubules and hippocampus

2.10.1. Sample homogenate preparation

For hippocampal homogenate, isolated brains were rinsed with ice-cold isotonic saline (0.9% w/v NaCl). The hippocampus region of brains was dissected and were homogenized using ice-cold 0.1 M phosphate buffer (pH 7.4) in ten times (w/v) volume, followed by centrifugation at 10,000 g for 15 min (4 °C) (Sharma and Taliyan, 2016). For proximal tubules, we directly taken the isolated proximal tubular fraction and added 0.1 M phosphate buffer (pH 7.4) in ten times (w/v) volume. Then, we centrifuged the samples at 10,000 g for 15 min. Finally, the aliquots of supernatant were separated and further used for biochemical estimations.

2.10.2. Protein determination

Protein content in the proximal tubules and hippocampal samples were measured by the method of Lowry et al. (Classics Lowry et al., 1951) using bovine serum albumin (1 mg/ml) as a standard.

2.10.3. Malondialdehyde (MDA) estimation

MDA is an end product of lipid peroxidation, was assessed using proximal tubules and hippocampal homogenate as described by previously (Sharma et al., 2015). The absorbance of MDA was observed after the reaction of MDA with thiobarbituric acid, at 532 nm. Then, the concentration of MDA was assessed from a standard curve and stated as nanomoles per milligram of protein.

2.10.4. Nitrite levels estimation

Nitrite, an indicator of nitric oxide production, was done as described by Sharma S. et al., (Sharma et al., 2015). Briefly, nitrite levels were determined by Griess reagent (0.1% N-(1-naphthyl) ethylenediamine dihydrochloride, 1% sulfanilamide, and 2.5% phosphoric acid).

Equal volumes of Griess reagent and tissue (proximal tubules/hippocampus) supernatant were mixed together and was incubated in the dark light for 10 min (24 °C). Absorbance was taken at 540 nm and the concentration of nitrite was assessed from a sodium nitrite standard curve and expressed as micromoles per milligrams protein.

2.11. ELISA to determine RAS components levels in proximal tubules and hippocampus

Isolated proximal tubular fraction and hippocampus tissues were homogenized in the recommended buffer solution, followed by total protein estimation. Protein equalised proximal tubular, hippocampal samples, and diluted urine were assayed for AGT, ACE, ACE2, Ang II and Ang-(1–7) protein levels by using ELISA kits (n = 6 rats/group) (Goru et al., 2017).

2.12. Quantitative real-time polymerase chain reaction

RNA isolation from hippocampal tissue and qRT-PCR were performed according to a previously described protocol (Malek and Gaikwad, 2018; Sharma et al., 2019b). Briefly, RNA was isolated from hippocampal tissue and reverse transcribed. qRT-PCR was conducted on the LightCycler® 96 Real-Time PCR System using the FastStart Essential DNA Green Master and results were analysed by LightCycler® Software (Roche, Germany). mRNA levels were normalised against 18s rRNA contents. All the primers were designed and produced by Eurofins, India (Supplementary data, Table S1). Experiments were carried out in triplicate for each sample and results are expressed as fold changes over respective controls.

2.13. Statistical analysis

Experimental values are represented as mean ± S.D., and 'n' refers to the number of samples studied. Statistical comparison between groups was performed using one-way analysis of variance (ANOVA) followed by Tukey's Multiple Comparison *post hoc* test or two-way ANOVA followed by Tukey's Multiple Comparison *post hoc* test. Data with $P < 0.05$, were considered statistically significant. GraphPad Prism software version 8.0.2 (San Diego, CA, USA) was used for all statistical processing. All the statistical analysis was performed according to suggested experimental design and analysis in the field of pharmacology (Curtis et al., 2015).

3. Results

3.1. Hyperglycaemia worsens renal functions under ischemic renal injury

DM rats had increased plasma glucose (Supplementary Fig. 1A) levels compared to ND rats. Further, we found that IRI in ND and DM rats significantly increased PCr (Supplementary Fig. 1B) and BUN (Supplementary Fig. 1C) levels compared to respective controls. DM-IRI rats showed significantly higher BUN and PCr levels compared to ND-IRI rats (28.66 ± 3.1 vs. 20.33 ± 2.5, 92.7 ± 9.4 vs. 66.41 ± 8.3). Kim-1, a type 1 trans-membrane protein, having an immunoglobulin and mucin domain, whose levels are said to be elevated under proximal tubular damage upon ischemic renal injury (Han et al., 2008). In our study, DM-IRI rats showed significantly increased urinary kim-1 protein levels as compared to ND-IRI rats (16.52 ± 1.5 vs. 9.34 ± 2.3, Supplementary Fig. 1D).

3.2. Hyperglycaemia impairs locomotor activity and aggravates brain inflammatory mediators after ischemic renal injury

To determine whether the findings of an abrupt alterations in kidney functional parameters was accompanied by impaired behavioural parameter and distant organ (brain) cellular inflammation, we checked locomotor activity using actophotometer, and performed ELISA for inflammatory molecules like GCSF and GFAP in plasma, hippocampus and cerebral cortex tissue. IRI has severe effect on the locomotor activity response in DM rats compared to ND rats (Supplementary Fig. 1E). Further, after IRI, both DM-IRI and ND-IRI had shown increase in plasma (Supplementary Fig. 1F) and hippocampal (Supplementary Fig. 1G) GCSF levels, compared to their respective controls. However, in comparison to ND-IRI group, DM-IRI group showed significant increase in GCSF levels in plasma and hippocampus (548.6 ± 34.2 vs. 441.1 ± 50.2, 50.02 ± 6.9 vs. 40.56 ± 4.4; Supplementary Figs. 1F and G). GFAP, an indicator for activated glial cells during brain inflammation, found to get elevated in plasma (Supplementary Fig. 1H) as well as in cerebral cortex (Supplementary Fig. 1I) of DM-IRI and ND-IRI rats. However, DM-IRI rats has shown marked elevation in plasma and cerebral cortex GFAP levels, as compared to ND-IRI rats (6.33 ± 0.43 vs. 4.84 ± 0.64, 332.4 ± 20.8 vs. 252.4 ± 21.7; Supplementary Figs. 1H and I).

3.3. AT2R and ACE2 activation accentuated renal functions in diabetic and non-diabetic rats upon ischemic renal injury

We adjured to check the role of RAS depressor arms' regulations on brain after IRI. We treated ND-IRI and DM-IRI rats with AT2R agonist (C21, 0.3 mg/kg/day, *i.p.*) and ACE2 activator (Dize, 5 mg/kg/day, *p.o.*), either alone as monotherapy or together as combination therapy (Fig. 1A and B). Plasma biochemical parameters revealed that none of the therapies had any effect on increased plasma glucose levels in DM group (Fig. 2A). ND-IRI and DM-IRI rats' receiving C21 and Dize combination therapy significantly reduced BUN levels, while both the monotherapies had no effect on BUN levels when compared to respective controls (Fig. 2B). On the other hand, both monotherapies and combination therapy showed significant reduction in PCr levels when compared to ND-IRI and DM-IRI rats. Interestingly, the combination therapy exhibited lower levels of PCr compared to both monotherapies in ND and DM conditions (Fig. 2C). Moreover, in ND-IRI rats, combination therapy has significantly reduced PCr levels compared to DM-IRI rats (60.92 ± 10.4 vs. 41.36 ± 9.1).

In ND group, the increased urinary Kim-1 level was significantly decreased by C21 and Dize monotherapies and combination therapy (Fig. 2D). In DM group, only combination therapy had effect on decreasing urinary kim-1 levels compared to DM-IRI and both monotherapies (Fig. 2D). Moreover, ND-IRI + CD rats has significantly lowered the urinary Kim-1 levels compared to DM-IRI + CD rats (9.55 ± 1.9 vs. 3.63 ± 1.2).

3.4. AT2R and ACE2 activation improved cognitive functions and diminished oxidative stress

As compared to ND-IRI rats, DM-IRI rats had a significant decrease in locomotor activity (Fig. 3A). Interestingly, concomitant activation of AT2R and ACE2 had improved the activity counts in ND-IRI and DM-IRI rats, while ND-IRI rats showed marked recovery as compared to DM-IRI rats (222.3 ± 32.56 vs. 178.1 ± 24.58). Neither of the monotherapies had improved the locomotor-cognitive function in ND-IRI and DM-IRI rats (Fig. 3A). Further, we tested MDA and nitrite levels to determine whether hyperglycaemia aggravated IRI-associated brain functional abnormalities are linked with brain oxidative stress levels. In proximal tubules, DM-IRI rats showed higher MDA (31.87 ± 2.87 vs. 20.48 ± 2.35) and nitrite (52.29 ± 4.07 vs. 38.11 ± 3.72) levels as compared to ND-IRI rats (Fig. 3B and C). In ND group, C21 and Dize monotherapies has reduced the MDA and nitrite levels compared to ND-IRI rats. However, combination therapy significantly reduced the MDA and nitrite levels compared to C21 and Dize monotherapies (Fig. 3B and C). In DM group, C21 and Dize monotherapies had no effect on MDA and nitrite levels, but combination therapy significantly lessened MDA and nitrite levels compared to DM-IRI rats (Fig. 3B and C).

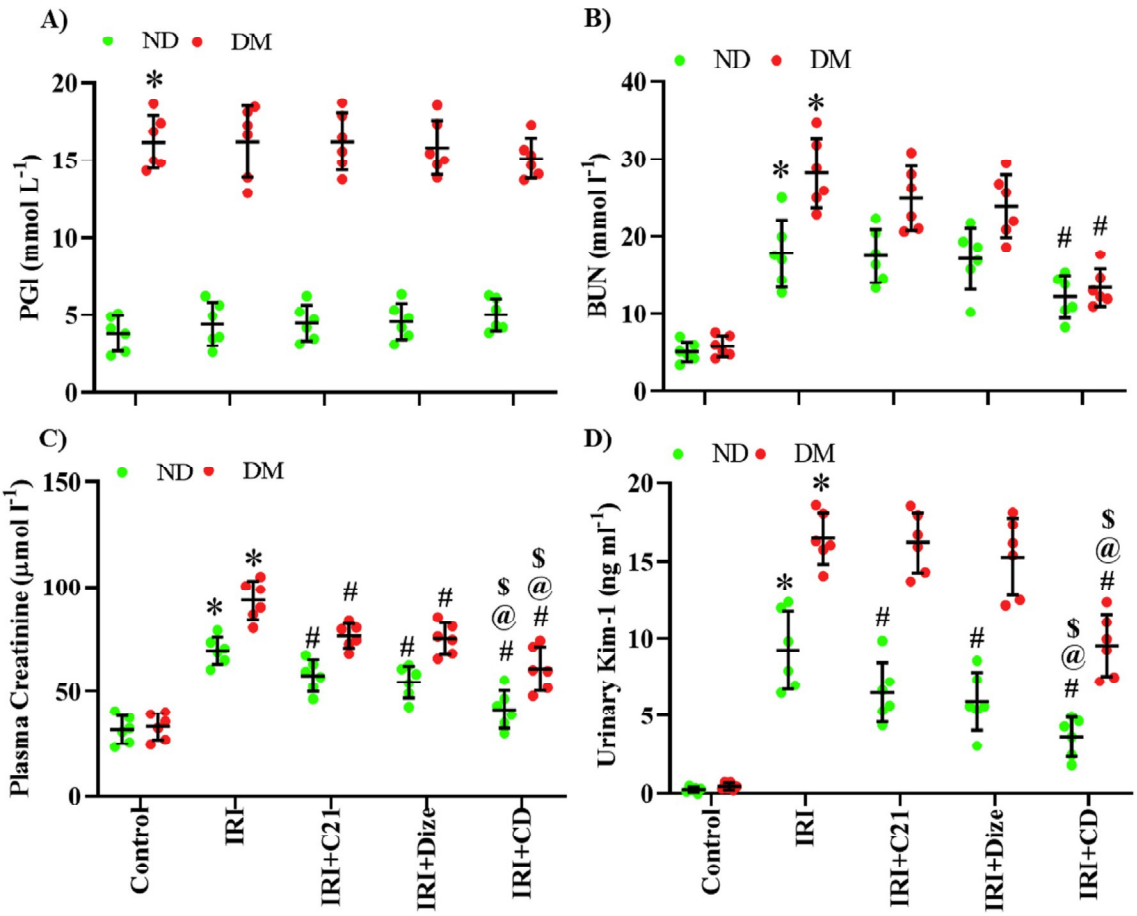

Fig. 2. Effect of AT2R and ACE2 activation on plasma and urine biochemistry. A–D: Representative scattered plots of plasma glucose (PGl) (A), creatinine (PCr) (B), blood urea nitrogen (BUN) (C) and urinary kidney injury molecule-1 (Kim-1) (D). Data are represented as mean ± S.D. (n = 6). For statistical comparison, two-way ANOVA with Tukey's multiple comparison test was used where $^{(*)}$ $P < 0.05$ vs control; $^{(\#)}$ $P < 0.05$ vs IRI; $^{(@)}$ $P < 0.05$ vs IRI-C21; $^{(\$)}$ $P < 0.05$ vs IRI-Dize.

In hippocampal tissue, DM-IRI rats showed significant elevation of MDA (9.22 ± 0.847 vs. 7.075 ± 0.91) and nitrite (24.58 ± 1.81 vs. 19.44 ± 1.52) levels compared to ND-IRI rats (Fig. 3D and E). Neither of the monotherapies lowered the hippocampal MDA and nitrite levels (Fig. 3D and E). However, the combination therapy significantly attenuated the MDA and nitrite levels as compared to ND-IRI and DM-IRI rats (Fig. 3D and E).

3.5. AT2R and ACE2 activation suppressed pyknotic neurons in hippocampal CA1 region of diabetic and non-diabetic rats after ischemic renal injury

Light microscopic data of H&E-stained brain sections showed healthy neurons in CA1 region of hippocampus in ND and DM rats (Fig. 4A). Healthy neurons seemed robust, spherical or slightly oval nucleus with clear visible cytoplasm as indicated by green arrows. However, the ND-IRI and DM-IRI groups showed disorganization and cell loss in CA1 region as indicated by red arrows (Fig. 4A and B). The pyknotic cells count were more prominent with DM-IRI group in comparison to ND-IRI group (47.33 ± 4.76 vs. 30.67 ± 4.33, Fig. 4B). The size of pyramidal cells was substantially shrunken with darkened nuclei. Remarkably, there was a reduction in the pyknotic neurons and apoptosis, and preservation of pyramidal cells following treatment with C21 and Dize combination therapy compared to ND-IRI and DM-IRI groups (Fig. 4A and B). In ND group, combination therapy significantly reduced pyknotic cells count compared to DM group with combination therapy (35.5 ± 5.89 vs. 14.67 ± 4.37, Fig. 4A and B). In contrast, both monotherapies were unable to produce significant reduction in pyknotic cells counts compared to ND-IRI and DM-IRI rats (Fig. 4A and B).

3.6. AT2R and ACE2 activation curbed systemic and brain soluble inflammatory mediator-GFAP in diabetic and non-diabetic rats upon ischemic renal injury

Regarding GCSF, DM-IRI rats showed significant increase in its plasma and hippocampal GCSF levels as compared to ND-IRI rats (Fig. 5A and B). Neither monotherapies nor combination therapies have observed to persuade a significant difference in the plasma and hippocampal GCSF protein levels compared with ND-IRI and DM-IRI rats (Fig. 5A and B). In plasma and cerebral cortex homogenate samples, DM-IRI rats showed significant increase in GFAP protein levels compared to ND-IRI rats (Fig. 5C and D). C21 and Dize monotherapies showed no effect on GFAP protein levels compared to ND-IRI and DM-IRI rats. In ND and DM studies, combination therapy significantly lowers the GFAP levels as compared to IRI and monotherapies groups (Fig. 5C and D). In combination therapy, DM-IRI rats showed less reduction GFAP levels compared to ND-IRI rats in plasma (4.966 ± 0.52 vs. 3.66 ± 0.35) and cerebral cortex (274.4 ± 22.2 vs. 200.5 ± 20.85, Fig. 5C and D) samples.

3.7. AT2R and ACE2 activation attenuated TNF-alpha expression in the hippocampal CA1 region after ischemic renal injury

We observed that DM-IRI and ND-IRI rats presented marked elevation of TNF-α expressions in the CA1 hippocampal region compared to

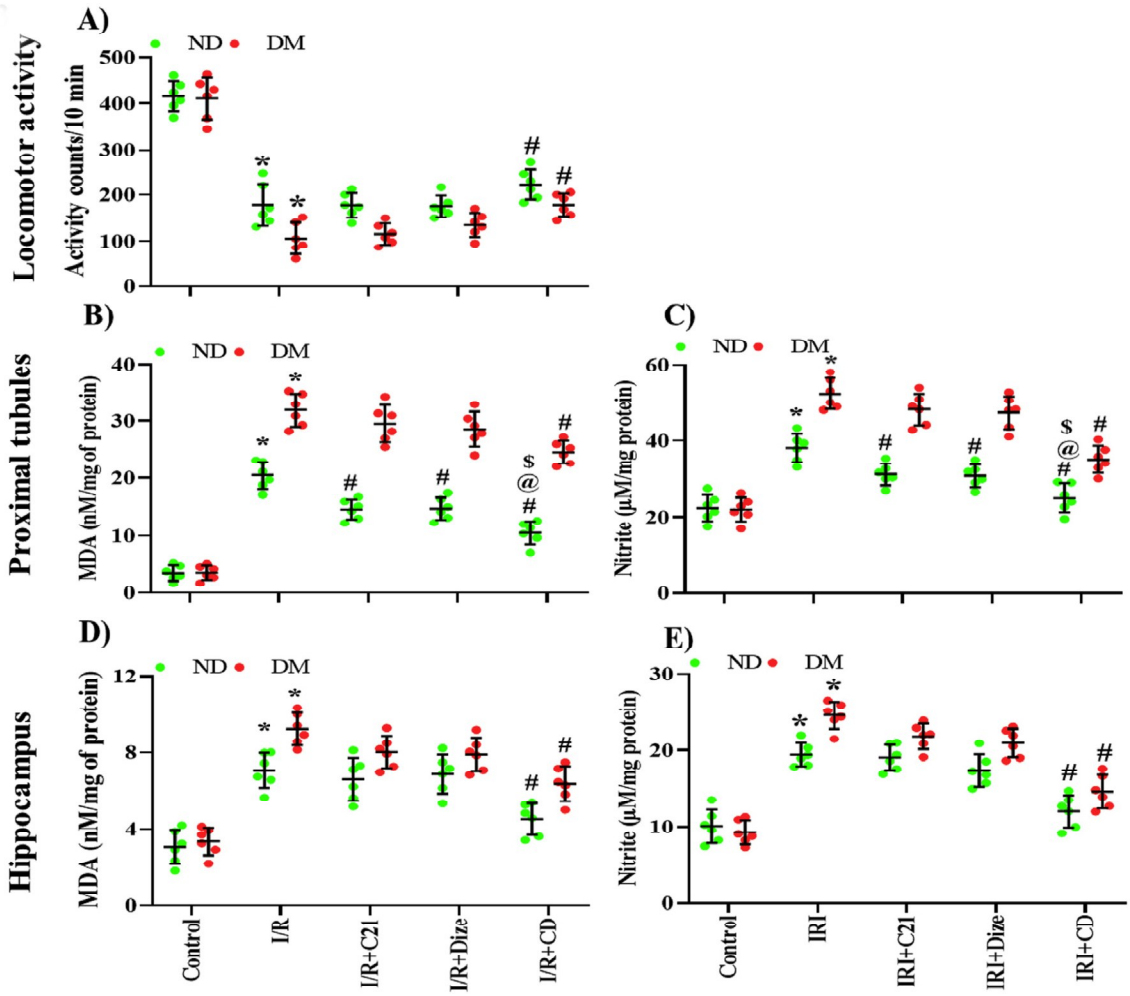

Fig. 3. Effect of AT2R and ACE2 activation on locomotor activity, and proximal tubular and hippocampal oxidative stress. A–B: Estimation of oxidative stress markers e.g. malondialdehyde (MDA) (A), nitrite (B) levels in isolated proximal tubular fraction from rat kidneys (n = 6). C–D: Estimation of oxidative stress markers; malondialdehyde (MDA) (A), nitrite (B) levels in hippocampal homogenate obtained from rat brain tissue (n = 6). Scattered plot (E) of locomotor activity which was evaluated by the times breaking laser beam during the test. Data are represented as mean ± S.D. from three independent experiments. Two-way ANOVA with Tukey's multiple comparison test for statistical comparison. $^{(*)}$ $P < 0.05$ vs control; $^{(\#)}$ $P < 0.05$ vs IRI; $^{(@)}$ $P < 0.05$ vs IRI-C21; $^{(\$)}$ $P < 0.05$ vs IRI-Dize.

respective controls (Fig. 6A and B). Here, DM-IRI group showed higher TNF-α expressions compared to ND-IRI group (67.17 ± 7.36 vs. 51.67 ± 5.68, Fig. 6B). In ND and DM studies, C21 and Dize combination treatment had significantly reduced the TNF-α expressions as compared to IRI and monotherapies group. In combination therapy, ND-IRI rats showed marked reduction in TNF-α expressions compared to DM-IRI rats (47.67 ± 8.75 vs. 39.2 ± 11.23, Fig. 6B).

3.8. AT2R and ACE2 activation modulated RAS components in the proximal tubular cells of diabetic and non-diabetic rats upon ischemic renal injury

We have checked the proximal tubular levels of pressor arm and depressor arm of RAS. In Fig. 7, the ACE and Ang II levels of ND-IRI and DM-IRI were significantly greater than their respective controls. The DM-IRI rats showed significant increase in ACE and Ang II levels compared to ND-IRI rats (14.64 ± 1.86 vs. 8.86 ± 1.1; 86.75 ± 7.56 vs. 56.62 ± 6.8, Fig. 7A, C). C21 and Dize alone and in combination did not reduced the ACE levels. However, combination therapy of C21 and Dize has markedly reduced the Ang II levels as compared to in ND/DM-IRI and monotherapies groups (Fig. 7C). Here, combination treatment in DM-IRI rats showed comparatively lesser reduction of Ang II levels as compared to ND-IRI rats (61.8 ± 8.2 vs. 37.93 ± 6.72). Further, depressor arm components: ACE2 (Fig. 7B) and Ang-(1–7) (Fig. 7D) levels were significantly reduced in proximal tubules of ND-IRI and DM-IRI groups compared to their respective controls. ND-IRI rats showed less significant reduction in ACE2 and Ang-(1–7) levels compared to DM-IRI rats (1.95 ± 0.51 vs. 1.022 ± 0.34; 11.09 ± 1.9 vs. 6.457 ± 1.7, Fig. 7B and D). Among monotherapies, only Dize treatment increased ACE2 (Fig. 7B) and Ang-(1–7) (Fig. 7D) levels compared to ND-IRI and DM-IRI rats. Moreover, combination therapy significantly increased ACE2 (Fig. 7B) and Ang-(1–7) levels (Fig. 7D) compared to ND/DM-IRI and monotherapies groups.

In Fig. 7E, urinary AGT levels were significantly elevated in ND-IRI and DM-IRI rats in comparison to ND and DM rats. Though, DM-IRI rats showed higher urinary AGT levels compared to ND-IRI rats (109.1 ± 11.6vs. 82.35 ± 7.45, Fig. 7E). Combination therapy has significantly reduced urinary AGT levels compared to ND-IRI and DM-IRI rats. However, combination treatment in DM-IRI rats showed comparatively lesser reduction of urinary AGT levels than ND group of combination therapy (85.77 ± 10.4 vs. 65.87 ± 7.05).

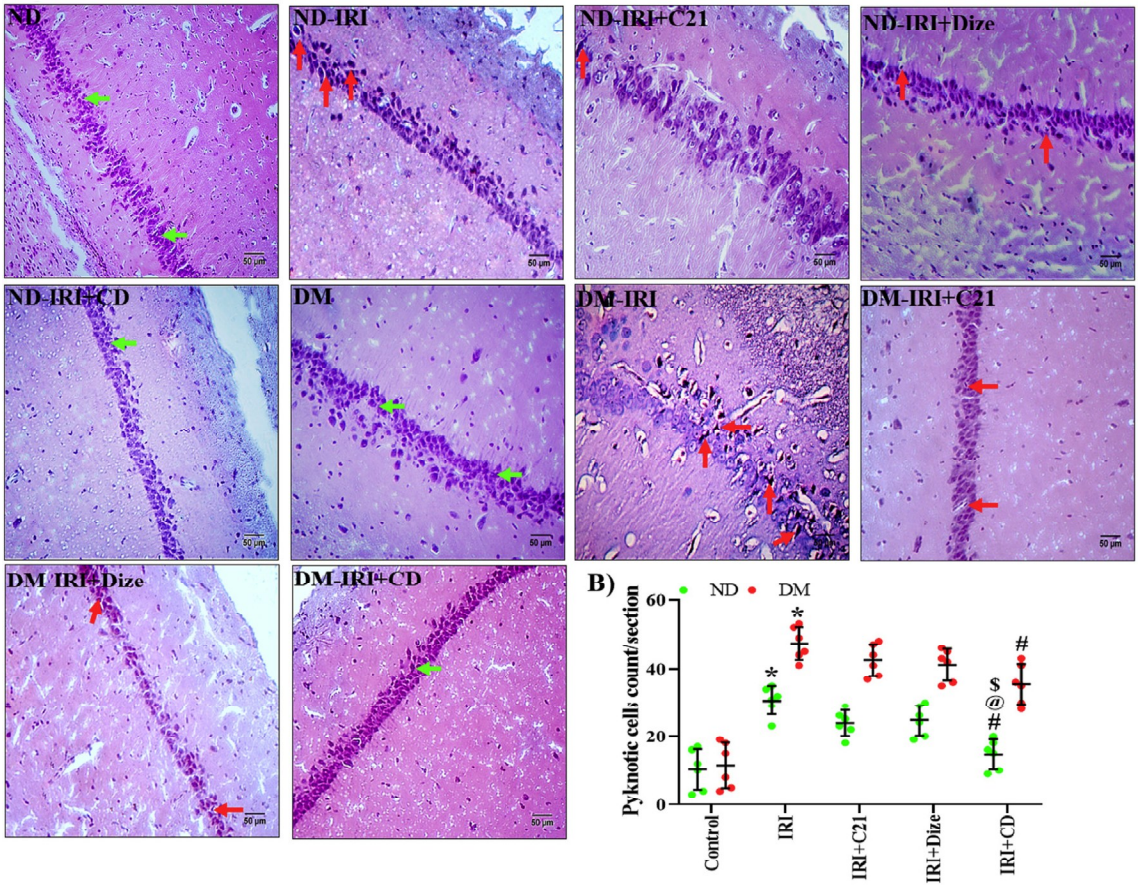

Fig. 4. Effect of AT2R and ACE2 activation on pyknotic neurons in the hippocampus of the brain. The brain samples from each group were collected at 24 h after surgery and were processed for histological examination by H and E staining. Representative images of brain sections magnifying CA1 region of hippocampus (original magnification 400× and scale bar- 50 μm). At least 4–5 images from each stained brain section and a total of six different brains per group were observed by a blinded observer for healthy (Green arrow) and pyknotic neuronal cells (Red arrow) (A). The pyknotic cell count was analysed semi-quantitatively (B). Data are represented as mean ± S.D. Two-way ANOVA with Tukey's multiple comparison test was applied for statistical comparison. $^{(*)}$ $P < 0.05$ vs control; $^{(\#)}$ $P < 0.05$ vs IRI; $^{(@)}$ $P < 0.05$ vs IRI-C21; $^{(\$)}$ $P < 0.05$ vs IRI-Dize.

3.9. AT2R and ACE2 activation improved hippocampal depressor arm and suppressed pressor arm components of diabetic and non-diabetic rats upon ischemic renal injury

In AKI, neurons get activated in stress-sensitive brain regions including hippocampus (Palkovits et al., 2009). In ND-IRI and DM-IRI rats, the hippocampal levels of Ang II (Fig. 8A) and Ang-(1–7) (Fig. 8B) were significantly increased and decreased, respectively, as compared to ND and DM rats. For hippocampal Ang II levels, DM-IRI rats showed higher Ang II levels as compared to ND-IRI rats (20.08 ± 1.5 vs. 15.49 ± 1.3). After combination therapy, ND-IRI rats showed significant reduction in Ang II levels compared to DM-IRI rats (11.68 ± 1.9 vs. 14.79 ± 1.5). For hippocampal Ang-(1–7) levels, ND-IRI rats showed lesser reduction in Ang-(1–7) levels as compared to DM-IRI rats (15.59 ± 3.1 vs. 9.52 ± 2.2). Among monotherapies, only Dize therapy has increased the Ang-(1–7) levels as compared to ND-IRI and DM-IRI rats. The combination therapy with C21 and Dize results in significant increased Ang-(1–7) levels as compared to ND/DM-IRI and both monotherapies groups (Fig. 8A and B).

IRI has significantly increased the hippocampal *At1r* mRNA expressions compared to ND and DM rats (Fig. 8C). DM-IRI rats showed significant elevated *At1r* mRNA expressions in comparison to ND-IRI rats (3.07 ± 0.39 vs. 2.11 ± 0.34). Here, neither monotherapies nor combination therapy normalised the *At1r* mRNA expression compared to ND-IRI and DM-IRI rats (Fig. 8C). On the other hand, the key receptors of depressor arm of RAS i.e. *At2r, Masr* mRNA expressions got elevated in ND-IRI and DM-IRI rats compared to ND and DM rats (Fig. 8D and E). Additionally, the combination treatment significantly raised the *At2r* and *Masr* mRNA expressions as compared to ND-IRI and DM-IRI rats (Fig. 8D and E). However, none of the monotherapies up-regulated the *At2r* and *Masr* mRNA expressions.

4. Discussion

Alteration in RAS plays a major role in neurological sequalae under diabetes and various kidney diseases (Cao et al., 2015; Padda et al., 2015). Individually, diabetes and AKI episodes reported to cause neurological dysfunction via disruption of blood brain barrier, activation of inflammatory cascade, derangement of neurotransmitters and altercation in RAS arms (Liu et al., 2008; Lu et al., 2015; Cao et al., 2017). Cao et al. have established the role of reno-cerebral RAS pathway under AKI as well as CKD (Cao et al., 2015, 2017).

Recently, depressor arm of RAS has gained the popularity as an important molecular target involved in various neurological dysfunctions like ischemic stroke and cognitive impairment (Bennion et al., 2017; Ahmed et al., 2019). However, its role in the pathophysiology of AKI abides poorly understood. Therefore, in the present study, we investigated the role of depressor arm of RAS on the neurological dysfunction induced by AKI in non-diabetic and diabetic rats. We found that IRI simultaneously activated the reno-cerebral RAS in ND and DM rats. The damaged kidneys and brain showed marked elevated oxidative stress levels and inflammatory cascade that impaired the cognitive

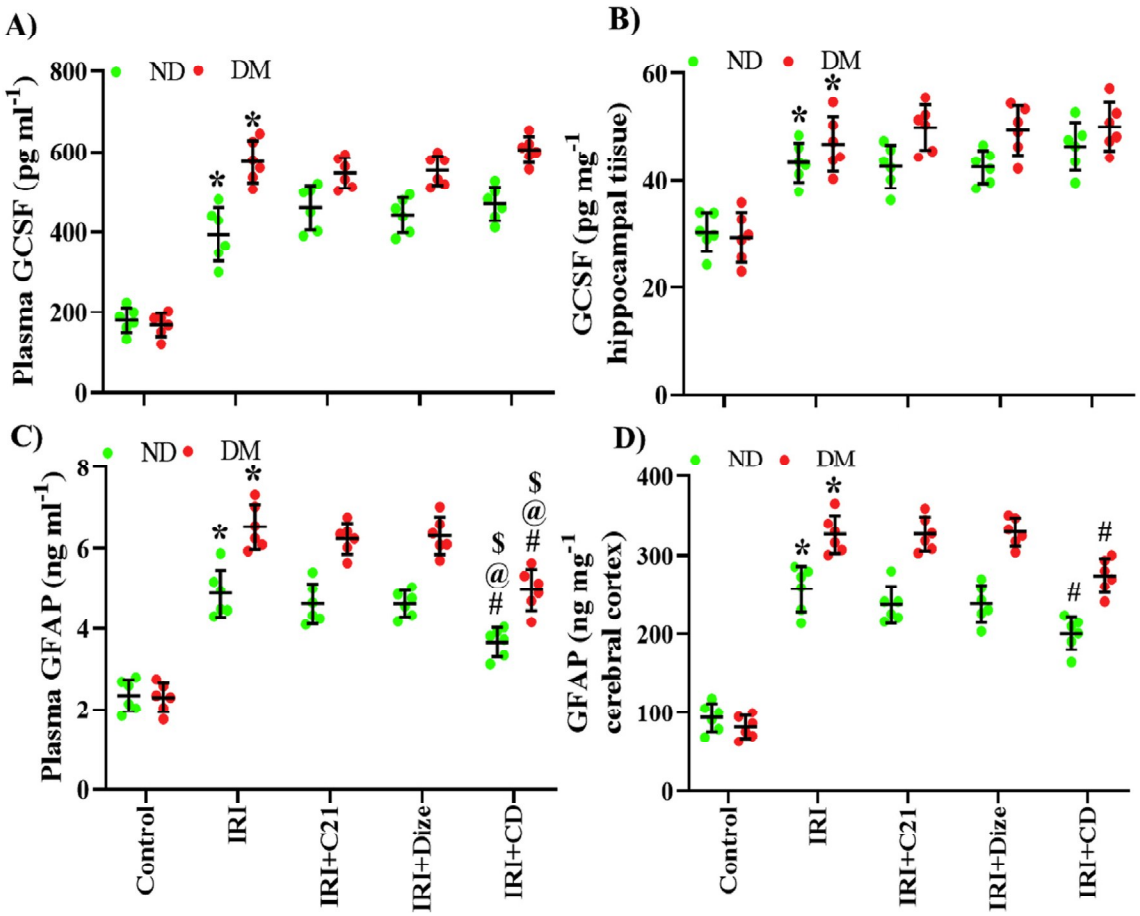

Fig. 5. Effect of C21 and Dize on systemic, hippocampal and cerebral cortex levels of GCSF and GFAP. A–B: Protein levels of GCSF in plasma (A) and hippocampal tissue (B); C–D: Protein levels of GFAP in plasma (C) and cerebral cortex (D) as measured by ELISA (n = 6). Data are represented as mean ± S.D. Two-way ANOVA with Tukey's multiple comparison test was applied for statistical comparison. $^{(*)}$ $P < 0.05$ vs control; $^{(\#)}$ $P < 0.05$ vs IRI; $^{(@)}$ $P < 0.05$ vs IRI-C21; $^{(\$)}$ $P < 0.05$ vs IRI-Dize.

behaviour of ND and DM rats. The alteration in reno-cerebral RAS leads to activation of pressor arm that result in increased Ang II levels and suppression of depressor arm causes depletion of Ang-(1–7) levels in renal and hippocampal tissue. Interestingly, the above-mentioned outcomes were significantly pronounced in DM-IRI rats compared to ND-IRI rats.

Treatment with the combination of two major depressor arm modulators, C21 (0.3 mg/kg/day, *i.p.*) and Dize (5 mg/kg/day, *p.o.*), attenuated the IRI induced increased in BUN, PCr and urinary KIM-1 levels in ND and DM rats. Thus, suggesting the potential of AT2R agonist and ACE2 activator in normalising the kidney functional parameters (Fig. 2). Similar results were obtained in previous reports, where improved BUN and PCr levels was observed in IRI and diabetic rats as a result of Dize administration (Malek and Nematbakhsh, 2014; Goru et al., 2017).

Both AKI and diabetes have been reportedly elevated the cerebral oxidative damage (Kovalcikova et al., 2018; Etienne et al., 2019). Increased brain oxidative stress markers (MDA, nitrite levels) most prominently found in hippocampal region of brain after IRI episode (Kovalcikova et al., 2018). In this study, DM-IRI rats showed marked increase in MDA and nitrite levels in isolated proximal tubular and hippocampal homogenates compared to ND-IRI rats. Combination therapy of C21 and Dize has significantly attenuated the increased MDA and nitrite levels in ND-IRI rats. However, a similar suppression was not observed in DM-IRI rats (Fig. 3).

Next, we performed behavioural assessment using actophotometer in DM-IRI and ND-IRI rats. IRI has severely impaired locomotor activity in DM rats compared to ND rats. Regarding the mechanism of altered motor activity, increased uremia leads to change in monoamine metabolism (specifically dopamine) and further altered motor activity (Adachi et al., 2001; Verma et al., 2018). The connecting link of reno-cerebral RAS axis remains the another possibility to alter motor activity in IRI rats (Cao et al., 2017). Combination therapy of C21 and Dize has improved the motor activity to a greater extent in ND rats compared to DM rats (Fig. 3).

Histopathological evaluation by H and E staining revealed elevated pyknotic neuronal cells in CA1 of the hippocampus. The hippocampus imparts a kin role in learning and memory as well as in anxiety and depression (Hollands et al., 2016; Anacker and Hen, 2017). Selectively, CA1 region remains the highly vulnerable hippocampal part to degenerate in various pathological anomalies (Bordi et al., 2016; Lee et al., 2017). Previous reports in Alzheimer's disease and diabetes showed the existence of CA1 pathology and inflammation along with hypoactivity in actophotometer (Sharma et al., 2015; Wei et al., 2019). Therefore, IRI induced damage to hippocampal CA1 neurons could account for hypoactivity of the rats. Whereas, concomitant therapy of C21 and Dize showed significant alleviation of neuronal damage in these regions in ND rats compared to DM rats (Fig. 4).

GCSF is a hematopoietic growth factor that regulates proliferation and differentiation of neural stem cells. Studies has revealed its neuroprotective role under Alzheimer disease and cerebral ischemia (Li et al., 2015; Wu et al., 2017). In our study, IRI results in elevated circulating and hippocampal GCSF levels in ND and DM rats. However, none of the treatment has further enhanced the GCSF levels. In higher vertebrates,

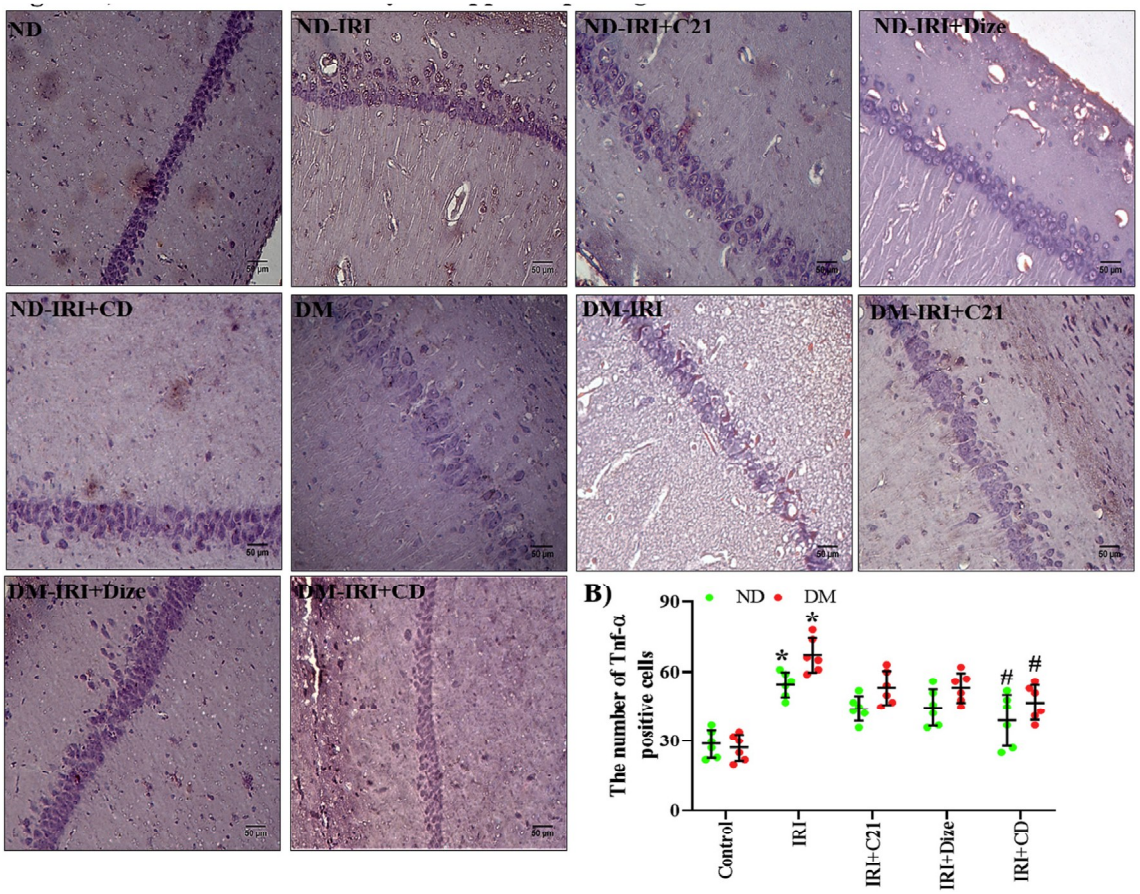

Fig. 6. Immunohistochemistry for TNF-α in the CA1 region of hippocampus. A: Representative images of IHC staining for TNF-α in the CA1 region of hippocampus (original magnification 400 × and scale bar 50 μm). Around 4–5 sections from each stained brain microscopy slide and total six different brain slides per group were seen under microscope and images were captured. B: Semi-quantitative analysis of all the images via ImageJ (colour deconvolution plugin was utilised for analysis) for calculating DAB-positive area. All Data are represented as mean ± S.D. Two-way ANOVA with Tukey's multiple comparison test was used for statistical comparison. $^{(*)}$ $P < 0.05$ vs control; $^{(\#)}$ $P < 0.05$ vs IRI; $^{(@)}$ $P < 0.05$ vs IRI-C21; $^{(\$)}$ $P < 0.05$ vs IRI-Dize.

brain injury resulted from chemical insult, trauma, genetic disorders or AKI, consequently elevated the reactive astrocytes which increased the GFAP synthesis in cerebral cortex, hippocampus, GFAP considered as inflammatory sign in brain tissue and is proved by protein levels and immunostaining GFAP (Liu et al., 2008; Cao et al., 2017). Similarly, we also observed the elevated GFAP protein levels in both plasma and cerebral cortices of DM-IRI rats compared to ND-IRI rats. After combination therapy, ND rats showed marked reduction in GFAP levels compared to DM rats (Fig. 5).

Both clinical and laboratory reports evidenced that IRI results in an upsurge of brain inflammation via over-expressing of pro-inflammatory cytokines such as keratinocyte derived chemoattractant (KC), IL-1, TNF-α, macrophage inflammatory protein (MIP)-1, and monocyte chemoattractant protein-1 (MCP-1) (Lee et al., 2018). With respect to these results, our study also showed increased TNF-α expression evaluated by immunostaining. In ND rats, combination therapy significantly attenuated the TNF- α levels as compared to DM rats (Fig. 6). These results are in streak with previous studies indicating the ability of AT2R and ACE2 stimulation to reduce inflammatory cytokines production and mediate neuro-protective role in cerebral stroke and Alzheimer's Disease (Min et al., 2014; Kamel et al., 2018).

Available literature established a mechanistic link between the down regulation of RAS depressor arm [AT2R/ACE2/Ang-(1–7)/MasR axis] and neurological dysfunction (Bennion et al., 2017; Kangussu et al., 2017). In this regards, depressor arm modulators strongly proved their neuro-protective role in vascular stroke, Alzheimer's disease, and anxiety conditions by virtue of increasing AT2R, ACE2, Ang-(1–7) and MasR expressions (Chen et al., 2014; Dai et al., 2015; Fuchtemeier et al., 2015; Wang et al., 2016). In line with these findings, we first examined the RAS components in the renal proximal tubules and urine samples. In proximal tubules, IRI resulted in significant elevation of ACE, Ang II levels and marked reduction of Ang-(1–7) and ACE2 levels of DM rats compared to ND rats. However, combination treatment significantly reduced the ACE, Ang II levels, and augmented the Ang-(1–7), ACE2 levels in ND and DM rats. On the other hand, increased urinary AGT levels were markedly reduced with concomitant AT2R and ACE2 stimulation in ND and DM rats (Fig. 7). IRI reported to stimulate a sympathetic reflex that interconnect the renal and cerebral RAS and promotes free radical generation, eventually progression of renal injury (Cao et al., 2017). Similarly, we observed the effect of IRI on hippocampal RAS, and found elevation in pressor arm and suppression of depressor arm components in ND and DM rats. Combination therapy has effectively normalised the Ang II levels, however; Ang-(1–7) protein levels, At2r and MasR mRNA expressions were significantly upregulated in ND and DM rats. Interestingly, we found that the aforesaid results were more distinct in ND rats compared to DM rats (Fig. 8).

The current study is aimed to explore the neuroprotective benefits of targeting the depressor arm of RAS against the acute responses of IRI. Recent epidemiological and experimental data have provided substantial information that AKI imparts to the development and progression of chronic kidney diseases and its associated distant organ dysfunction such as neurological dysfunction (Chawla et al., 2014; Ferenbach and Bonventre, 2015; Shiao et al., 2015; Venkatachalam et al., 2015; Basile et al., 2016). Though, it remains a notable query of

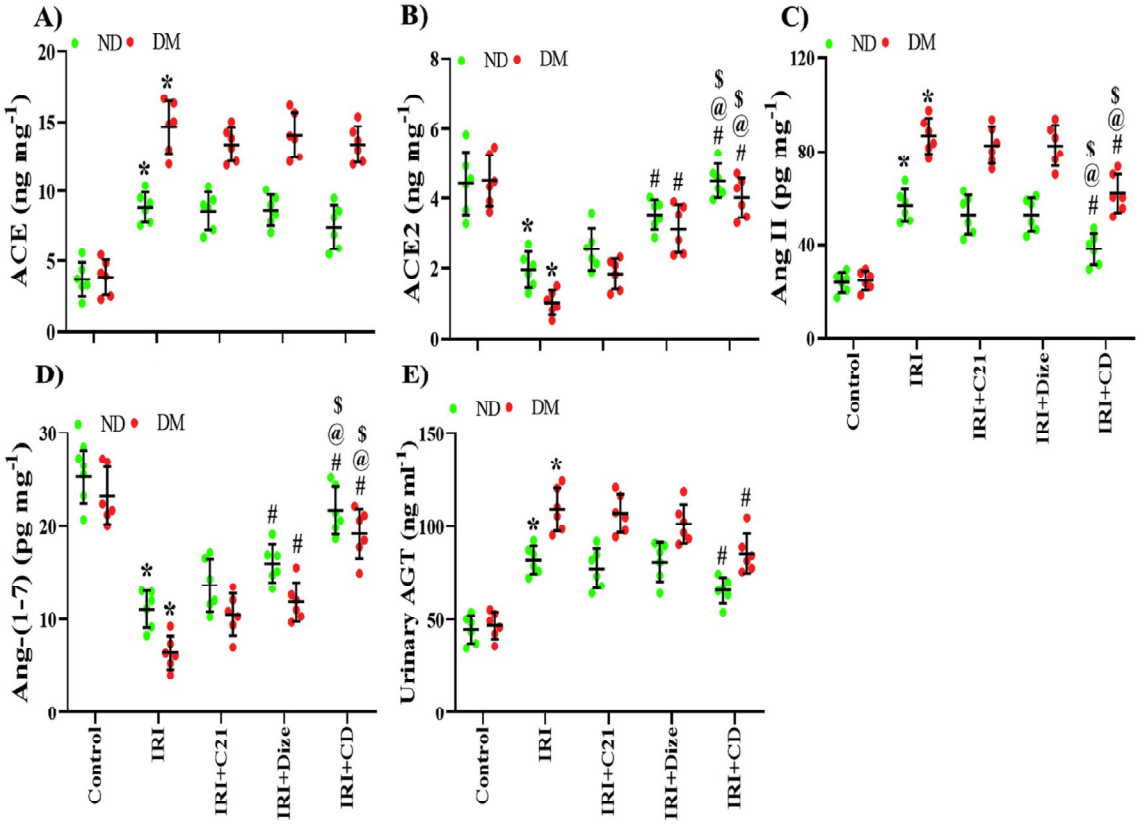

Fig. 7. AT2R and ACE2 activation modulates protein levels of pressor and depressor components of RAS in proximal tubules. A–D: Protein levels of ACE, ACE2, Ang II and Ang-(1–7) in isolated proximal tubules, and urinary AGT (E) was measured by ELISA (n = 6). Data are represented as mean ± S.D. Two-way ANOVA with Tukey's multiple comparison test was applied for statistical comparison. (*) $P < 0.05$ vs control; (#) $P < 0.05$ vs IRI; (@) $P < 0.05$ vs IRI-C21; ($) $P < 0.05$ vs IRI-Dize.

the impact of depressor arm modulators (C21 and Dize) treatment on longer-term neurological outcomes, which is the limitation of the present study. Therefore, we expect that future studies are required in this area where substantial changes would be detected at later time points post-IRI and will determine the effects of C21 and Dize under such pathological condition.

It has been proven difficult to target CNS with pharmacotherapy because the blood brain barrier (BBB) prohibits several molecules and restricts their activity centrally (Pardridge, 2005). Altogether, small and lipophilic molecules having molecular mass less than 400–500 g/mol crosses BBB (Ghose et al., 1999). However, BBB disruption occurs following ischemic renal insult, which consequently increases the BBB permeability (Nongnuch et al., 2014). Regarding the drug distribution profile, C21 and Dize effectively circulates among kidney, heart, liver and brain (Kuriakose and Uzonna, 2014; Namsolleck et al., 2014). Interestingly, intraperitoneal administration of C21 and Dize have already been reported for their neuroprotective role either directly, or by the anti-inflammatory action (secondary neuroprotection) under stroke and Alzheimer's disease (Joseph et al., 2014; Bennion et al., 2015; Evans et al., 2020). As the current study is limited to the peripheral treatment strategy for IRI-associated neurological dysfunction, future studies focusing on the intracerebroventricular administration of C21 and Dize would provide crucial neurological data which would be more direct to the brain.

5. Conclusion

To the best of our knowledge, this is the first study revealing that down-regulation of depressor arm of RAS played a major role in IRI-induced neurological dysfunction, which are significantly halted by combination therapy of AT2R agonist and ACE2 activator. The observed beneficial effects of C21 and Dize therapy is likely to be mediated by increased ACE2/Ang-(1–7)/AT2R/MasR axis expressions, which concurrently diminished brain soluble inflammatory mediator, GFAP and other cytokines like, TNF-α. It also diminished brain oxidative stress along with improved locomotor activity. Therefore, this study strongly holds the potential of depressor arm activation as novel therapeutic approaches to attenuate neurological sequalae associated with IRI under diabetic and non-diabetic condition.

Funding

This research was funded by the Science & Engineering Research Board -Department of Science & Technology (SERB - DST), Govt. of India [SERB/ECR/2017/000317].

CRediT authorship contribution statement

Nisha Sharma: Methodology, Data curation, Formal analysis, Validation, Visualization, Writing - original draft, Writing - review & editing. **Anil Bhanudas Gaikwad:** Conceptualization, Funding acquisition, Supervision, Writing - review & editing.

Declaration of competing interest

The authors declare no potential conflicts of interest.

Acknowledgements

N.S. sincerely acknowledges the Indian Council of Medical Research (ICMR) for providing senior research fellowship [45/54/2019/PHA/

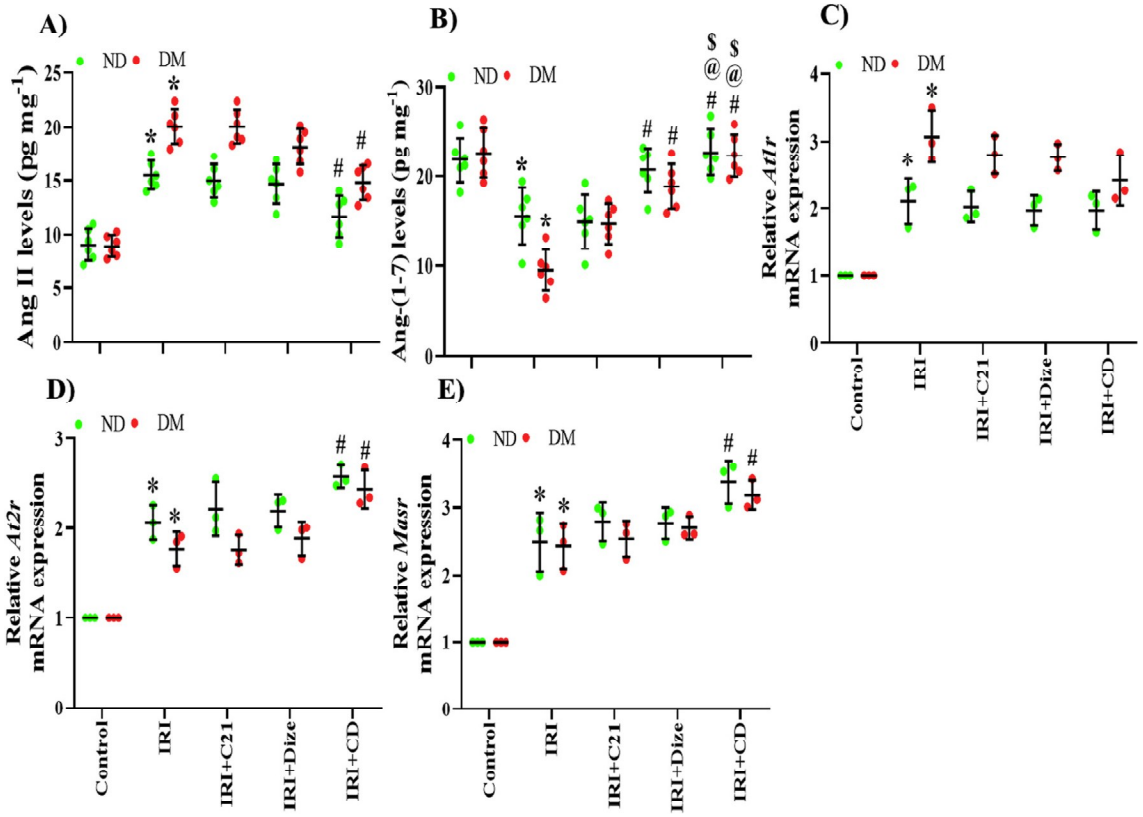

Fig. 8. Effect of C21, Dize and their combination therapy on protein and mRNAexpressions of RAS components in hippocampal tissue. A–B: Protein expression of Ang II and Ang-(1–7) in hippocampal tissue homogenate was assessed by ELISA (n = 6). C–D: mRNA expressions of *At1r*, *At2r* and *Masr* was checked by qRT-PCR in brain hippocampus. 18s rRNA expression was used as internal control. Data are represented as mean ± S.D. from three independent experiments. Two-way ANOVA with Tukey's multiple comparison test was utilised for statistical comparison. (*) $P < 0.05$ vs control; (#) $P < 0.05$ vs IRI; (@) $P < 0.05$ vs IRI-C21; ($) $P < 0.05$ vs IRI-Dize.

BMS]. The authors also thank Anders Ljunggren, Vicore Pharma, Sweden, for his suggestions and for offering the drug sample, Compound 21.

Appendix A. Supplementary data

Supplementary data to this article can be found online at https://doi.org/10.1016/j.ejphar.2020.173241.

References

Adachi, N., Lei, B., Deshpande, G., et al., 2001. Uraemia suppresses central dopaminergic metabolism and impairs motor activity in rats. Intensive Care Med. 27, 1655–1660. https://doi.org/10.1007/s001340101067.

Ahmed, H.A., Ishrat, T., Pillai, B., et al., 2019. Angiotensin receptor (AT2R) agonist C21 prevents cognitive decline after permanent stroke in aged animals—a randomized double-blind pre-clinical study. Behav. Brain Res. 359, 560–569. https://doi.org/10.1016/j.bbr.2018.10.010.

Anacker, C., Hen, R., 2017. Adult hippocampal neurogenesis and cognitive flexibility—linking memory and mood. Nat. Rev. Neurosci. 18, 335. https://doi.org/10.1038/nrn.2017.45.

Basile, D.P., Bonventre, J.V., Mehta, R., et al., 2016. Progression after AKI: understanding maladaptive repair processes to predict and identify therapeutic treatments. J. Am. Soc. Nephrol. 27, 687–697. https://doi.org/10.1681/ASN.2015030309.

Baumgaertel, M.W., Kraemer, M., Berlit, P., 2014. Neurologic complications of acute and chronic renal disease. In: Handbook of Clinical Neurology, vol. 119. Elsevier, pp. 383–393.

Bennion, D.M., Haltigan, E.A., Irwin, A.J., et al., 2015. Activation of the neuroprotective angiotensin-converting enzyme 2 in rat ischemic stroke. Hypertension 66, 141–148. https://doi.org/10.1016/B978-0-7020-4086-3.00024-2.

Bennion, D.M., Isenberg, J.D., Harmel, A.T., et al., 2017. Post-stroke angiotensin II type 2 receptor activation provides long-term neuroprotection in aged rats. PloS One 12, e0180738. https://doi.org/10.1161/HYPERTENSIONAHA.115.05185.

Bordi, M., Berg, M.J., Mohan, P.S., et al., 2016. Autophagy flux in CA1 neurons of Alzheimer hippocampus: increased induction overburdens failing lysosomes to propel neuritic dystrophy. Autophagy 12, 2467–2483. https://doi.org/10.1080/15548627.2016.1239003.

Campbell, D.J., 2014. Clinical relevance of local renin angiotensin systems. Front. Endocrinol. 5, 113. https://doi.org/10.3389/fendo.2014.00113.

Cao, W., Li, A., Wang, L., et al., 2015. A salt-induced reno-cerebral reflex activates renin-angiotensin systems and promotes CKD progression. J. Am. Soc. Nephrol. 26, 1619–1633. https://doi.org/10.1681/ASN.201405051.

Cao, W., Li, A., Li, J., et al., 2017. Reno-cerebral reflex activates the renin-angiotensin system, promoting oxidative stress and renal damage after ischemia-reperfusion injury. Antioxidants Redox Signal. 27, 415–432. https://doi.org/10.1089/ars.2016.6827.

Chawla, L.S., Eggers, P.W., Star, R.A., et al., 2014. Acute kidney injury and chronic kidney disease as interconnected syndromes. N. Engl. J. Med. 371, 58–66. https://doi.org/10.1056/NEJMra1214243.

Chen, J., Zhao, Y., Chen, S., et al., 2014. Neuronal over-expression of ACE2 protects brain from ischemia-induced damage. Neuropharmacology 79, 550–558. https://doi.org/10.1016/j.neuropharm.2014.01.004.

Chou, A.-H., Lee, C.-M., Chen, C.-Y., et al., 2014. Hippocampal transcriptional dysregulation after renal ischemia and reperfusion. Brain Res. 1582, 197–210. https://doi.org/10.1016/j.brainres.2014.07.030.

Classics Lowry, O., Rosebrough, N., Farr, A., et al., 1951. Protein measurement with the Folin phenol reagent. J. Biol. Chem. 193, 265–275.

Curtis, M.J., Bond, R.A., Spina, D., et al., 2015. Experimental design and analysis and their reporting: new guidance for publication in BJP. Br. J. Pharmacol. 172, 3461–3471. https://doi.org/10.1111/bph.12856.

Dai, S.-Y., Peng, W., Zhang, Y.-P., et al., 2015. Brain endogenous angiotensin II receptor type 2 (AT2-R) protects against DOCA/salt-induced hypertension in female rats. J. Neuroinflammation 12, 1–11. https://doi.org/10.1186/s12974-015-0261-4.

Etienne, I., Magalhães, L.V.B., Cardoso, S.A., et al., 2019. Oxidative stress markers in cognitively intact patients with diabetic neuropathy. Brain Res. Bull. 150, 196–200. https://doi.org/10.1016/j.brainresbull.2019.06.001.

Evans, C.E., Miners, J.S., Piva, G., et al., 2020. ACE2 activation protects against cognitive decline and reduces amyloid pathology in the Tg2576 mouse model of Alzheimer's disease. Acta Neuropathol. 139, 485–502.

Ferenbach, D.A., Bonventre, J.V., 2015. Mechanisms of maladaptive repair after AKI leading to accelerated kidney ageing and CKD. Nat. Rev. Nephrol. 11, 264–276. https://doi.org/10.1038/nrneph.2015.3.

Fuchtemeier, M., Brinckmann, M.P., Foddis, M., et al., 2015. Vascular change and opposing effects of the angiotensin type 2 receptor in a mouse model of vascular cognitive impairment. J. Cerebr. Blood Flow Metabol. 35, 476–484. https://doi.org/10.

1038/jcbfm.2014.221.
Ghose, A.K., Viswanadhan, V.N., Wendoloski, J.J., 1999. A knowledge-based approach in designing combinatorial or medicinal chemistry libraries for drug discovery. 1. A qualitative and quantitative characterization of known drug databases. J. Comb. Chem. 1, 55–68. https://doi.org/10.1021/cc98000718.
Goru, S.K., Kadakol, A., Malek, V., et al., 2017. Diminazene aceturate prevents nephropathy by increasing glomerular ACE2 and AT2 receptor expression in a rat model of type1 diabetes. Br. J. Pharmacol. 174, 3118–3130. https://doi.org/10.1111/bph.13946.
Han, W., Waikar, S., Johnson, A., et al., 2008. Urinary biomarkers in the early diagnosis of acute kidney injury. Kidney Int. 73, 863–869. https://doi.org/10.1038/sj.ki.5002715.
Hollands, C., Bartolotti, N., Lazarov, O., 2016. Alzheimer's disease and hippocampal adult neurogenesis; exploring shared mechanisms. Front. Neurosci. 10, 178. https://doi.org/10.3389/fnins.2016.00178.
Joseph, J.P., Mecca, A.P., Regenhardt, R.W., et al., 2014. The angiotensin type 2 receptor agonist Compound 21 elicits cerebroprotection in endothelin-1 induced ischemic stroke. Neuropharmacology 81, 134–141. https://doi.org/10.1016/j.neuropharm.2014.01.044.
Kamel, A.S., Abdelkader, N.F., Abd El-Rahman, S.S., et al., 2018. Stimulation of ACE2/ANG(1-7)/mas Axis by diminazene ameliorates Alzheimer's disease in the D-galactose-ovariectomized rat model: role of PI3K/akt pathway. Mol. Neurobiol. 55, 8188–8202. https://doi.org/10.1007/s12035-018-0966-3.
Kangussu, L.M., Almeida-Santos, A.F., Moreira, F.A., et al., 2017. Reduced anxiety-like behavior in transgenic rats with chronically overproduction of angiotensin-(1–7): role of the Mas receptor. Behav. Brain Res. 331, 193–198. https://doi.org/10.1016/j.bbr.2017.05.026.
Kilkenny, C., Browne, W.J., Cuthill, I.C., et al., 2010. Improving bioscience research reporting: the ARRIVE guidelines for reporting animal research. PLoS Biol. 8, e1000412. https://doi.org/10.1371/journal.pbio.1000412.
Kovalcikova, A., Gyuraszova, M., Vavrincova-Yaghi, D., et al., 2018. Oxidative stress in the brain caused by acute kidney injury. Metab. Brain Dis. 33, 961–967. https://doi.org/10.1155/2019/8690805.
Kumar, S., 2018. Cellular and molecular pathways of renal repair after acute kidney injury. Kidney Int. 93, 27–40. https://doi.org/10.1016/j.kint.2017.07.030.
Kuriakose, S., Uzonna, J.E., 2014. Diminazene aceturate (Berenil), a new use for an old compound? Int. Immunopharm. 21, 342–345. https://doi.org/10.1016/j.intimp.2014.05.027.
Lee, J.C., Park, J.H., Kim, I.H., et al., 2017. Neuroprotection of ischemic preconditioning is mediated by thioredoxin 2 in the hippocampal CA1 region following a subsequent transient cerebral ischemia. Brain Pathol. 27, 276–291. https://doi.org/10.1111/bpa.12389.
Lee, S.A., Cozzi, M., Bush, E.L., et al., 2018. Distant organ dysfunction in acute kidney injury: a review. Am. J. Kidney Dis. 72, 846–856. https://doi.org/10.1053/j.ajkd.2018.03.028.
Li, L., McBride, D.W., Doycheva, D., et al., 2015. G-CSF attenuates neuroinflammation and stabilizes the blood–brain barrier via the PI3K/Akt/GSK-3β signaling pathway following neonatal hypoxia-ischemia in rats. Exp. Neurol. 272, 135–144. https://doi.org/10.1016/j.expneurol.2014.12.020.
Lima-Posada, I., Fontana, F., Pérez-Villalva, R., et al., 2019. Pirfenidone prevents acute kidney injury in the rat. BMC Nephrol. 20, 158. https://doi.org/10.1186/s12882-019-1364-4.
Liu, M., Liang, Y., Chigurupati, S., et al., 2008. Acute kidney injury leads to inflammation and functional changes in the brain. J. Am. Soc. Nephrol. 19, 1360–1370. https://doi.org/10.1681/ASN.2007080901.
Lu, R., Kiernan, M.C., Murray, A., et al., 2015. Kidney–brain crosstalk in the acute and chronic setting. Nat. Rev. Nephrol. 11, 707–719. https://doi.org/10.1038/nrneph.2015.131.
Malek, M., Nematbakhsh, M., 2014. The preventive effects of diminazene aceturate in renal ischemia/reperfusion injury in male and female rats. Adv. Prevent. Med. 2014, 740647. https://doi.org/10.1155/2014/740647. 2014.
Malek, V., Gaikwad, A.B., 2018. Telmisartan and thiorphan combination treatment attenuates fibrosis and apoptosis in preventing diabetic cardiomyopathy. Cardiovasc. Res. 115, 373–384. https://doi.org/10.1093/cvr/cvy226.
Mansfield, K.E., Nitsch, D., Smeeth, L., et al., 2016. Prescription of renin–angiotensin system blockers and risk of acute kidney injury: a population-based cohort study BMJ Open 6, e012690. https://doi.org/10.1136/bmjopen-2016-012690.
Min, L.J., Mogi, M., Tsukuda, K., et al., 2014. Direct stimulation of angiotensin II type 2 receptor initiated after stroke ameliorates ischemic brain damage. Am. J. Hypertens. 27, 1036–1044. https://doi.org/10.1093/ajh/hpu01.
Monseu, M., Gand, E., Saulnier, P.-J., et al., 2015. Acute kidney injury predicts major adverse outcomes in diabetes: synergic impact with low glomerular filtration rate and albuminuria. Diabetes Care 38, 2333–2340. https://doi.org/10.2337/dc15-1222.
Namsolleck, P., Recarti, C., Foulquier, S., et al., 2014. AT2 receptor and tissue injury: therapeutic implications. Curr. Hypertens. Rep. 16, 1–10. https://doi.org/10.1007/s11906-013-0416-6.
Nongnuch, A., Panorchan, K., Davenport, A., 2014. Brain–kidney crosstalk. Crit. Care 18, 225. https://doi.org/10.1186/cc13907.
Padda, R.S., Shi, Y., Lo, C.-S., et al., 2015. Angiotensin-(1-7): a novel peptide to treat hypertension and nephropathy in diabetes? J. Diabetes Metabol https://doi.org/10.4172/2155-6156.1000615.
Palkovits, M., Sebekova, K., Gallatz, K., et al., 2009. Neuronal activation in the CNS during different forms of acute renal failure in rats. Neuroscience 159, 862–882. https://doi.org/10.1016/j.neuroscience.2008.12.062.
Pandey, A., Gaikwad, A.B., 2017. Compound 21 and Telmisartan combination mitigates type 2 diabetic nephropathy through amelioration of caspase mediated apoptosis. Biochem. Biophys. Res. Commun. 487, 827–833. https://doi.org/10.1016/j.bbrc.2017.04.13.
Pardridge, W.M., 2005. The blood-brain barrier: bottleneck in brain drug development. NeuroRx 2, 3–14. https://doi.org/10.1602/neurorx.2.1.
Sharma, N., Anders, H.-J., Gaikwad, A.B., 2019a. Fiend and friend in the renin angiotensin system: an insight on acute kidney injury. Biomed. Pharmacother. 110, 764–774. https://doi.org/10.1016/j.biopha.2018.12.018.
Sharma, N., Malek, V., Mulay, S.R., et al., 2019b. Angiotensin II type 2 receptor and angiotensin-converting enzyme 2 mediate ischemic renal injury in diabetic and non-diabetic rats. Life Sci. 235, 116796. https://doi.org/10.1016/j.lfs.2019.116796.
Sharma, S., Taliyan, R., 2016. Epigenetic modifications by inhibiting histone deacetylases reverse memory impairment in insulin resistance induced cognitive deficit in mice. Neuropharmacology 105, 285–297. https://doi.org/10.1016/j.neuropharm.2016.01.025.
Sharma, S., Taliyan, R., Ramagiri, S., 2015. Histone deacetylase inhibitor, trichostatin A, improves learning and memory in high-fat diet-induced cognitive deficits in mice. J. Mol. Neurosci. 56, 1–11. https://doi.org/10.1007/s12031-014-0461-x.
Shiao, C.C., Wu, P.C., Huang, T.M., et al., 2015. Long-term remote organ consequences following acute kidney injury. Crit. Care 19, 438. https://doi.org/10.1186/s13054-015-1149-5.
Venkatachalam, M.A., Weinberg, J.M., Kriz, W., et al., 2015. Failed tubule recovery, AKI-CKD transition, and kidney disease progression. J. Am. Soc. Nephrol. 26, 1765–1776. https://doi.org/10.1681/ASN.2015010006.
Verma, L., Agrawal, D., Jain, N.S., 2018. Enhanced central histaminergic transmission attenuates compulsive-like behavior in mice. Neuropharmacology 138, 106–117. https://doi.org/10.1016/j.neuropharm.2018.05.031.
Wang, L., de Kloet, A.D., Pati, D., et al., 2016. Increasing brain angiotensin converting enzyme 2 activity decreases anxiety-like behavior in male mice by activating central Mas receptors. Neuropharmacology 105, 114–123. https://doi.org/10.1016/j.neuropharm.2015.12.026.
Wei, J., Yang, F., Gong, C., et al., 2019. Protective effect of daidzein against streptozotocin-induced Alzheimer's disease via improving cognitive dysfunction and oxidative stress in rat model. J. Biochem. Mol. Toxicol., e22319. https://doi.org/10.1002/jbt.22319.
Wu, C.C., Wang, I.F., Chiang, P.M., et al., 2017. G-CSF-mobilized bone marrow mesenchymal stem cells replenish neural lineages in Alzheimer's disease mice via CXCR4/SDF-1 chemotaxis. Mol. Neurobiol. 54, 6198–6212. https://doi.org/10.1007/s12035-016-0122-x.
Wu, V.C., Wu, P.C., Wu, C.H., et al., 2014. The impact of acute kidney injury on the long-term risk of stroke. J. Am. Heart Assoc. 3, e000933. https://doi.org/10.1161/JAHA.114.000933.

Environmental Toxicology and Pharmacology 80 (2020) 103501

Contents lists available at ScienceDirect

Environmental Toxicology and Pharmacology

journal homepage: www.elsevier.com/locate/etap

Ameliorative effect of AT2R and ACE2 activation on ischemic renal injury associated cardiac and hepatic dysfunction

Nisha Sharma, Anil Bhanudas Gaikwad *

Laboratory of Molecular Pharmacology, Department of Pharmacy, Birla Institute of Technology and Science Pilani, Pilani Campus, Rajasthan, 333031, India

ARTICLE INFO

Keywords:
Ischemic renal injury
Diabetes
Renin-angiotensin system
AT2R agonist
ACE2 activator

ABSTRACT

This study explored the role of the depressor arm of renin angiotensin system (RAS) on ischemic renal injury (IRI)-associated cardio-hepatic sequalae under non-diabetic (ND) and diabetes mellitus (DM) conditions. Firstly, rats were injected with Streptozotocin (55 mg/kg *i.p.*) to develop DM. ND and DM rats underwent Bilateral IRI followed by 24 h of reperfusion. Further, ND and DM rats were subjected to AT2R agonist-Compound 21 (C21) (0.3 mg/kg/day, *i.p.*) or ACE2 activator- Diminazene Aceturate (Dize), (5 mg/kg/day, *p.o.*) per se or its combination therapy. As results, IRI caused cardio-hepatic injuries via altered oxidant/anti-oxidant levels, elevated inflammatory events, and altered protein expressions of ACE, ACE2, Ang II, Ang (1–7) and urinary AGT. However, concomitant therapy of AT2R agonist and ACE2 activator exerts a protective effect in IRI-associated cardio-hepatic dysfunction as evidenced by inhibited oxidative stress, downregulated inflammation, and enhanced cardio-hepatic depressor arm of RAS under ND and DM conditions.

1. Introduction

Acute kidney injury (AKI) is one of the major challenging medical conditions for which there is no defined therapy so far (Vanmassenhove et al., 2017). Under clinical settings, the association of co-morbidities, such as diabetes made patients more vulnerable to AKI (Monseu et al., 2015). Among various factors, ischemic renal injury (IRI) remains the most common cause of AKI. Moreover, AKI-induced multiorgan dysfunction is of serious concern because it results in a higher mortality rate (Lee et al., 2018). Due to the organ crosstalk, the renal injury may cause damage to distant organs such as liver, heart, brain, lungs, intestines and bone marrow; however, the precise mechanism behind is still elusive. Nevertheless, possible pathways proposed by the scientists such as vascular inflammation, metabolic acidosis, electrolyte imbalances triggered life-threatening arrhythmias, reactive oxygen species (ROS), upregulation of systemic cytokines, neurohumoral factors, and proapoptotic pathways (Bucsics and Krones, 2017; Lee et al., 2018; Panicoa et al., 2019). Besides these known characteristic mechanisms, there is another crucial factor with immediate impact on distant organs, i.e., the renin-angiotensin system (RAS) (Bucsics and Krones, 2017; Panicoa et al., 2019).

Recently, we have thoroughly reviewed the role of RAS controlling several pathological signalling that contributes to AKI (Sharma et al., 2019a). In clinical settings, treatment with pressor arm modulators, i.e. angiotensin converting enzyme inhibitor (ACEi) and angiotensin II type 2 receptor blockers (ARBs) claimed to worsens the patients' condition via deteriorating glomerular filtration rate (Mansfield et al., 2016). Hence, we established the role of depressor arm of RAS in IRI under normal- and hyperglycaemia condition (Sharma et al., 2019b). Our report explained that diabetic unilateral-ischemic rats presented up- and downregulation of pressor RAS and depressor RAS, respectively, resulted in a rapid upsurge of free radical generation, inflammation, apoptotic markers along with severe histological alterations in the proximal tubules. Further, treatment with depressor arm modulators; Compound 21 (C21) and Diminazene aceturate (Dize), the depressor arm components get over-expressed which suppressed the pathological signalling in IRI and protected the proximal tubular morphological alterations (Sharma et al., 2019b). Remarkably, the clinical relevance proposed that all the organs have their own local RAS, which remains compartmentalised from the circulation (Campbell, 2014). Following a similar approach, recent reports have demonstrated the activation of local RAS in distant organs; heart and liver (Taskin and Guven, 2017;

Abbreviations: AKI, acute kidney injury; ACE, angiotensin-converting enzyme; ACE2, angiotensin-converting enzyme 2; Ang II, angiotensin II; Ang-(1–7), angiotensin-(1–7); AT2R, angiotensin II type 2 receptor; DM, diabetes mellitus; IRI, ischemic renal injury; ND, non-diabetic; RAS, renin-angiotensin system.

* Corresponding author at: Department of Pharmacy, Birla Institute of Technology and Science Pilani, Pilani Campus, Pilani, 333031, Rajasthan, India.
E-mail address: anil.gaikwad@pilani.bits-pilani.ac.in (A.B. Gaikwad).

https://doi.org/10.1016/j.etap.2020.103501
Received 5 April 2020; Received in revised form 12 September 2020; Accepted 17 September 2020
Available online 23 September 2020

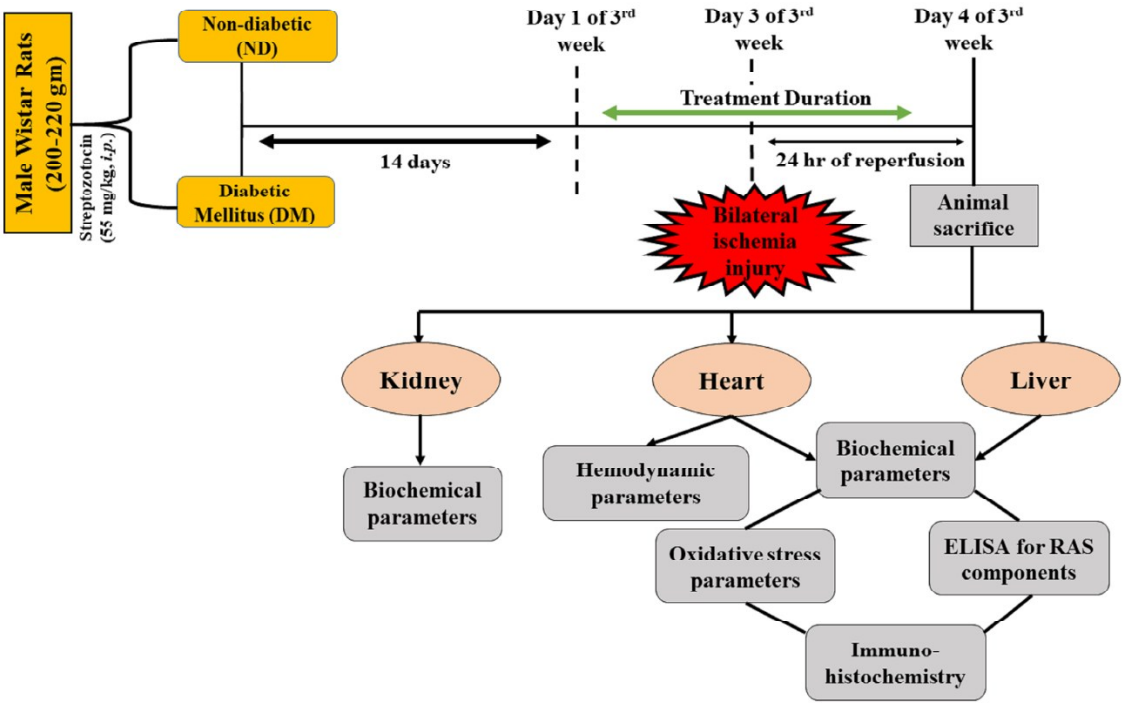

Fig. 1. Experimental study design.

Panicoa et al., 2019). Nevertheless, the role of the depressor arm of RAS in IRI-induced cardio-hepatic dysfunction remains elusive. Hence, in the current study, we utilised a bilateral renal IRI model of diabetic and nondiabetic rats to test the hypothesis that IRI could alter the cardio-hepatic levels of AT2R and ACE2 which could arbitrate inflammation and oxidative stress in the same.

2. Materials and methods

2.1. Chemicals

Glucose, plasma creatinine (PCr), blood urea nitrogen (BUN), Creatine kinase-MB (CK-MB), Lactate dehydrogenase (LDH), Aspartate aminotransferase (AST), alanine transaminase (ALT) kits obtained from Accurex (Mumbai, India). Chemicals like Streptozotocin and Diminazene aceturate (Dize) obtained from Sigma (St. Louis, MO, USA). ELISA kits for Kidney injury molecule-1 (Kim-1), ACE, ACE2, Ang-(1–7), Ang II, AGT and Myeloperoxidase (MPO) purchased from Elabsciences (China). Primary antibody of tumour necrosis factor-alpha (TNF-α) purchased from Santa Cruz Biotechnology (Dallas, TX, USA), and secondary antibody purchased from Cell Signaling Technology (Danvers, MA, USA). Other chemicals used in the study were of analytical grade. Drugs/chemical solutions were always prepared anew before use.

2.2. Animal studies

The male adult Wistar rats (200−220 g) acquisition and experimentation were carried out at the Central Animal Facility (CAF) of Birla Institute of Technology and Science Pilani (BITS-Pilani) as per the protocol approved by the Institutional Animal Ethics Committee (IAEC), BITS-Pilani (Protocol Approval No: IAEC/RES/23/19/Rev-2/25/18). Animals kept under standard environmental conditions, with feed and water *ad lib*. Reported animal studies adhered to ARRIVE guidelines (Kilkenny et al., 2010). The study was performed following the protocol for type 1 diabetes, as described previously (Sharma et al., 2019b). Briefly, diabetes was induced by a single dose of Streptozotocin [55 mg/kg, *i.p.*, vehicle- sodium citrate buffer (0.01 M, pH 4.4)] (Sharma et al., 2019b) and ND rats were injected only with ice-cold sodium citrate buffer. After 48 h of Streptozotocin-injection, rats having plasma glucose levels >250 mg/dL included in the study as DM rats.

Further, bilateral IRI was performed on ND and DM rats as described by Peng et, al. (Peng et al., 2015). Briefly, rats were anaesthetised with pentobarbital sodium (50 mg/kg, *i.p.*) and were kept on a surgical platform in the dorsal position. Rats were administered with saline (20 mL/kg, *s.c.*) to prevent the fluid loss during laparotomy, and body temperature (37°C) was maintained with a homoeothermic blanket. Two flank incisions were made to expose both kidneys, and renal pedicles were occluded using non-traumatic clamps. After 20 min, the clamps were removed and after observing renal blood flow (kidney appearance), the skeletal muscle and skin layers were sutured separately with absorbable and non-absorbable sutures, respectively. Topical application of (Betadine™) antiseptic and parenteral (Augmentin™, 324 mg/kg, *i.p.*) antibiotics were given to rats to avoid post-surgery infection. Sham control animals were subjected to identical operation and length of time of surgery but without renal vascular pedicles clamping. After 24 h of reperfusion, animals were re-anesthetised with pentobarbital sodium (50 mg/kg, *i.p.*), and systolic blood pressure (SBP) was measured using ADInstruments PowerLab system (Bella Vista, NSW, Australia) (Malek and Gaikwad, 2018). A lethal dose of pentobarbital sodium was administered to sacrifice rats; blood was collected from vena cava with a 5 mL syringe for plasma biochemistry. The kidney, heart and liver tissues were then removed, washed and blotted dry, weighed and kept at −80 °C for further experimentations (Fig. 1).

2.3. Experimental design

Both ND and DM rats were divided into five groups each: 1) ND/DM-serve as respective controls, 2) ND-/DM-IRI- ND or DM rats subjected to bilateral IRI after completion of two weeks of diabetes induction 3) ND-/DM-IRI + C21- ND- IRI or DM- IRI rats treated with compound 21 (C21) (0.3 mg/kg/day, *i.p.*) (Pandey and Gaikwad, 2017a), 4) ND /DM IRI + Dize- ND- IRI or DM- IRI rats treated with Dize (5 mg/kg/day, *p.o.*) (Goru et al., 2017), 5) ND-/DM-IRI + CD- ND- IRI or DM- IRI rats treated with C21 (0.3 mg/kg/day, *i.p.*) and Dize (5 mg/kg/day, *p.o.*) combination therapy. Both monotherapies and combination therapy were administered two days before bilateral IRI and continual to next day (24

h of reperfusion time) (Fig. 1).

2.4. Assessment of renal, cardiac and hepatic functions by plasma and urine biochemistry

Biochemical estimations were conducted as described previously (Sharma et al., 2019b). After reperfusion time, blood samples were taken and plasma was separated by centrifugation (5 min at 5000 g, 4 °C). The plasma samples were used for estimation of kidney, heart and liver-Specific functional parameters (BUN, PCr, CK-MB, LDH, AST, ALT) using spectrometric kits. For urinary Kim-1 estimation, urine samples were collected using metabolic cages, and urinary Kim-1 was assessed using ELISA kits.

2.5. Measurements of oxidative stress level in heart and liver tissues

a) Sample homogenate preparation

For heart and liver homogenate, isolated tissues were rinsed with ice-cold isotonic saline (0.9 % w/v NaCl) followed by dissection and homogenised using ice-cold 0.1 M phosphate buffer (pH 7.4) in ten times (w/v) volume. The homogenised samples were centrifugation at 10,000 g for 15 min at 4 °C (Sharma and Taliyan, 2016). Finally, the aliquots of supernatant were prepared and further used for biochemical estimations.

b) Protein determination

Protein content in the heart and liver samples were measured by the method of Lowry et al. (Classics Lowry et al., 1951) using bovine serum albumin (1 mg/mL) as a standard.

c) Malondialdehyde (MDA) estimation

MDA, an end product of lipid peroxidation, was assessed using heart and liver homogenates, as described previously (Sharma et al., 2015). The absorbance of MDA was observed after the reaction of MDA with thiobarbituric acid, at 532 nm. Then, the concentration of MDA was assessed from a standard curve and stated as nanomoles per milligram of protein.

d) Reduced Glutathione (GSH) estimation

Reduced glutathione levels in the heart and liver were estimated according to the method described by Pandey et al. (2017b). Briefly, the assay mixture contains 1 mL of 4% sulfosalicylic acid and 1 mL of supernatant allowed to cold-digested at 4 °C for 1 h. The samples were centrifuged at 1200 g for 15 min, in 1 mL of collected supernatant, 2.7 mL of phosphate buffer and 0.2 mL of Ellman's reagent were added. Finally, the developed yellow colour of 5-thio-2-nitrobenzoate-SH was measured immediately at 412 nm using a spectrophotometer.

e) Myeloperoxidase (MPO) Activity

MPO activity in heart and liver tissues of rats was measured as described previously (Yang et al., 2017). Briefly, Aliquots of supernatants were analysed using *o*-dianisidine dihydrochloride, 0.0005 % hydrogen peroxide and 0.1 mM H2O2, and incubated to 37 °C. MPO activity was determined at 450 nm using a spectrophotometer, and was further normalised to protein content and expressed as U/mg protein.

2.6. Haematoxylin and eosin staining

Liver and heart histology was examined by Hematoxylin and Eosin (H and E) staining (Sharma et al., 2019b). Briefly, after formalin fixation (10 %) and dehydration process, paraffin-embedded liver sections (5 microns) were stained with H and E staining. At least 4–5 sections (one microscopy slide) from each liver and heart and a total of n = 6 from each group were observed and captured at an original magnification of 40x (liver) and 100x (heart) by using "Zeiss" microscope (model: Vert. A1) and "Optika TCB5″ microscope (Optika Research Microscope, Italy), respectively.

Table 1
Kidney functional parameters.

Groups	PGL (mg/dL)	BUN (mmol/L)	PCr (μmol/L)	Urinary Kim-1 (ng/mL)
ND	101.2 ± 13.1	7.22 ± 1.2	34.48 ± 6.6	0.23 ± 0.2
ND-IRI	94.6 ± 6.7	17.46 ± 4.3*	112.3 ± 6.5*	7.59 ± 2.1*
ND-IRI + C21	96.7 ± 7.2	17.29 ± 3.4	101.2 ± 6.3	6.12 ± 0.9$^{@}$
ND-IRI + Dize	98.7 ± 8.1	17.07 ± 3.9	99.89 ± 5.7	6.06 ± 1.2$^{@}$
ND-IRI + CD	99.3 ± 7.5	12.51 ± 2.7$^{@}$	62.36 ± 5.4$^{@}$	4.21 ± 1.0$^{@}$
DM	273.8 ± 24.3*	7.31 ± 1.6	32.99 ± 6.4	0.43 ± 0.2
DM- IRI	290.1 ± 30.3	23.32 ± 4.5$^{\#,@}$	131.23 ± 9.4$^{\#,@}$	15.47 ± 2.2$^{\#}$
DM- IRI + C21	288.5 ± 34.7	21.82 ± 4.3	120.97 ± 7.4	13.45 ± 1.7
DM- IRI + Dize	282.4 ± 29.9	20.98 ± 4.7	115.30 ± 7.5	13.12 ± 2.1
DM- IRI + CD	284.9 ± 33.7	15.19 ± 3.6$^{\$}$	77.97 ± 7.9$^{\$}$	9.71 ± 1.9$^{\$}$

Note: Each data is represented as mean ± SD (n = 6). $^{(*)}$ $p < 0.05$ vs ND; $^{(@)}$ $p < 0.05$ vs ND-IRI; $^{(\#)}$ $p < 0.05$ vs DM; $^{(\$)}$ $p < 0.05$ vs. DM-IRI.

2.7. Immunohistochemistry

In immunohistochemistry (IHC), the deparaffinisation of the paraffin-embedded liver and heart sections (5 microns) was followed by antigen retrieval by heating in citrate buffer (10 mmol/L). Mouse TNF-α (Dilution: 1:200 v/v) primary antibody incubation was performed, followed by secondary antibody incubation with HRP-conjugated anti-mouse IgG. For detection, diaminobenzidine (DAB) was used as a chromogen. The slides were counterstained with haematoxylin, dehydrated with alcohol and xylene and mounted in DPX. We observed around 4–5 sections (one microscopy slide) from each liver/heart, and a total of n = 6 from each group. Images were taken at 40x (liver) and 100x (heart) original magnification by using "Zeiss" microscope (model: Vert A1) and "Optika TCB5″ microscope (Optika Research Microscope, Italy), respectively. Then, DAB-positive area was calculated on 5–6 images from each stained liver/heart microscopy slide using ImageJ software (NIH, Bethesda, MD, USA).

2.8. ELISA to determine RAS components levels in samples of plasma, urine, heart and liver tissues

The heart and liver tissues were homogenised in the recommended buffer solution, followed by total protein estimation. Heart and liver samples normalised for protein content, and diluted plasma (dilution factor = 3) was assayed for ACE, ACE2, Ang II and Ang-(1–7), whereas AGT protein levels were measured using urine samples (dilution factor = 3) (n = 6 rats/group) (Goru et al., 2017).

2.9. Statistical analysis

Experimental values are represented as mean ± SD, and 'n' refers to the number of samples studied. Statistical comparison between groups was performed by two-way ANOVA followed by Tukey's Multiple Comparison *post hoc* test using GraphPad Prism software version 8.0.2

Table 2
Effect of AT2R and ACE2 activation on cardiac and liver specific parameters.

Groups	SBP (mmHg)	CK-MB (IU/L)	LDH (IU/L)	ALT (IU/L)	AST (IU/L)
ND	105 ± 4.7	307.4 ± 38.2	273.3 ± 33.1	27.28 ± 2.4	23.84 ± 5.8
ND-IRI	104 ± 5.2	802.7 ± 52.4*	982.4 ± 48.4*	64.23 ± 3.7*	54. 24 ± 4.9*
ND-IRI + C21	105 ± 6.4	751.2 ± 42.5	832.9 ± 75.2	52.13 ± 4.6	50.32 ± 8.3
ND-IRI + Dize	106 ± 6.9	724.7 ± 55.3	743.1 ± 63.9	48.53 ± 5.2	47.96 ± 6.8
ND-IRI + CD	107 ± 5.5	461.9 ± 34.8@	412.4 ± 43.1@	32.94 ± 3.7@	36.24 ± 4.2@
DM	105 ± 4.7	312.3 ± 53.5	280.2 ± 37.2	28.01 ± 1.9	24.13 ± 4.5
DM- IRI	106 ± 3.9	1220.8 ± 93.7#,@	1343.6 ± 78.8 #,@	84.94 ± 4.1 #,@	60. 65 ± 3.9#,@
DM- IRI + C21	104 ± 3.8	1038.2 ± 72.9	1047.9 ± 69.2	70.29 ± 3.8	55.87 ± 4.1
DM- IRI + Dize	106 ± 4.5	1091.4 ± 87.2	1098.7 ± 84.7	67.38 ± 5.7	56.12 ± 4.6
DM- IRI + CD	109 ± 6.1	726.7 ± 56.2$	628.8 ± 81.3$	43.92 ± 3.2$	43.56 ± 3.5$

Note: Each data is represented as mean ± SD (n = 6). (*) $p < 0.05$ vs ND; (@) $p < 0.05$ vs ND-IRI; (#) $p < 0.05$ vs DM; ($) $p < 0.05$ vs DM-IRI.

(San Diego, CA, USA). Data with $p < 0.05$, were considered statistically significant.

3. Results

3.1. Effect of AT2R and ACE2 activation on kidney functional parameters

Under the hyperglycemic condition, DM rats showed increased ($P <$ 0.05) plasma glucose levels compared to ND rats (Table 1). However, either IRI or AT2R/ACE2 activation did not decreased the level of plasma glucose (Table 1). In ND and DM rats, IRI had significantly elevated ($P < 0.05$) the BUN and PCr levels, where DM-IRI group showed significant elevation in BUN and PCr levels as compared to ND-IRI group. Urinary Kim-1, a type 1 transmembrane protein, served as the biomarker of AKI was found to be profoundly elevated ($P < 0.05$) in DM-IRI rats compared to ND-IRI rats (Table 1). After the administration of C21 and Dize, the combination therapy significantly reduced BUN ($P <$ 0.05), PCr ($P < 0.05$) and urinary Kim-1 levels ($P < 0.05$) in IRI rats of ND and DM groups.

3.2. Effect of AT2R and ACE2 activation on cardiac and hepatic functional parameters

After surgery, IRI showed no significant changes in SBP in ND and DM rats. Either alone or combination therapy had not exerted any alteration in SBP of ND/DM-IRI rats (Table 2). Further, cardiac injury markers CK—MB and LDH, and hepatic dysfunction markers ALT and AST significantly elevated in ND, and DM rats that underwent IRI (Table 2). However, DM-IRI rats showed significant elevation ($P < 0.05$) in cardiac and hepatic injury markers compared to ND-IRI rats. Combination therapy of C21 and Dize markedly reduced ($P < 0.05$) the plasma levels of CK—MB, LDH, ALT and AST compared to IRI groups of ND and DM rats. However, monotherapies reduced the plasma levels of CK—MB, LDH, ALT and AST in ND/DM IRI rats, but not significantly.

3.3. Effect of AT2R and ACE2 activation on oxidative/ antioxidant status

Oxidative stress is one of the major inflammation triggering factor for the progression of AKI and its associated distant organ dysfunction (Kanagasundaram, 2015). In heart and liver tissue homogenates,

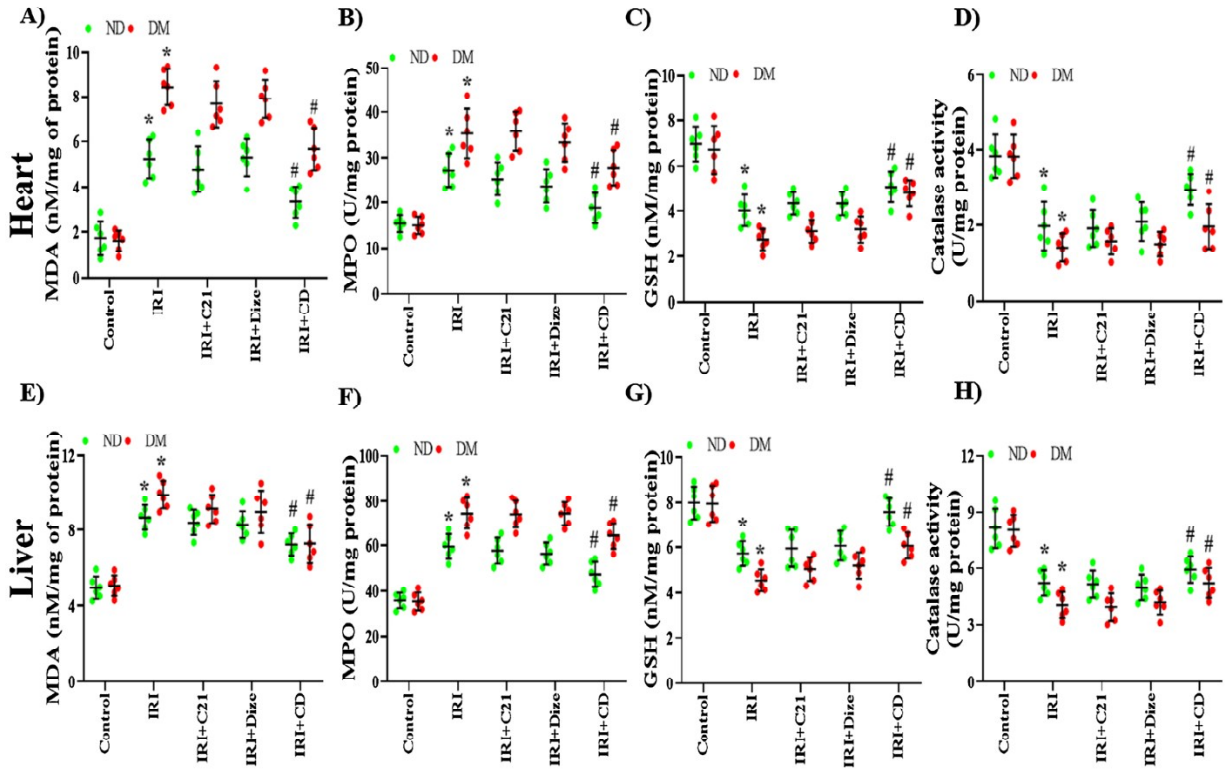

Fig. 2. Effect of AT2R and ACE2 activation on heart and liver oxidative stress.
A-H: Estimation of oxidative stress markers, e.g. malondialdehyde (MDA) levels (A, E), Myeloperoxidase (MPO) activity (B, F), glutathione (GSH) levels (C, G), catalase activity (D, H) in isolated heart and liver tissues (n = 6). Data are represented as mean ± SD from three independent experiments. Two-way ANOVA with Tukey's multiple comparison test for statistical comparison. (*) $p < 0.05$ vs ND; (@) $p < 0.05$ vs ND-IRI; (#) $p < 0.05$ vs DM; ($) $p < 0.05$ vs DM-IRI.

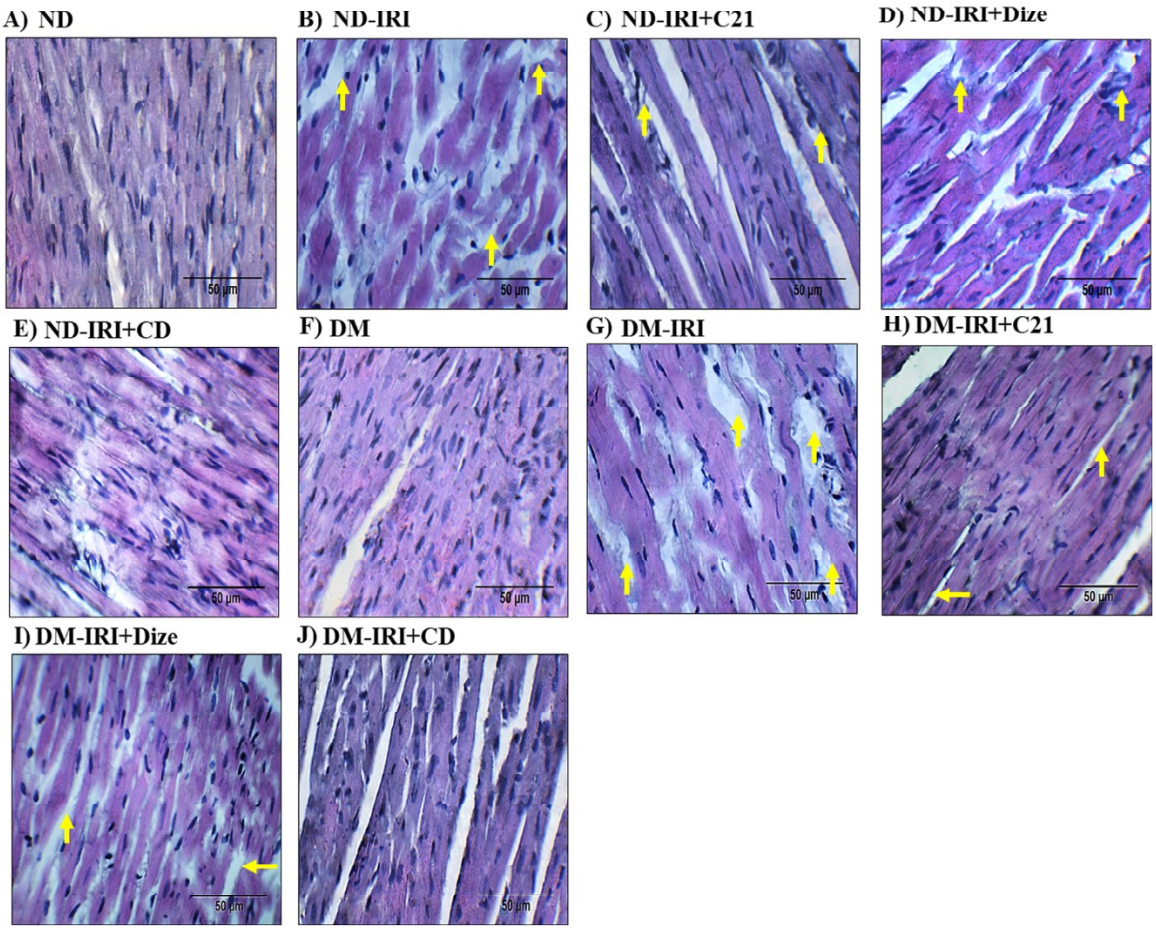

Fig. 3. Effect of AT2R and ACE2 activation on histopathological findings in the heart.
The heart samples from each group were collected after reperfusion and were processed for histological examination by H and E staining. A-J: Representative images of heart sections magnifying cardiac muscle fibres (original magnification 100x and scale bar- 50 µm). 4–5 images from each stained heart section and a total of six different heart per group were observed by a blinded observer for healthy as well as disarrayed cardiac muscle fibres (Yellow arrow) (A).

oxidative stress was elevated significantly ($P < 0.05$) in ND/DM-IRI rats, owing to an increase in MDA levels (Fig. 2 A, E). DM-IRI rats showed a more significant increase in heart and liver MDA levels as compared to ND-IRI rats (8.43 ± 0.7 vs 5.42 ± 0.5); (9.96 ± 0.7 vs 8.71 ± 0.5). However, only combination therapy of C21 and Dize effectively reduced MDA levels ($P < 0.05$) in ND/DM IRI rats (Fig. 2A-E). Both ND/DM-IRI rats showed elevated MPO activity, the DM-IRI rats, however, showed significant increased heart and liver MPO activity compared to ND-IRI rats (35.31 ± 2.4 vs 27.31 ± 3.1), (74.48 ± 6.1 vs 59.53 ± 4.7) (Fig. 2B, F). Treatment with combination therapy has effectively depleted the heart and liver MPO activity in comparison to monotherapies and IRI groups under ND and DM conditions (Fig. 2B, F).

On the other hand, anti-oxidant defence mechanism was impaired by IRI, demonstrated by reduced ($P < 0.05$) GSH levels and catalase activity in heart and liver tissues of ND/DM IRI rats (Fig. 2C-D, G–H). DM-IRI rats showed a significant reduction in heart and liver GSH levels in comparison to ND-IRI rats (2.74 ± 0.4 vs 4.02 ± 0.6); (4.55 ± 0.3 vs 5.72 ± 0.9). Similarly, DM-IRI rats showed significant depletion in catalase activity as compared to ND-IRI rats (1.40 ± 0.3 vs 2.03 ± 0.5); (4.01 ± 0.4 vs 5.23 ± 0.7) (Fig. 2G H). Interestingly, the combination therapy effectively normalised the GSH and catalase activity in heart and liver tissues. Moreover, both monotherapies showed no effect on IRI rats under ND and DM conditions.

3.4. Histopathological findings

In the current study, histopathological changes in hepatic and cardiac tissue samples obtained from all groups were evaluated using microscopy. The cardiac histological architecture in tissue from ND and DM rats appeared as regularly arranged cardiac myofibers having several cardiac myocytes comprising mainly of single, ovoid and centrally located nuclei (Fig. 3A, F). After IRI, histopathology revealed severe myocardial degenerative changes, which were identified by disarrayed cardiac muscle fibres (shown by the yellow arrow) (Fig. 3D, G). Meanwhile, IRI rats with combination therapy exhibited mild myocardial degenerative changes (Fig. 3E, J).

The hepatic histological architecture in tissue sections from ND and DM rats showed normal, lobular structure with finely arranged hepatic cords embracing large polyhedral cells with spherical vesicular nuclei. Besides, Kupffer cells and hepatic sinusoids were located in-between the radiating hepatic cords (Fig. 4A, F). After IRI, ND/DM rat livers showed sinusoidal dilatation and vacuolisation of hepatocytes along with leukocyte infiltration (shown by the yellow arrow), pyknotic nuclei and Kupffer cell proliferation (Fig. 4B, G). Interestingly, combination therapy of C21 and Dize markedly reduced the histopathological alterations such as reduced vacuolisation of hepatocytes and decreased hepatocellular degeneration (Fig. 4E, J). On the other hand, both monotherapies mildly reduced the vacuolisation of hepatocytes (Fig. 4C-D, H–I).

3.5. Effect of AT2R and ACE2 activation on TNF-α mediated cardiac and hepatic inflammation

We have checked the immunohistochemical TNF-α expressions to evaluate whether the C21 and Dize reduced the IRI-induced cardio-

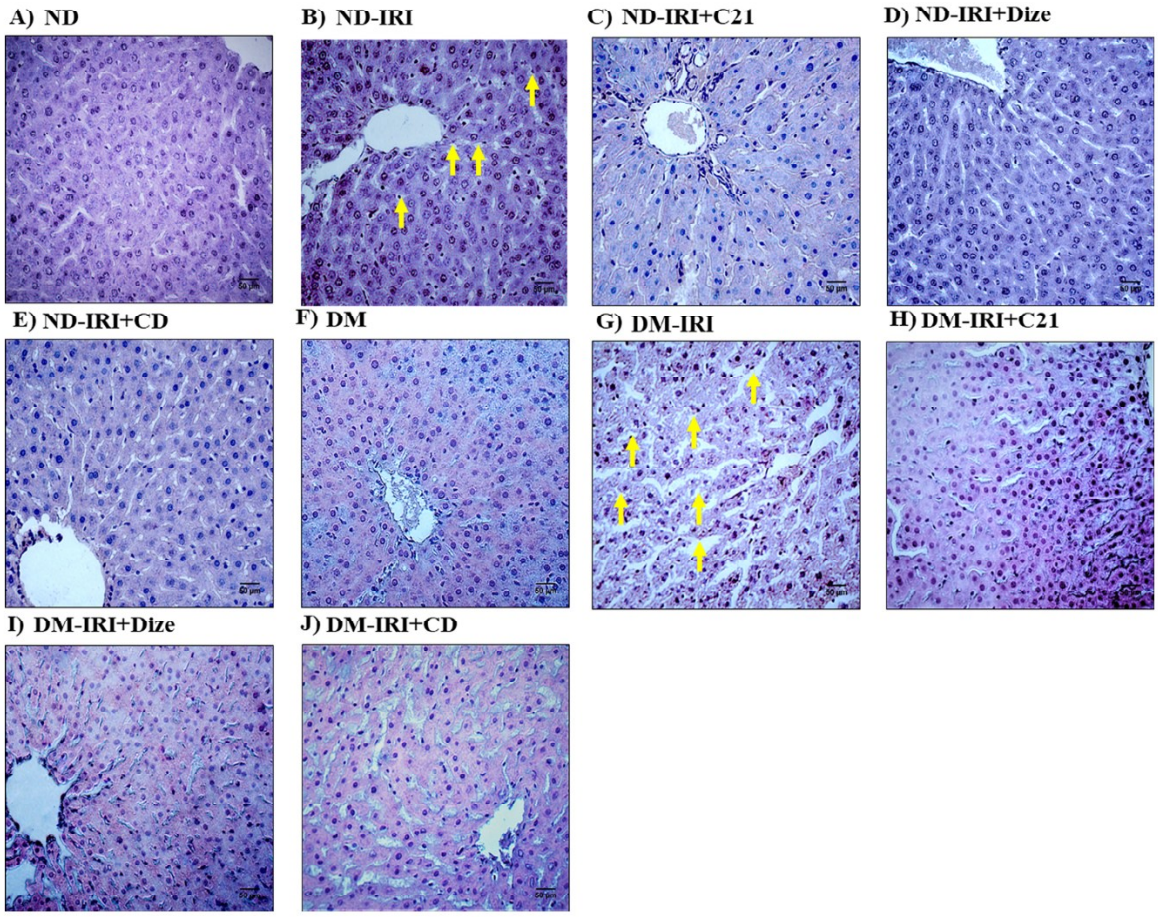

Fig. 4. Effect of AT2R and ACE2 activation on histopathological findings in the liver.
The liver samples from each group were collected after reperfusion and were processed For histological examination by H and E staining. A-J: Representative images of liver sections (original magnification 100x and scale bar- 50 μm). A blinded observer observed 4–5 images from each stained liver section and a total of six different liver per group: sinusoidal dilatation and vacuolisation of hepatocytes along with leukocytes infiltration (shown by the yellow arrow).

hepatic inflammation. In cardiac tissue sections, we found that IRI in ND and DM rats increased ($P < 0.05$) the TNF-α expression as compared to their respective controls (Fig. 5A, F). In comparison to ND IRI, DM IRI group showed significant elevation ($P < 0.05$) in the TNF-α expression (10.49 + 1.3 vs 6.65 + 0.9). Both monotherapies decreased the TNF-α expressions in ND/DM-IRI rats. Interestingly, simultaneous activation of AT2R and ACE2 by combination therapy of C21 and Dize significantly decreased ($P < 0.05$) the TNF-α expressions in comparison to ND and DM rats underwent IRI (Fig. 5B, G). Moreover, combination therapy has a more pronounced effect in reducing TNF-α expression as compared to C21 and Dize monotherapies under normal and hyperglycemic condition (Fig. 5K).

In hepatic tissue sections, we found the drastic increase in inflammation, as demonstrated by the multi-fold increase ($P < 0.05$) in TNF-α expressions in IRI groups of ND and DM rats (Fig. 6B, G). In the DM group, DM-IRI rats showed significant elevation of TNF-α expression as compared to ND-IRI rats (12.02 ± 2.1 vs 7.60 ± 1.5). TNF-α mediated inflammation was significantly controlled ($P < 0.05$) by the combination treatment as compared to the ND/DM-IRI rats (Fig. 6E, J). Besides, both the monotherapies significantly suppressed the hepatic TNF-α expression as compared to ND/DM-IRI rats (Fig. 6K).

3.6. Effect of AT2R and ACE2 on systemic and cardio-hepatic depressor arm and pressor arm of RAS

In the systemic circulation, heart and liver tissues, we have checked the pressor and depressor arm of RAS specific enzymes i.e. ACE and ACE2. Here, IRI resulted in the significant increase ($P < 0.05$) in ACE levels compared to ND and DM rats (Fig. 7A-C). In plasma, ACE levels were found to be higher in DM rats compared to ND rats that underwent IRI (10.08 ± 2.0 vs 6.86 ± 1.1). Interestingly, C21 and Dize combination therapy significantly reduced the plasma, heart and liver ACE levels when compared to ND/DM-IRI rats. However, none of the monotherapies was effective to reduce ACE levels (Fig. 7A-C).

On the other hand, the important enzyme of depressor arm of RAS, ACE2, was significantly depleted in the heart and liver samples of IRI rats under ND and DM conditions (Fig. 7E, F). However, combination therapy effectively normalised the ACE2 levels in comparison to ND/DM-IRI rats (Fig. 7E, F). In contrast, systemic ACE2 levels remain unchanged across all the groups (Fig. 7D). We have also checked the levels of urinary AGT and found significantly elevated levels in ND/DM-IRI (Fig. 7G). Urinary AGT was significantly higher in DM IRI rats compared to ND-IRI rats (96.58 + 7.8 vs 75.72 + 6.2). The C21 and Dize combination therapy significantly reduced ($P < 0.05$) the urinary AGT levels in comparison to ND/DM-IRI and monotherapy groups (Fig. 7G).

Likewise, plasma, cardiac and hepatic Ang II levels were markedly increased ($P < 0.05$) after IRI in ND and DM rats as compared to respective controls (Fig. 8A-C). In cardiac and hepatic tissue, treatment with monotherapies reduced Ang II levels, but not significantly (Fig. 8B, C). C21 and Dize combination therapy effectively reduced Ang II levels compared to both monotherapies and ND/DM-IRI groups (Fig. 8A-C). Further, we also determined the Ang-(1–7) levels in systemic circulation, heart and liver tissue homogenates. We found that the Ang (1–7) levels were significantly reduced ($P < 0.05$) by IRI in comparison to ND and

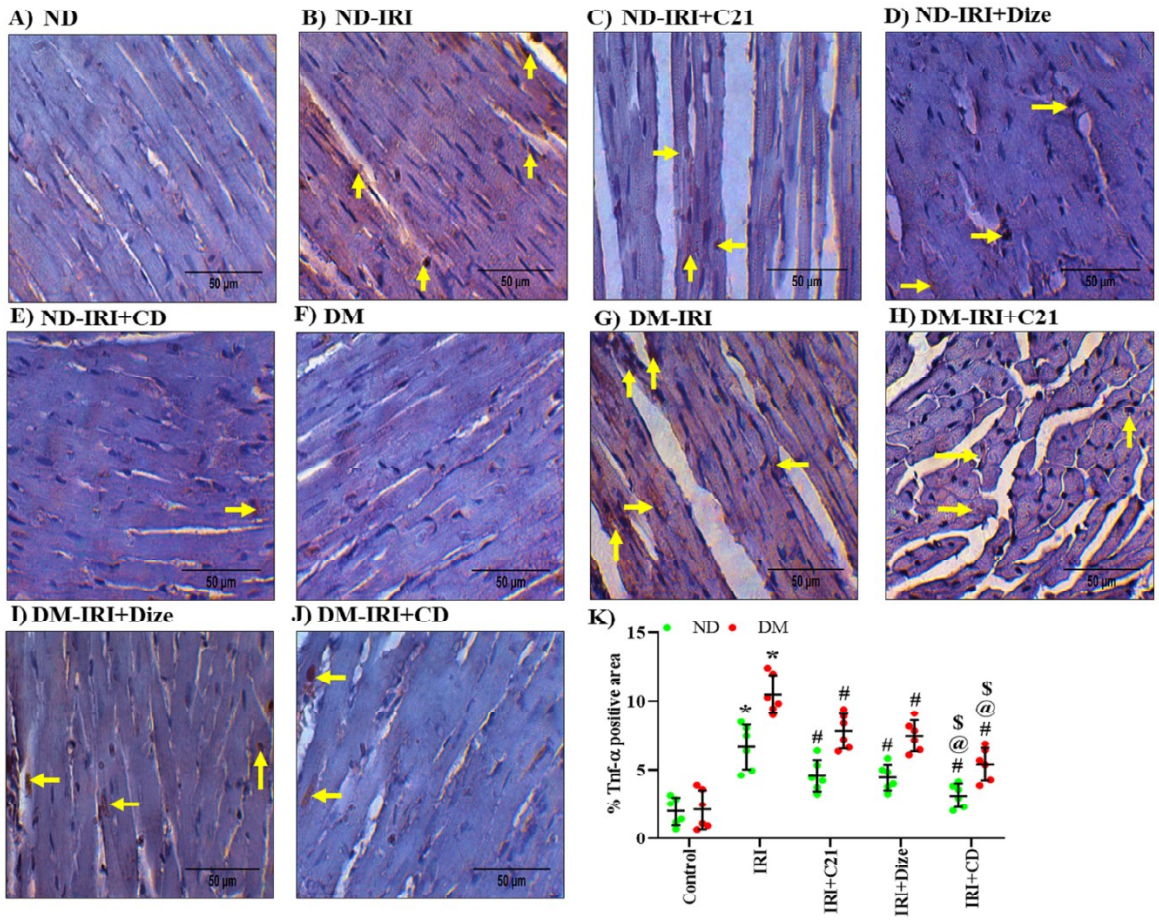

Fig. 5. Effect of AT2R and ACE2 activation on TNF-α expression in the heart.
A-J: Representative images of IHC staining for TNF-α in the heart (original magnification 100x and scale bar 50 μm). Around 4–5 sections from each stained heart microscopy slide and total six different heart slides per group were seen under microscope and images were captured. K: Semi-quantitative analysis of all the images via ImageJ (colour deconvolution plugin was utilized for analysis) for calculating DAB-positive area. All Data are represented as mean ± SD. Two-way ANOVA with Tukey's multiple comparison test was used for statistical comparison. $^{(*)}$ $p < 0.001$ vs ND; $^{(\#)}$ $p < 0.001$ vs DM; $^{(@)}$ $p < 0.001$ vs ND-IRI, $^{(\$)}$ $p < 0.001$ vs DM-IRI.

DM rats (Fig. 8D-F). Further, combination treatment significantly improved ($P < 0.05$) the Ang-(1–7) levels in plasma, cardiac and hepatic tissue in comparison to ND/DM IRI rats (Fig. 8D F). None of the mon otherapy altered the Ang II and Ang-(1–7) levels across the groups (Fig. 8A-F).

4. Discussion

Mounting shreds of evidence demonstrated that several cellular and molecular mechanisms play specific roles in the IRI, instead of the usual possible treatments, no effective therapy has been appraised, so far (Doyle and Forni, 2016). Clinical reports have demonstrated that mortality rate soared from 45 % to 60 % when AKI was associated with distant organ insufficiency and co-morbidities (such as diabetes) (Lee et al., 2018). As compared to non-diabetics, diabetic patients endure a higher risk of AKI under critically ill hospitalised conditions (Hursh et al., 2017). Because of the complexity of pathological signals, the IRI associated heart and liver dysfunction are inadequately understood (Husain-Syed et al., 2019). Nevertheless, studies have revealed the possible mechanisms behind the multiorgan dysfunction under IRI settings, including vascular inflammation, metabolic acidosis, electrolyte imbalances triggered life-threatening arrhythmias, reactive oxygen species (ROS), upregulation of inflammatory cytokines and pro-apoptotic molecules (Bucsics and Krones, 2017; Lee et al., 2018; Panicoa et al., 2019). Beside these distinctive mechanisms, there is an imperative factor with immediate impact on distant organs, i.e., the RAS (Bucsics and Krones, 2017; Panicoa et al., 2019).

Recently, the depressor arm of RAS has gained acceptance as an essential molecular target involved in various cardiac and hepatic dys functions like diabetic cardiomyopathy, pulmonary hypertension and NAFLD (Macedo et al., 2016; Cao et al., 2019; Malek et al., 2019). However, its role in the pathophysiology of IRI-associated cardiac and hepatic dysfunctions is still elusive. Therefore, in the present study, we aimed to investigate the role of depressor arm of RAS in IRI-associated cardio-hepatic dysfunction under normal and hyperglycemic condition. In this study, we utilised the bilateral IRI model of AKI. During animal model standardisation, we carried out 30 or 20 min of ischemia by clamping both renal pedicles. Animals with 30 min of bilateral IRI showed a drastic decline in the survival rate as compared to 20 min of bilateral IRI (Supplementary Fig. 1 A, B).

Additionally, the BUN levels reached a peak between 24 and 72 h following reperfusion (Supplementary Fig. 1 C). At the same time, PCr levels remain at peak with 24 h of reperfusion (Supplementary Fig. 1 D). Therefore, we have chosen 20 min of bilateral renal ischemia followed by 24 h of reperfusion. Given due weightage to existing literature and our previous reports, we have designed the treatment groups with depressor arm modulators, C21 (0.3 mg/kg/day, *i.p.*) and Dize (5 mg/kg/day, *p.o.*) monotherapies as well as their combination therapy to evaluate their efficacy against IRI induced cardiac and hepatic dysfunction in ND and DM conditions (Fig. 1). Clinically IRI is characterised by elevated BUN, PCr levels along with increased urinary KIM-1 levels (Bonventre and Yang, 2011). Here, we observed similar changes

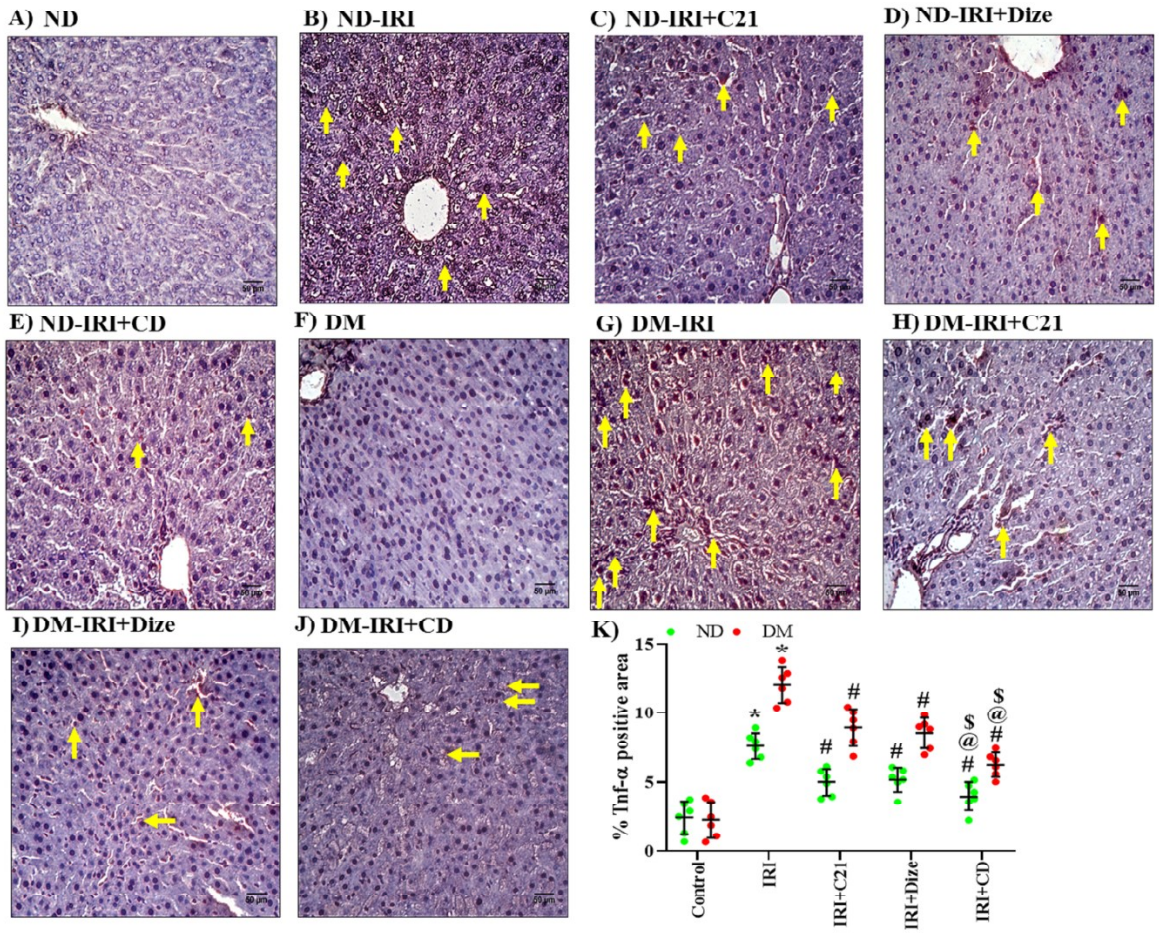

Fig. 6. Effect of AT2R and ACE2 activation on TNF-α expression in the liver.
A-J: Representative images of IHC staining for TNF-α in the liver (original magnification 40x and scale bar 50 μm). Around 4–5 sections from each stained liver microscopy slide and total six different liver slides per group were seen under microscope and images were captured. B: Semi-quantitative analysis of all the images via ImageJ (colour deconvolution plugin was utilized for analysis) for calculating DAB-positive area. All Data are represented as mean ± SD. Two-way ANOVA with Tukey's multiple comparison test was used for statistical comparison. $^{(*)}$ $p < 0.05$ vs ND; $^{(\#)}$ $p < 0.05$ vs DM; $^{(@)}$ $p < 0.05$ vs ND-IRI, $^{(\$)}$ $p < 0.05$ vs DM-IRI.

in IRI rats which were significantly attenuated by the proposed combination therapy (Table 1). These results suggested the potential of AT2R agonist and ACE2 activator in improving kidney functional parameters. Various clinical and preclinical studies have found the development of cardiac and hepatic dysfunction in patients with AKI, signified by increased myocardial and hepatic injury markers (Liaño et al., 1998; Sun et al., 2012; Amini et al., 2019; Mohammadi et al., 2019). In the present study, IRI cause myocardial and hepatic dysfunctions which were manifested by raised systemic activities of LDH, CK—MB and AST, ALT under two different physiological (normal and hyperglycemic) conditions. There is a significant reduction of biomarkers, as mentioned above by combination therapy (Table 2). Nonetheless, we have not observed any changes in the SBP level after 24 h of reperfusion (Table 2).

The subsequent mechanism for the progression of cardio-hepatic dysfunction involves a combination of oxidative stress, lipid peroxidation under AKI and diabetic conditions (Abdellatief et al., 2017; Bigagli and Lodovici, 2019). In experimental studies, the initiation and perpetuation of cellular injury in IRI affected cardiac and hepatic tissue, is associated with the upsurge in free radicals and the depletion of endogenous antioxidant defence (Fadillioglu et al., 2008; Amini et al., 2019). MDA, an index of lipid peroxidation, plus GSH and catalase, indexes of anti-oxidant defence mechanism, have been shown to increase in remote cardiac and liver injury augmented by IRI (Park et al., 2012; Yap and Lee, 2012; Zhao et al., 2018). In the current study, we observed that hyperglycaemia resulted in significant increase in MDA and depleted antioxidant defence mechanism (GSH and catalase activity) after IRI, which were significantly controlled by the combination therapy (Fig. 2).

MPO, a neutrophil-specific enzyme referred as an indicator of leukocyte infiltration whose expression elevated in the tissue injuries, including remote organ injuries (Kelly, 2003; Brochner et al., 2014). In our study, the elevated aforementioned cardiac and hepatic oxidative stress is accompanied by increased MPO activity in IRI groups of ND and DM rats (Fig. 2). Here, the presence of hyperglycaemia with IRI severely increased the MPO activity as compared to the ND-IRI group, which was significantly controlled by the administration of C21 and Dize combination therapy.

Under AKI settings, kidney-heart and liver interaction resulted in morphological alteration (Abdellatief et al., 2017). In this study, the heart tissue of IRI groups showed severe myocardial degenerative changes, which were identified by disarrayed cardiac muscle fibres (Fig. 3). However, liver histology of IRI groups showed sinusoidal dilatation and vacuolisation of hepatocytes along with leukocytes infiltration, pyknotic nuclei and Kupffer cell proliferation (Fig. 4). In contrast, concomitant therapy of C21 and Dize significantly alleviated the cardio-hepatic structural damage in IRI groups of ND and DM rats.

Both clinical and laboratory reports demonstrated that IRI resulted in an upsurge of heart and liver inflammation via upregulation of pro-inflammatory cytokines such as IL-1, IL-6, IL-17A, monocyte chemoattractant protein-1 (MCP-1) and TNF-α (Lee et al., 2018; Lai et al., 2019). To explore the role of the inflammatory mechanism in regulating IRI under ND and DM conditions, we have checked the expression of

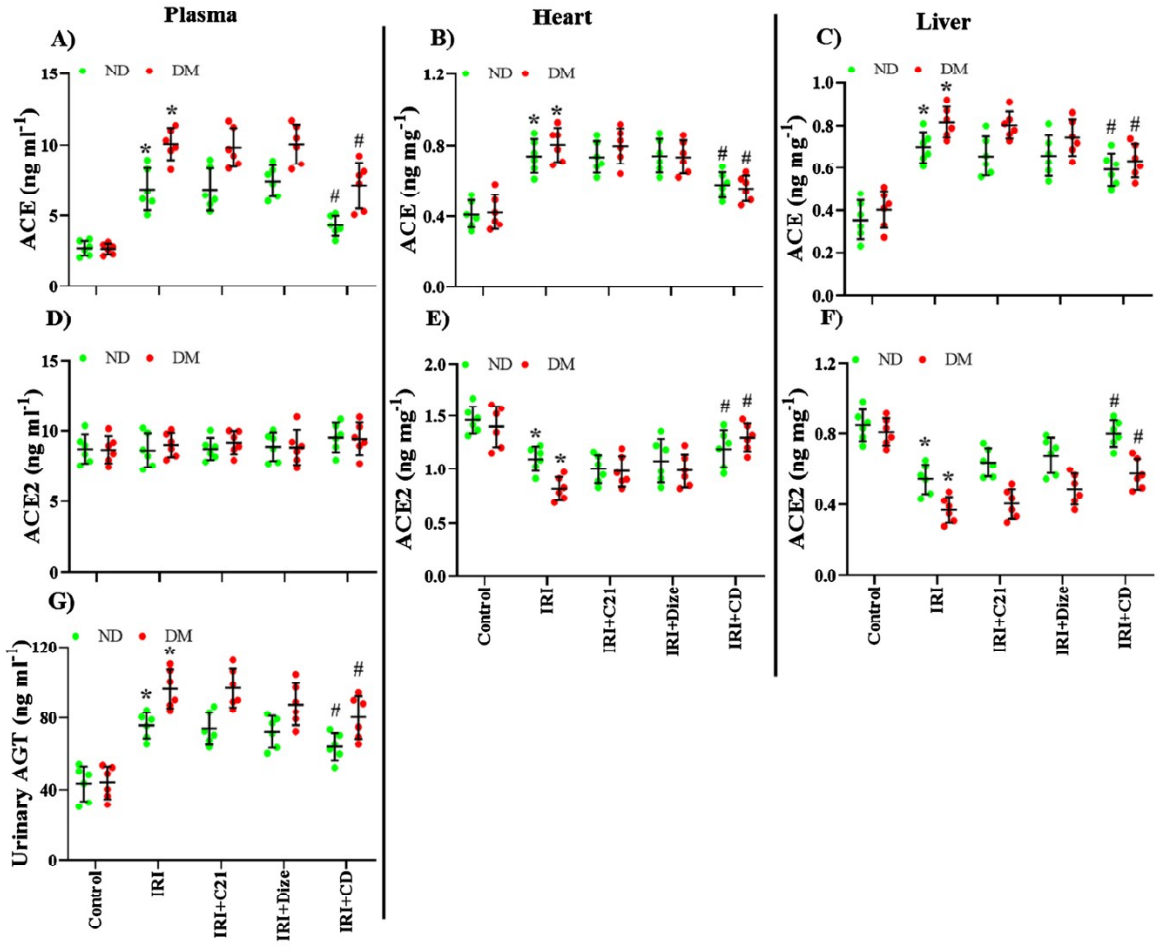

Fig. 7. Effect of AT2R and ACE2 activation on protein levels of ACE, ACE2 in plasma, heart and liver tissues along with urinary AGT.
A-F: Protein expression of ACE and ACE2 in plasma (A, D), heart (B, E) and liver (C, F), whereas protein expression of urinary AGT (G) was assessed by ELISA (n = 6). Data are represented as mean ± SD from three independent experiments. Two-way ANOVA with Tukey's multiple comparison test was utilised for statistical comparison. $^{(*)}$ $p < 0.05$ vs ND; $^{(\#)}$ $p < 0.05$ vs DM; $^{(@)}$ $p < 0.05$ vs ND-IRI, $^{(\$)}$ $p < 0.05$ vs DM-IRI.

TNF-α. It is the first report to explain the AKI induced overexpression of TNF-α in the cardiac and hepatic tissues under both ND and DM conditions, where DM-IRI group showed a marked rise in TNF-α expression compared to ND-IRI group (Figs. 5,6). Treatment with C21 and Dize alone and in combination have significantly down the expressions of TNF-α in cardiac and hepatic tissues; however, combination therapy has proven to be better in reducing the TNF-α expressions. Our previous studies indicating the ability of AT2R and ACE2 stimulation to reduce inflammatory cytokines production and diabetes-related microvascular complications (Pandey and Gaikwad, 2017a; Malek et al., 2019).

Numerous studies have provided mechanistic evidence in support of the depressor arm of RAS required for suitable cardiac and hepatic function. These studies proposed that repression of AT2R/ACE2/Ang-(1–7)/MasR axis diminished the protective functions of the depressor arm (Santos et al., 2006; Silva et al., 2013). Nevertheless, depressor arm modulators strongly reveal their cardio-hepatic protective role in hypertension, atherosclerosis, insulin resistance (Bruce et al., 2015; Chow et al., 2016; Quiroga et al., 2018; Rajapaksha et al., 2018) as evidenced by increased ACE2, Ang-(1–7), AT2R and MasR expressions. Following these findings, we first examined the RAS components in the systemic circulation and urine. IRI results in marked reduction of ACE2 and Ang-(1–7) levels followed by a significant increase in ACE, Ang II and urinary AGT levels in DM rats as compared to ND rats. However, combination therapy normalised the pressor and depressor arm components in plasma as well as urine (Figs. 7,8). Most recent study revealed the novel mechanism of kidney-heart interaction under IRI condition and suggested that cardiac inflammatory cascades triggered by the simultaneous upregulation of sympathetic reflex and RAS in the cardiac tissue (Panicoa et al., 2019). In the current study, we observed the impact of IRI on cardiac and liver RAS, where there was significant increased Ang II and ACE levels plus decreased in Ang-(1–7) and ACE2 levels. On the contrary, the novel combination therapy managed to normalise the pressor and depressor arm components in ND and DM rats (Figs. 7,8).

Under clinical settings, AKI remains a major risk factor to induce further distant organ dysfunction including cardiac and hepatic dysfunction in hospitalised patients (Lee et al., 2018). Therefore, the outcome of this study suggests that the combination of C21 and Dize could be a novel approach for the prevention of IRI associated with distant organ dysfunction. Further, extensive clinical studies should be conducted to check the efficacy of C21 and Dize alone and in combination in order to carry these novel targeting treatments from the bench to the bedside. The present study has some limitations. Firstly, the effect of renal ischemia on cardiac function parameters was only assessed by SBP measurement; future studies should use echocardiography analysis to provide a clearer indication of ventricular function. Secondly, we have done CK-MB and LDH estimation to assess cardiac functioning; however, future studies should also estimate the plasma electrolyte concentrations (Na^+, Cl^-, K^+) to provide a clear indication of electrolyte imbalance in AKI-induced cardiac dysfunction.

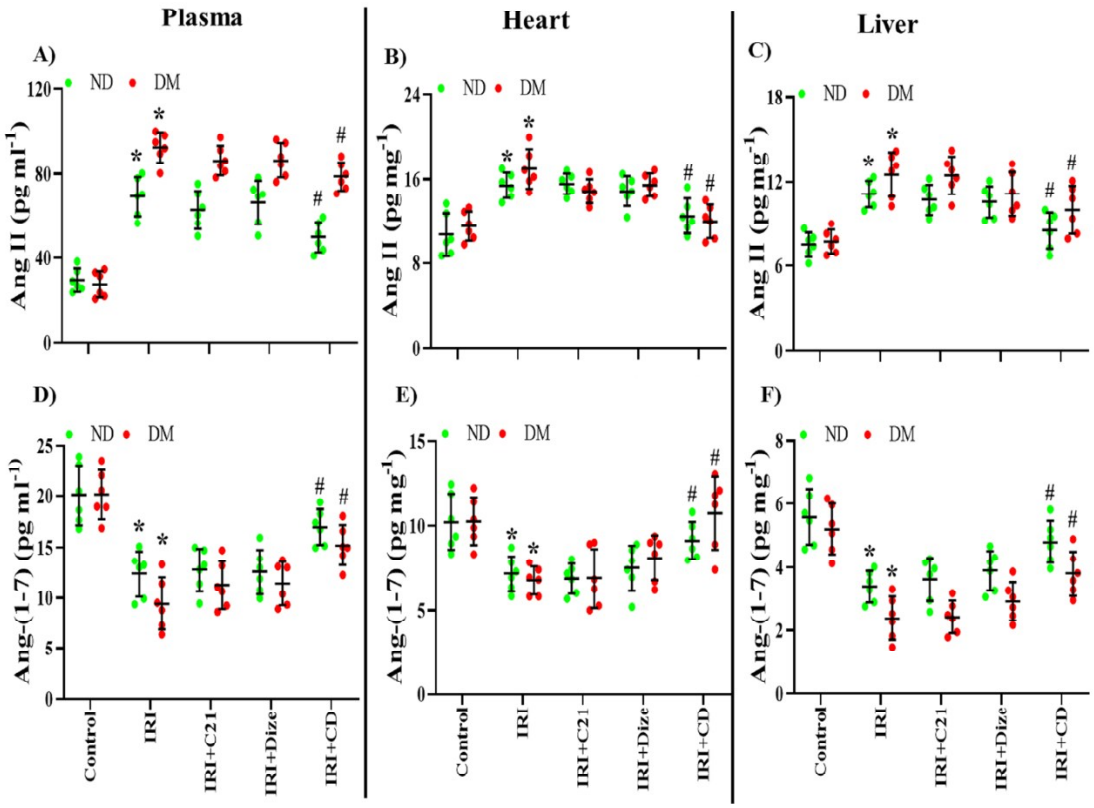

Fig. 8. Effect of AT2R and ACE2 activation on protein levels of Ang II, Ang-(1-7) in plasma, heart and liver tissues.
A-F: Protein expression of Ang II and Ang-(1 7) in plasma (A, D), heart (B, E) and liver (C, F) were assessed by ELISA (n = 6). Data are represented as mean ± SD from three independent experiments. Two-way ANOVA with Tukey's multiple comparison test was utilised for statistical comparison. $^{(*)}$ $p < 0.05$ vs ND; $^{(\#)}$ $p < 0.05$ vs DM; $^{(@)}$ $p < 0.05$ vs ND-IRI, $^{(\$)}$ $p < 0.05$ vs DM-IRI.

5. Conclusion

In conclusion, to the best of our knowledge, this is the first report that upregulation of depressor arm of RAS exerted significant protective effects on the heart and liver during IRI in ND and DM conditions. This potential mechanism of combination therapy of AT2R and ACE2 activation is associated with normalised biochemical markers, antioxidative and anti-inflammatory capability. These results support the proposition that depressor arm modulators hold potential for novel therapeutic approaches to curb cardio-hepatic sequelae associated with AKI under diabetic and non-diabetic conditions.

Author contributions

N.S. perceived the idea and A.B.G. framed and supervised the experiments. N.S. performed the experiments and completed the manuscript writing. Both authors read and approved the manuscript.

Funding

This research was funded by the Science & Engineering Research Board -Department of Science & Technology (SERB-DST), Govt. of India [SERB/ECR/2017/000317].

CRediT authorship contribution statement

Nisha Sharma: Conceptulization, Data curation, Methodology, Formal analysis, Writing - original draft. **Anil Bhanudas Gaikwad:** Supervision, Validation, Writing - review & editing.

Declaration of Competing Interest

The authors report no declarations of interest.

Acknowledgements

N.S. sincerely grateful to the Indian Council of Medical Research (ICMR) for providing senior research fellowship [45/54/2019/PHA/BMS]. The authors also acknowledge Anders Ljunggren, Vicore Pharma, Sweden, for his valuable suggestions and for offering the drug sample, Compound 21.

Appendix A. Supplementary data

Supplementary material related to this article can be found, in the online version, at doi:https://doi.org/10.1016/j.etap.2020.103501.

References

Abdellatief, S.A., Galal, A.A., Farouk, S.M., et al., 2017. Ameliorative effect of parsley oil on cisplatin-induced hepato-cardiotoxicity: a biochemical, histopathological, and immunohistochemical study. Biomed. Pharmacother. 86, 482–491.

Amini, N., Sarkaki, A., Dianat, M., et al., 2019. Protective effects of naringin and trimetazidine on remote effect of acute renal injury on oxidative stress and myocardial injury through Nrf-2 regulation. Pharmacol. Rep. 71 (6), 1059–1066.

Bigagli, E., Lodovici, M., 2019. Circulating oxidative stress biomarkers in clinical studies on type 2 diabetes and its complications. Oxid. Med. Cell. Longev. 2019 https://doi.org/10.1155/2019/5953685.

Bonventre, J.V., Yang, L., 2011. Cellular pathophysiology of ischemic acute kidney injury. J. Clin. Invest. 121, 4210–4221.

Brochner, A.C., Dagnaes-Hansen, F., Hojberg-Holm, J., et al., 2014. The inflammatory response in blood and in remote organs following acute kidney injury. APMIS: Acta Pathologica, Microbiologica, et Immunologica Scandinavica 122, 399–404.

Bruce, E., Shenoy, V., Rathinasabapathy, A., et al., 2015. Selective activation of angiotensin AT 2 receptors attenuates progression of pulmonary hypertension and inhibits cardiopulmonary fibrosis. Br. J. Pharmacol. 172, 2219–2231.
Bucsics, T., Krones, E., 2017. Renal dysfunction in cirrhosis: acute kidney injury and the hepatorenal syndrome. Gastroenterol. Rep. (Oxf) 5, 127–137.
Campbell, D.J., 2014. Clinical relevance of local renin angiotensin systems. Front. Endocrinol. 5, 113. https://doi.org/10.3389/fendo.2014.00113.
Cao, X., Song, L.N., Zhang, Y.C., et al., 2019. Angiotensin-converting enzyme 2 inhibits endoplasmic reticulum stress–associated pathway to preserve nonalcoholic fatty liver disease. Diabetes Metab. Res. Rev. 35, e3123.
Chow, B.S., Koulis, C., Krishnaswamy, P., et al., 2016. The angiotensin II type 2 receptor agonist Compound 21 is protective in experimental diabetes-associated atherosclerosis. Diabetologia 59, 1778–1790.
Classics Lowry, O., Rosebrough, N., Farr, A., et al., 1951. Protein measurement with the Folin phenol reagent. J. Biol. Chem. 193, 265–275.
Doyle, J.F., Forni, L.G., 2016. Acute kidney injury: short-term and long-term effects. Crit. Care 20, 188.
Fadillioglu, E., Kurcer, Z., Parlakpinar, H., et al., 2008. Melatonin treatment against remote organ injury induced by renal ischemia reperfusion injury in diabetes mellitus. Arch. Pharm. Res. 31, 705–712.
Goru, S.K., Kadakol, A., Malek, V., et al., 2017. Diminazene aceturate prevents nephropathy by increasing glomerular ACE2 and AT2 receptor expression in a rat model of type1 diabetes. Br. J. Pharmacol. 174, 3118–3130.
Hursh, B.E., Ronsley, R., Islam, N., et al., 2017. Acute kidney injury in children with type 1 diabetes hospitalized for diabetic ketoacidosis. JAMA Pediatr. 171, e170020.
Husain-Syed, F., Rosner, M.H., Ronco, C., 2019. Distant organ dysfunction in acute kidney injury. Acta Physiol., e13357
Kanagasundaram, N.S., 2015. Pathophysiology of ischaemic acute kidney injury. Ann. Clin. Biochem. 52, 193–205.
Kelly, K., 2003. Distant effects of experimental renal ischemia/reperfusion injury. J. Am. Soc. Nephrol. 14, 1549–1558.
Kilkenny, C., Browne, W.J., Cuthill, I.C., et al., 2010. Improving bioscience research reporting: the ARRIVE guidelines for reporting animal research. PLoS Biol. 8, e1000412.
Lai, Y., Deng, J., Wang, M., et al., 2019. Vagus nerve stimulation protects against acute liver injury induced by renal ischemia reperfusion via antioxidant stress and anti-inflammation. Biomed. Pharmacother. 117, 109062.
Lee, S.A., Cozzi, M., Bush, E.L., et al., 2018. Distant organ dysfunction in acute kidney injury: a review. Am. J. Kidney Dis. 72, 846–856.
Liaño, F., Junco, E., Pascual, J., et al., 1998. The spectrum of acute renal failure in the intensive care unit compared with that seen in other settings. The Madrid Acute Renal Failure Study Group. Kidney Int. Suppl. 66, S16–24.
Macedo, L.M., da Silva Souza, ÁP., De Maria, M.Ld A., et al., 2016. Cardioprotective effects of diminazene aceturate in pressure overloaded rat hearts. Life Sci. 155, 63–69.
Malek, V., Gaikwad, A.B., 2018. Telmisartan and thiorphan combination treatment attenuates fibrosis and apoptosis in preventing diabetic cardiomyopathy. Cardiovasc. Res. 115, 373–384.
Malek, V., Sharma, N., Gaikwad, A.B., 2019. Simultaneous inhibition of Neprilysin and activation of ACE2 prevented diabetic cardiomyopathy. Pharmacol. Rep. 71 (5), 958–967.
Mansfield, K.E., Nitsch, D., Smeeth, L., et al., 2016. Prescription of renin–angiotensin system blockers and risk of acute kidney injury: a population-based cohort study. BMJ Open 6, e012690.
Mohammadi, M., Najafi, H., Yarijani, Z.M., et al., 2019. Piperine pretreatment attenuates renal ischemia-reperfusion induced liver injury. Heliyon 5, e02180.
Monseu, M., Gand, E., Sauniier, P.-J., et al., 2015. Acute kidney injury predicts major adverse outcomes in diabetes: synergic impact with low glomerular filtration rate and albuminuria. Diabetes Care 38, 2333–2340.
Pandey, A., Gaikwad, A.B., 2017a. Compound 21 and Telmisartan combination mitigates type 2 diabetic nephropathy through amelioration of caspase mediated apoptosis. Biochem. Biophys. Res. Commun. 487, 827–833.
Pandey, A., Raj, P., Goru, S.K., et al., 2017b. Esculetin ameliorates hepatic fibrosis in high fat diet induced non-alcoholic fatty liver disease by regulation of FoxO1 mediated pathway. Pharmacol. Rep. 69, 666–672.
Panicoa, K., Abrahãoa, M.V., Trentin-Sonodaa, M., et al., 2019. Cardiac inflammation after ischemia-reperfusion of the kidney: role of the sympathetic nervous system and the renin-angiotensin system. Cell. Physiol. Biochem. 53, 587–605.
Park, S.W., Kim, M., Kim, J.Y., et al., 2012. Paneth cell–mediated multiorgan dysfunction after acute kidney injury. J. Immunol. 189, 5421–5433.
Peng, J., Li, X., Zhang, D., et al., 2015. Hyperglycemia, p53, and mitochondrial pathway of apoptosis are involved in the susceptibility of diabetic models to ischemic acute kidney injury. Kidney Int. 87, 137–150.
Quiroga, D.T., Muñoz, M.C., Gil, C., et al., 2018. Chronic administration of the angiotensin type 2 receptor agonist C21 improves insulin sensitivity in C57 BL/6 mice. Physiol. Rep. 6, e13824.
Rajapaksha, I.G., Mak, K.Y., Huang, P., et al., 2018. The small molecule drug diminazene aceturate inhibits liver injury and biliary fibrosis in mice. Sci. Rep. 8, 10175.
Santos, R.A., Castro, C.H., Gava, E., et al., 2006. Impairment of in vitro and in vivo heart function in angiotensin-(1-7) receptor MAS knockout mice. Hypertension 47, 996–1002.
Sharma, S., Taliyan, R., 2016. Epigenetic modifications by inhibiting histone deacetylases reverse memory impairment in insulin resistance induced cognitive deficit in mice. Neuropharmacology 105, 285–297.
Sharma, S., Taliyan, R., Ramagiri, S., 2015. Histone deacetylase inhibitor, trichostatin A, improves learning and memory in high-fat diet-induced cognitive deficits in mice. J. Mol. Neurosci. 56, 1–11.
Sharma, N., Anders, H.-J.-J., Gaikwad, A.B., 2019a. Fiend and friend in the renin angiotensin system: an insight on acute kidney injury. Biomed. Pharmacother. 110, 764–774.
Sharma, N., Malek, V., Mulay, S.R., et al., 2019b. Angiotensin II type 2 receptor and angiotensin-converting enzyme 2 mediate ischemic renal injury in diabetic and non-diabetic rats. Life Sci. 235, 116796.
Silva, A.R., Aguilar, E.C., Alvarez-Leite, J.I., et al., 2013. Mas receptor deficiency is associated with worsening of lipid profile and severe hepatic steatosis in ApoE-knockout mice. American J. Physiol. Regulatory Integrative Comparative Physiol. 305, R1323–R1330.
Sun, J., Shannon, M., Ando, Y., et al., 2012. Serum metabolomic profiles from patients with acute kidney injury: a pilot study. J. Chromatogr. B 893, 107–113.
Taskin, E., Guven, C., 2017. Local Renin angiotensin System at Liver and Crosstalk with Hepatic Diseases. In. Renin-angiotensin System-past, Present and Future. IntechOpen.
Vanmassenhove, J., Kielstein, J., Jörres, A., et al., 2017. Management of patients at risk of acute kidney injury. Lancet 389, 2139–2151.
Yang, Y., Yin, B., Lv, L., et al., 2017. Gastroprotective effect of aucubin against ethanol-induced gastric mucosal injury in mice. Life Sci. 189, 44–51.
Yap, S.C., Lee, H.T., 2012. Acute kidney injury and extrarenal organ DysfunctionNew concepts and experimental evidence. Anesthesiology: J. American Soc. Anesthesiologists 116, 1139–1148.
Zhao, H., Huang, H., Alam, A., et al., 2018. VEGF mitigates histone-induced pyroptosis in the remote liver injury associated with renal allograft ischemia–reperfusion injury in rats. Am. J. Transplant. 18, 1890–1903.